# Data reconciliation and optimal operation

## With applications to refinery processes

*by*

*Tore Lid*

*A Thesis Submitted for the Degree of Dr. Ing.*

Department of Chemical Engineering
Norwegian University of Science and Technology

May 16, 2007

# Preface

This Ph.D. study was originally Statoils contribution to the INCOOP project (Integrated Process Unit Control and Plantwide Optimization) with a planned start in January 1998. The funding of this Ph.D study was planned to be an equal split between Statoil and INCOOP. Unfortunately INCOOP did not initially get the required funding from the EU (European Union) and Statoil withdrew from the project. In spite of this, Statoil decided to continue the funding of the Ph.D. study, now with a 100% share.

The Ph.D. work was carried out in the period from January-1998 to December 2006 with a full three year stay at NTNU in Trondheim from December 1998 to December 2001. I did not manage to complete the Ph.D. work during this time and continued the work at spare time working full time as a control engineer at the Statoil Mongstad Refinery. In 2005 and 2006, Statoil contributed with funding of an additional six months of full time Ph.D work in order to finalize the research and this Thesis.

During the Ph.D. study, I have completed several interesting courses, at graduate and postgraduate level, and had the privilege of carrying out research with relevance to my profession and personal interest.

# Acknowledgment

First, I want to thank my Ph.D. advisor professor Ph.D. Sigurd Skogestad at NTNU for excellent supervision, his always positive and constructive feedback and patience.

Second, my advisor supervisor at the Statoil Research Center, Stig Strand. He was the initiator of this project and has contributed with valuable advice, challenging discussions and encouragement during difficult times with low progress. I also acknowledge his contribution to establish the financial support for my study.

The generosity of Statoil, financing this Ph.D. study, is greatly appreciated and hopefully Statoil will get a profitable return of their investment during the years to come. In particular, I want to thank my current and former leaders, Bernt Vagstad, Per Birger Møvik and Ole Langeland, Ellinor Hoemsnes and Birger Tenden, for their encouragement and interests in my studies.

In addition, I thank my colleges at NTNU, Marius Govatsmark, with whom I shared office for three years, Truls Larsson, Ivar J. Halvorsen and Audun Faanes for "good times" and many interesting discussions (with and without relevance to the research discipline).

Finally, I want to thank, now my wife, Karianne for sharing the last ten years with me. During these years we have bought an apartment, we have got three great children, Mari, Magnus and Andreas, sold the apartment, bought a house, we got married and more. I thank my family for being supportive, patient and inspiring and I look forward to many years to come.

# Contents

# Chapter 1

# Introduction

## 1.1 Motivation

Optimization of the operation of chemical processes is primarily a search for profitable operational opportunities. The objective is to maximize profit, given the process and constraints in feeds and products. In this context the maximum profit is achieved by adjusting operational parameters like mass flows, temperatures and pressures optimally.

The improvement in profit due to optimal adjustments in operational parameters are small (in the range of 0-5%) compared to the total income. The day to day improvement, compared operation without optimization, can also be difficult to measure due to measurement errors and long term changes like changes in feed and product quality, catalyst degradation. It may be necessary to use estimation methods, like data reconciliation, to verify the improvements made by optimization. Still, when these small day-to-day improvements are summarized over a longer time (like one year) a significant contribution to the overall profit is achieved.

A process model is necessary to perform data reconciliation and optimization. It can also describe the relation between the state of the process equipment, operation and the process economics. Which parameters have a significant influence on the process economics and which have only a small or negligible influence? What is the cost of instrument malfunction or a "sticky" valve? What is the cost of poor control? What is the cost of a product quality constraint? There is a long list of interesting questions to be answered and decisions to be made.

The word optimization is used in many contexts in the chemical industry and this may in some cases be confusing. In this thesis the word optimization is used to describe the minimization of a mathematical objective function subject to a set of constraints. If the objective function describes the negated profit and the constraints a process model, the solution of this problem yields the optimal operation of the process.

## 1.2 Summary

The key elements of on-line process optimization are data validation, model update, optimization, result conditioning and implementation (Forbes and Marlin, 1996).

In this thesis, these key elements are groped into three main functions, data reconciliation, optimization and control. First, the current process state is estimated using data reconciliation (data validation and model update). The estimate is based on all measured values and a first principles process model. Then, the optimal operation is computed as the maximum profit, given the estimated current process state, the process model and operational constraints (optimization) . Finally, the optimal operation is implemented as set points in the control system (implementation).

The basis for data reconciliation and optimization is a process model. In chapter 2 a modelling framework for deriving physically-based (first principle) nonlinear models is proposed. The model is based on a unit model structure where first-order derivatives, scaling and initial values are properties of each unit model. A new scaling procedure based on equation and variable pairing is used to improve the numerical properties of the model. The modeling framework and the use of the proposed scaling procedure are demonstrated in two case studies. Case 1 is simulation of a simple pipe model. Case 2 is simulation, data reconciliation and optimization of a flash process.

Chapter 3 gives a detailed introduction to data reconciliation. This chapter does not contain any new material but provides a justification for the methods used in later chapters. It is also written to get a "hands on" understanding of what is actually gained using data reconciliation methods. In general, process measurements are contaminated with random and possibly systematic errors. For this reason, they do not obey the conservation laws of the process, like the mass and energy balance. Data reconciliation is a method of optimally adjusting these measurements, such that they obey the conservation laws or process model. The process model is incorporated as a set of equality constraints in an optimization problem where the objective is to minimize the deviation between the measurement and the corresponding variable values in the process model. As a basis for the adjustments or estimation, each process and its measurements should be analyzed. The measurements are classified as redundant or non redundant, the process model variables as measured or unmeasured, the unmeasured variables as observable or unobservable. The above classification and the computation of the estimate uncertainty give valuable information of the quality of the estimate. If systematic errors also named gross errors are present, they are removed or a robust objective function is used. These methods are applied to a small stream mixing process as an example. Individual measurement validation and steady state detection is not treated in this thesis.

Chapter 4, 5, and 6 are case studies where the modeling framework and the main functions of on-line optimization are applied to a naphtha reformer and a crude unit heat exchanger network.

The naphtha reforming process in chapter 4 converts low-octane gasoline blending com-

ponents to high-octane components for use in high-performance gasoline fuels. The reformer also has an important function as the producer of hydrogen to the refinery hydrotreaters. There are large seasonal variations in the reformer product price and two operational cases are studied. In case 1, the product price is high and throughput is maximized with respect to process and product quality constraints. In case 2, the product price is low and the throughput is minimized with respect to a low constraint on the hydrogen production. A process model based on a unit model structure is used for estimation of the process condition using data reconciliation. Measurements are classified as redundant or non-redundant and the model variables are classified as observable, barely observable or unobservable. The computed uncertainty of the measured and unmeasured variables shows that even if a variable is observable it may have a very large uncertainty and thereby practically unobservable. The process condition at 21 data points, sampled from two years of operation, is estimated and operation is optimized. Based on the characteristics of the optimal operation a "self optimizing" control structure is suggested for each of the two operational cases.

Chapter 5 describes modeling and on-line optimization of a crude unit heat exchanger network at the Statoil Mongstad refinery. The objective is to minimize the energy input in the gas fired heater by optimally distributing the cold crude oil in the heat exchanger network. The steady state mass and energy balance of the 20 heat exchangers in the network yields the process model. This model is fitted to the measured values using data reconciliation and unmeasured values like heat exchanger duty and heat transfer coefficients are computed. The fitted model is used to compute the optimal split fractions of crude in the network. This system has been implemented at the refinery and has resulted in a 2% reduction in energy consumption. In operational modes where the unit is constrained on energy input this gives a increased throughput and a significant contribution to the refinery profit.

Chapter 6 provides a case study on the selection of controlled variables for the implementation of real time optimization in a crude unit heat exchanger network. Two different control strategies with 22 different control structures are evaluated. The idea is to select the controlled variables that give the best plant economic (smallest loss) when there are disturbances (self-optimizing control). The disturbances are correlated and a simple principal component analysis is used to generate a more realistic set of disturbance variations for evaluation of the different control structures. This analysis shows a large variation of loss for different control structures and that a control structure evaluation is necessary to obtain the benefits from a RTO system.

**List of publications**

Chapter 2:
**Scaled steady state models for effective on-line applications**
Authors: Tore Lid and Sigurd Skogestad.
Published in Computers & Chemical Engineering (2007),
doi:10.1016/j.compchemeng.2007.04.003

Chapter 4:
**Data reconciliation and optimal operation of a catalytic naphtha reformer**
Authors: Tore Lid and Sigurd Skogestad
Submitted to Journal of Process Control, December, 2006

Chapter 5 :
**On line optimization of a crude unit heat exchanger network.**
Authors: Tore Lid, Sigurd Skogestad, and Stig Strand.

Presented at the sixth inernational conference on Chemical Process Control, Tucson, Arizona, 7-12 January, 2001.

Published in AIChE Symposium Series, Vol 98 No 326, p 403-407, 2002. ISBN 0-8169-0869-9.

Chapter 6:
**Implementation issues for real time optimization of a heat exchanger network.**
Authors: Tore Lid and Sigurd Skogestad.

Presented at the European Symposium On Computer Aided Engineering -11. ESCAPE-11, 27-30 May, 2001, Kolding, Denmark.

Published in Computer-Aided Chemical Engineering, European Symposium On Computer Aided Process Engineering-11, p 1041-1046, 2001. ISBN: 0-444-50709-4.

# Chapter 2

# Scaled steady state models for effective on-line applications

*Accepted for publication in Computers & Chemical Engineering*
*Authors: Tore Lid and Sigurd Skogestad*

## Abstract

*Applications for on-line data reconciliation and optimization must be efficient and numerically robust. The models in these applications are rarely changed and the same optimization problem is solved thousands of times with only minor changes in the parameters. This paper describes a suitable modeling framework for this type of applications that, with the aim of simplifying the creation of new models, makes the application robust and avoids numerical difficulties. The model is based on a unit model structure where first-order derivatives, scaling and initial values are properties of the unit model. A new scaling procedure is proposed based on equation and variable pairing. The modeling framework and the use of the proposed scaling procedure are demonstrated in two case studies, case 1 is simulation of a simple pipe model, case 2 is simulation, data reconciliation and optimization of a flash process.*

## 2.1 Introduction

Typical process modeling tools are based on a unit model structure library, and then using streams to connect these. Unit models typically included are heaters, flash drums, heat exchangers, distillation columns, reactors and so on (Westerberg et al., 1979). The resulting model equations are solved sequentially or simultaneously.

Most chemical engineers prefer tools like PRO/II from SIMSCI and Hysys from AspenTech. This may be due to an extensive unit model library, a high quality user interface

and a sequential solver that solves one unit model at a time. In this environment it is simple to locate a problem (like a non-converging unit model) and it is simple to do changes to the model on the worksheet level. On the other hand, sequential solvers are ineffective for solving optimization problems, including data reconciliation.

For optimization problems, as well as for simulation of more complex processes with energy and mass recycles, simultaneous solvers are preferred. Examples of tools for process modeling using simultaneous solvers are gProms from PSE, ASCEND from Carnegie Mellon University and Custom Modeler from AspenTech. See Marquardt (1996) for an overview of these tools and others.

The strength of the generic modeling tools mentioned above are the modeling capability, i.e. creation of new models, but this is rarely needed in on-line optimization applications. On-line optimization of a process plant is typically separated into three main tasks; estimation of current state (data reconciliation), optimization and implementation (White, 1997). Models for on-line applications should be derived with the following in mind:

- An optimization problem may be solved thousands of times a year with only small changes in objective functions and specifications and the models are only rarely changed. Changes in the model are only required when the plant is modified which may be only once every two to ten years.

- The execution of the optimizer is often automated and is generally not monitored by modeling experts. Robust convergence properties of the solver are critical.

- The optimizer must have on-line data exchange with the control and process planning systems. It is therefore often run on computers closely connected to the control system with limited access for changes.

In summary, the requirements for an on-line application are: a model with no overhead (unused functionality) to save computation time, an effective and robust solver and simple interfaces to other systems for data transfer. The actual application is typically "tailor made" and programmed in some object oriented programming language (C++ or similar).

This paper demonstrates a modeling procedure for this type of on-line applications. Our experience is that too much time in such projects is spent on finding model errors and avoiding numerical difficulties and too little time on result analysis. This modeling guideline will hopefully improve this. The models are based on a unit model structure and solved simultaneously using a general NLP (non-linear programming) solver. The equations and variables are organized such that the same process model is used for simulation, data reconciliation and optimization of the process.

Model residuals, first order derivatives of the models, scaling factors and initial values, are properties of the unit model. The model equations and numerical properties of each unit model are verified before they are added to the process model. The unit

model equations are standardized to reduce the possibility of errors and simplify the modeling work. For example, all mass balances have the same structure, similar scaling and same engineering units. This simplifies the development of new unit models and reduces the possibility of errors.

The examples given in this paper are simple, but the procedure has been applied industrially on a crude unit pre-heater train (Lid et al., 2002) where the resulting on-line application is still operating after several years. It has also successfully been applied to a naphtha reformer model with more than 500 equations and variables.

The model representation in this paper is very simple and a comprehensive definition, more suited for commercial use, can be found in Bogusch and Marquardt (1995).

In this paper all models are steady state, which is suitable for most process plants with continuous operation. In the case of processes where dynamic changes are central, the use of a dynamic model should be considered.

The most important notation is summarized in table 2.1.

## 2.2 Simulation, data reconciliation and optimization problems

This section defines the simulation, data reconciliation and optimization problems considered in this work.

All three problems use a nonlinear steady state model of the process, which is incorporated as a set of nonlinear equality constraints $f(z) = 0$. In addition, known variables are specified by linear equality constraints $Az = b$. For each specification $i$, the matrix $A$ has a row $A(i)$ with a single nonzero element $A(i, j) = 1$, such that the value of $z(j)$ is specified to equal $b(i)$.

The number of equations in the process model ($f(z) = 0, Az = b$) should be less than the number of variables, i.e. $n_f < n_z$. The difference $n_z - n_f - n_s$ is the number of degrees of freedom for the problem.

### 2.2.1 Simulation

In the simulation case, specifications are added in $A_s$ such that there are zero degrees of freedom, i.e. $n_z - n_f - n_s = 0$. The simulation problem is formally defined as

$$\begin{aligned} &\min_z \ J_s(z) \\ \text{s.t.} \quad &f(z) = 0 \\ &A_s z = b_s \end{aligned} \tag{2.1}$$

| | Description | Dimension |
|---|---|---|
| $z$ | process model variables | $n_z \times 1$ |
| $\tilde{z}$ | scaled process model variables | $n_z \times 1$ |
| $n_z$ | number of process model variables | |
| $f$ | process model equations | $n_f \times 1$ |
| $\tilde{f}$ | scaled process model equations | $n_f \times 1$ |
| $r$ | residual vector | $n_f \times 1$ |
| $n_f$ | number of process model equations | |
| $J$ | objective to be minimized | |
| $y$ | measurement vector | $n_y \times 1$ |
| $Q$ | measurement weighting matrix | $n_y \times n_y$ |
| $U$ | measurement incident matrix | $n_y \times n_z$ |
| $P_n$ | equation and variable pairing matrix | $n_f \times n_z$ |
| $P_s$ | equation and variable pairing matrix | $n_s \times n_z$ |
| $n_y$ | number of measurements | |
| $A_s$ | fixed values matrix | $n_s \times n_z$ |
| $b_s$ | vector of fixed values | $n_s \times 1$ |
| $n_s$ | number of specified variables | |
| $A_r$ | fixed values matrix | $n_r \times n_z$ |
| $b_r$ | vector of fixed values | $n_r \times 1$ |
| $n_r$ | number of specified variables | |
| $A_{opt}$ | fixed values matrix | $n_{opt} \times n_z$ |
| $b_{opt}$ | vector of fixed values | $n_{opt} \times 1$ |
| $n_{opt}$ | number of specified variables | |
| $z$ | model variables | $n_z \times 1$ |
| $z_s$ | simulation result | $n_z \times 1$ |
| $z_r$ | data reconciliation result | $n_z \times 1$ |
| $z_{opt}$ | optimization result | $n_z \times 1$ |
| $z_0$ | initial value | $n_z \times 1$ |
| $p$ | cost vector | $n_z \times 1$ |
| $S_n$ | nonlinear equations scaling matrix | $n_f \times n_f$ |
| $S_l$ | linear equations scaling matrix | $n_s \times n_s$ |
| $S_v$ | variable scaling matrix | $n_z \times n_z$ |
| $S_o$ | objective scaling factor | |
| $H$ | linearized equality constraints | |
| $\tilde{H}$ | scaled linearized equality constraints | |
| $d_{est}$ | Estimation error | |
| Init. | initial values | |
| Sim. | simulation results | |
| Rec. | data reconciliation results | |
| Opt. | optimization results | |

Table 2.1: Nomenclature

where the "dummy" objective function is chosen as $J_s(z) = 0$. This is because with no degrees of freedom the objective function has no influence on the solution. Note that the specifications in $A_s z = b_s$ must be selected such that there are no dependent equations in $f(z)$ and $A_s$, that is such that the matrix

$$\begin{bmatrix} \frac{\partial f}{\partial z} \\ A_s \end{bmatrix} \tag{2.2}$$

has full rank.

### 2.2.2 Data reconciliation

Data reconciliation is used to estimate the actual condition of the process and is obtained as the solution of

$$\begin{aligned} &\min_z \ J(z) \\ \text{s.t.} \quad &f(z) = 0 \\ &A_r z = b_r \\ &z_{r\,\min} \le z \le z_{r\,\max} \end{aligned} \tag{2.3}$$

where $J = (y - Uz)^{\mathrm{T}} Q (y - Uz)$. All $n_y$ measurements are collected in the measurement vector $y$. The "selection" matrix $U$ gives a mapping of the variables $z$ into the measurements, such that $Uz$ represents the estimated value of the measurements $y$. The matrix $U$ has $n_y$ rows and in each row there is only one nonzero element $U(i, j) = 1$, that is $y(i)$ corresponds to $z(j)$.

The diagonal weighting matrix $Q$ has elements $Q(i, i)$ equal to $1/\sigma(i)^2$, where $\sigma(i)^2$ is the variance of the measurement noise of measurement number $i$. Minimizing the objective function is the same as maximizing the Gaussian frequency function, $\sum_i f_i = 1/(\sigma(i)\sqrt{2\pi})\ \exp(-0.5(y(i) - U(i)z)^2/\sigma(i)^2)$, which results in a least squares or maximum likelihood estimate of the process state. More about this and other objective functions can be found in Tjoa and Biegler (1991) and Chen et al. (1998).

Upper and lower bounds on variables are used to limit the solution to acceptable values. For example all flows, temperatures and pressures must satisfy $z(j) \ge 0$.

If the value of a variable is known it can be specified using the linear constraints.

The variables must be observable based on the measured values and the process model (Stanley and Mah, 1981). A minimal requirement is that the number of measurements satisfies $n_y > n_z - n_f - n_r$, where $n_r$ is the number of rows in $A_r$. If some variables are not observable then measurements must be added or the actual variable value must be specified.

### 2.2.3 Optimization

Optimal operation is calculated by minimization of a cost function subject to the process model, specified values and operating constrains.

$$\begin{aligned} \min_{z} \ & J(z) \\ \text{s.t.} \quad & f(z) = 0 \\ & A_{opt} z = b_{opt} \\ & z_{opt\,\min} \leq z \leq z_{opt\,\max} \end{aligned} \tag{2.4}$$

where $J(z) = p(z)^{\mathrm{T}} z$. In most cases $p$ is a vector of fixed prices related to feed cost, energy cost and product values.

Values for variables like model parameters, feed conditions and other variables, not available for optimization, are specified using the linear equality constraints $A_{opt} z = b_{opt}$. These variables are set equal to the reconciled variable, $b_{opt} = A_{opt} z_r$.

Operating constraints are added as upper and lower bounds on variables, $z_{opt\,\min}$ and $z_{opt\,\max}$.

### 2.2.4 NLP Solver

An NLP solver is used for solving the simulation, data reconciliation and optimization problems. In this paper a general NLP solver is required to at least handle the following optimization problem definition:

| | |
|---|---|
| Objective to be minimized | $J(z)$ |
| Linear equality constraints | $Az = b$ |
| Nonlinear equality constraints | $f(z) = 0$ |
| Variable bounds | $z_{\min} < z < z_{\max}$ |

In addition it is expected to be able to utilize user specified first order derivatives of the objective and of the nonlinear constraint functions.

| | |
|---|---|
| Objective first order derivatives | $\frac{\partial J(z)}{\partial z}$ |
| NL constraints first order derivatives | $\frac{\partial f(z)}{\partial z}$ |

The linearized equality constraints

$$H = \begin{bmatrix} \frac{\partial f(z)}{\partial z} \\ A \end{bmatrix} \tag{2.5}$$

are used for analysis of the numerical properties of the optimization problem. If the condition number of $H$ is large, then the problem is said to be ill-conditioned and

numerical problems may be expected (based on personal experience large, in this case, means $> 10^6$).

In this paper the solver `fmincon` from the Matlab Optimization Toolbox® is used.

## 2.3 Modeling framework

### 2.3.1 Model structure

In the suggested model structure, a process model is a collection of one or more unit models. A unit model describes a small part of the process like a flash drum, heater or a reactor. The boundary of the unit model is selected such that the connection to other unit models is by process streams. A general unit model, as shown in figure 2.1, can

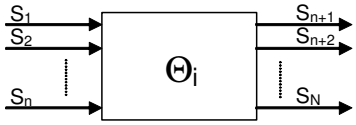


Figure 2.1: UnitModel

have one or more input and output streams, shown as $S_1 - S_N$ and internal variables shown as $\Theta_i$. A process stream, connecting two unit models, is simply a set of shared variables describing the properties of the process stream. A process model with three

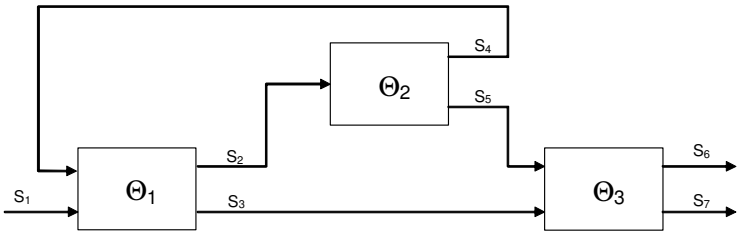


Figure 2.2: Process model

unit models and seven process streams is shown in figure 2.2. Each unit model has a set of equations $f_i(z) = 0$ and the overall process model is a collection of equations from these unit models.

$$r = f(z) = \begin{bmatrix} f_1(z) \\ f_2(z) \\ f_3(z) \end{bmatrix} \tag{2.6}$$

The process model, $r = f(z)$, as shown in equation (2.6), is a collection of unit models where each unit model is represented by equations written as $r_i = f_i(z)$.

All unit models share the variable vector $z$. This variable vector contains variables from all process streams and internal variables from all unit models.

$$z = \begin{bmatrix} S_1 \\ S_2 \\ \vdots \\ S_7 \\ \Theta_1 \\ \Theta_2 \\ \Theta_3 \end{bmatrix} \tag{2.7}$$

Variables describing a process stream are typically component molar fractions, flow, temperature and pressure. Some cases may require other variables. For example, in units with two-phase streams, enthalpy may replace temperature as a variable. In this paper process stream variables are selected as $S_i = [\boldsymbol{x}_j^{\mathrm{T}}\ F_j\ T_j\ P_j]^{\mathrm{T}}$

The unit model internal variables $\Theta_i$, can be heater duty, heat transfer coefficient and compressor efficiency.

With this fixed ordering of the variables in the variable vector $z$, a variable mapping is created. The variable mapping is used to obtain the values of input and output stream variables and internal variables from the variable vector $z$, within each unit model. This requires that the stream number of the input and output streams is known within each unit model. The stream numbers can be passed to the unit model as parameters in the actual function call.

The first order derivatives of the process model are also calculated on a unit model basis.

$$\frac{\partial f(z)}{\partial z} = \begin{bmatrix} \frac{\partial f_1(z)}{\partial z} \\ \frac{\partial f_2(z)}{\partial z} \\ \frac{\partial f_3(z)}{\partial z} \end{bmatrix} \tag{2.8}$$

where $\frac{\partial f_i(z)}{\partial z}$ is a $n_{fi} \times n_z$ matrix. The above mentioned variable mapping is used in the column mapping of the individual elements in $\frac{\partial f_i(z)}{\partial z}$.

### 2.3.2 Unit Models

A unit model describes the behavior of some process unit or process equipment and is based on equations of mass balance, energy balance and pressure-flow relations. Even if the individual units may be different, the equations describing their behavior is very similar and there are benefits of standardization of these equations.

The simplest unit model possible is a unit model with one inlet stream and one outlet stream. The unit model has no holdup, no reactions, no heat loss or pressure drop. It is visualized as a "pipe model" and is stated in equation (2.21).

This "pipe model" is of no practical use as a unit model but works well as a basic template for other unit models. Some examples:

- A heater unit model can be made by adding a simple heat input term $Q$ in the energy balance. The heat input is an internal variable in the model.
- A heat exchanger can be made by combining two pipes. The energy balance in the two models is modified by adding a heat term, one negative and one positive. One additional equation is added in the models describing the heat transfer. This can be based on LMTD (log mean temperature difference), $\epsilon$-Ntu or other.
- A CSTR reactor can be made by adding a reaction term, $VN^{\mathrm{T}}r$, in the pipe model mass balance, where $V$ is the reactor volume, $N$ is the reaction stoichiometric matrix and $r$ is a vector of reaction rates.
- A flash drum can be made as a pipe with two outlet streams, one vapor flow and one liquid flow. Equations for vapor-liquid equilibrium ($y - K(T, P)x = 0$), sum of vapor components, equal vapor-liquid pressure and temperature have to be added.

The idea in section 2.4 is to develop a "pipe model" with good numerical properties to serve as a template. Other unit models will then inherit these properties and only small adjustments will be necessary. See Appendix A for unit models of

- Heater
- Reactor (CSTR)
- Separator (flash drum)
- Compressor
- Heat exchanger
- Stream split
- Stream mix

In formulating models, it is easy to miss an equation. A general recommendation or rule in modeling is to use set assignment and formally pair equations and variables. Since most variables appear in more than one equation this pairing is not unique. Nevertheless this rule gives a valuable overview of the model and the pairing turns out to be useful in adding proper variable specifications and scaling of the variables and equations.

A systematic approach to the equation-variable pairing is found in Maurya et al. (2003) and Mah (1990) where the equations and variables are defined as nodes in a graph. The equations and variables are grouped into two disjoint subsets where arcs connect the variables and equations. If all equation nodes are connected to only one variable node and no nodes are left unmatched, the set of equations and variables is said to have perfect matching.

### 2.3.3 Initial values

When creating a large process model it is reasonable to start with a small part of the process, verify the results, and then add more process streams and process units until the total model is finalized.

In this construction process the variable vector $z$ will vary in size and the position of the individual variables in $z$ will change and the generation of initial values, $z_0$, will be a tedious task.

A simple solution is to let all unit models generate initial values for all unit model internal variables and for variables related to unit model exit streams. This may not result in initial values close to a solution but it may still be sufficient as a starting value for generation of an improved set of initial values by simulation. In addition, initial values for feed streams must be generated.

In a steady state model, assuming no multiple steady-states, the initial value may influence convergence properties but has no influence on the final solution itself. This is different for differential algebraic (DAE) systems where the initial value affects the solution and must be a valid solution of the DAE system at $t = 0$ (Pantelides, 1988). In this case the method described above may be an initial value for solving the DAE system at $t = 0$

### 2.3.4 Scaling

The performance of the NLP solver depends crucially on how the problem is formulated. An important issue is proper scaling. Note that the scaling is performed off-line. Thus, the computational complexity of the scaling itself is not important. Rather, the objective of the scaling is to minimize the computation time and robustness for the subsequent on-line computations.

An unconstrained optimization problem is said to be poorly scaled if a change in $x$ in one direction produces a much larger change in $f = f(x)$ than in another direction (Nocedal and Wright, 1999). The measure of poor scaling is not so clear in constrained optimization. Some of the methods are said to be scaling invariant, like the SQP algorithm with BFGS update of the Hessian (as used in this paper), but they are still influenced by scaling (Biegler and Cuthrell, 1985). This is related to two issues. First, the initial value of the Hessian is normally set equal to the identity matrix. If the true Hessian of the scaled problem is closer to the identity matrix than the case of the unscaled model this should result in an improved estimate of the Hessian and improved performance of the algorithm. Second, a poorly scaled model is likely to generate larger rounding errors which may degrade the performance of the algorithm.

Scaling methods used within or as a part of an NLP solver are in general based on properties of the estimated Hessian (Zhu, 2005; Roma, 2005). The scaling methods related to the process model or constraints are based on residuals, variable values and first order derivatives (Jacobian).

A scaled process model is written as

$$\tilde{f}(\tilde{z}) = 0 \tag{2.9}$$
$$\widetilde{A}_s \tilde{z} = \tilde{b} \tag{2.10}$$

where the scaled variable $\tilde{z} = S_v^{-1} z$. The scaled model $\tilde{f}(\tilde{z}) = S_n f(S_v \tilde{z})$ and for the scaled specification $\widetilde{A}_s = S_l A_s$ and $\tilde{b} = S_l b_s$. $S_l$, $S_n$ and $S_v$ are fixed diagonal scaling matrices.

The scaled objective function $\widetilde{J}(\tilde{z}) = S_o J(S_v \tilde{z})$ where $S_o$ is a fixed factor.

Three methods for scaling found in literature are:

**Method 1.** Scaling based on variable bounds and initial equation residual (Biegler and Cuthrell, 1985).

$$S_{v_{jj}} = 2^{a_j} \quad \text{where } a_j = \text{int}[\log_2(z_{\max_i} - z_{\min_i})] \tag{2.11}$$
$$S_{n_{ii}} = 2^{-a_i} \quad \text{where } a_i = \text{int}[\log_2(|f(z_0)|_i)] \tag{2.12}$$
$$S_{l_{ii}} = 2^{-a_i} \quad \text{where } a =_i \text{int}[\log_2(|A_s z_0 - b_s|_i)] \tag{2.13}$$

where $z_0$ is the initial value. The equation scaling factor is limited to some maximum value in case the equation residual is close to zero. More details and suggested improvements can be found in the reference.

**Method 2.** Scaling based on first order derivatives (Kelly, 2004).

$$\mathbb{C} = \begin{bmatrix} \frac{\partial f(z_0)}{\partial z} \\ A_s \end{bmatrix} \tag{2.14}$$
$$S_{v_{jj}} = ||\mathbb{C}_j||_2^{-1} \quad \text{where } j = 1...n_z \tag{2.15}$$
$$S_{n_{ii}} = ||\mathbb{C}_i||_2^{-1} \quad \text{where } i = 1...n_f \tag{2.16}$$
$$S_{l_{ii}} = ||\mathbb{C}_i||_2^{-1} \quad \text{where } j = n_f + 1...n_f + n_s \tag{2.17}$$

where $\mathbb{C}_j$ and $\mathbb{C}_i$ denotes the columns and rows of $\mathbb{C}$ respectively. Other norms like the 1-norm ($||\cdot||_1$) or the infinity norm ($||\cdot||_\infty$) may also be used.

**Method 3.** Scaling based on order of magnitude (Rodriguez-Toral et al., 2001).

$$S_{v_{jj}} = 10^{-a_j} \quad \text{where } a_j = \text{int}[\log_{10}(z_0)_j] \tag{2.18}$$

The equation scaling factor is the reciprocal of an integer power of 10 of the value of a given term or group of terms, normally related to the scale factor of a relevant variable. As an example, let a typical value of a mass balance term $x_i F$ be $0.5 \cdot 0.3 = 0.15$. The scaling factor for the mass balance equation is then $10^{(-\text{int}(\log_{10}(0.15)))} = 10$. The objective scaling factor is divided by an integer power of 10 close to its typical value.

**Method 4.** New proposed scaling method based on variable and equation pairing.

This new scaling method is similar to method number 3 but uses to a larger extent the structure of the model. The equation scaling factors are not based on the constraint term values but on values of the first order derivatives matrix. The proposed scaling procedure is

1. Make a pairing of equations and variables:

   The equation and variable pairing is given in the matrix $P$ where $P(i,j) = 1$ if variable number $j$ is paired with equation number $i$. All other elements in $P$ are zero.

   The equation and variable pairing for a unit model $f_i(z)$ is given in a matrix $P_{ni}$ of dimension $n_{f_i} \times n_z$ and variable pairing for the specifications $A_s z = b$ is stated in $P_s$ of dimension $n_s \times n_z$.

2. Scale all variables such that the scaled variable has a value close to one

   The variable scaling matrix $S_v(j,j) = \bar{z}_j$ where $\bar{z}_j$ is a typical value of variable number $j$. The initial value, $z_0$, is used in this case.

3. Scale all equations such that the absolute value of the elements of the first order derivatives, corresponding to the equation and variable pairing, is close to one.

$$S_{ni} = \left| \left[ I \times \left( \frac{\partial f_i(z)}{\partial z} S_v P_{ni}^{\mathrm{T}} \right) \right]^{-1} \right| \tag{2.19}$$

$$S_l = \left| [I \times (A_s S_v P_l^{\mathrm{T}})]^{-1} \right| \tag{2.20}$$

   where $\times$ denotes element by element multiplication so that $S_{ni}$ and $S_l$ are diagonal matrices.

4. The scaling factor for the objective function $S_o$ is selected such that the largest element of the first order derivative $\widetilde{J}(\tilde{z})$ has an absolute value close to one.

5. If any of the elements in the matrix $\widetilde{H} = \left[ \tilde{f}(\tilde{z})^{\mathrm{T}} \ \widetilde{A}_s^{\mathrm{T}} \right]^{\mathrm{T}}$ have large absolute values (where large is $> 100$) then the equation and variable pairing or variable scaling should be revised. A possible solution is to pair the equation with the variable corresponding to the large value in $\widetilde{H}$.

In order to illustrate the idea of this scaling strategy, assume that the variables and equations are reordered such that the elements along the diagonal of the first order derivatives correspond to the selected equation-variable pairing. The diagonal elements of this matrix are now all equal to one and the off-diagonal elements are preferably smaller than one. With this scaling the set of constraints will be balanced where a change in one variable will result in a change of same magnitude in the equation residual.

The condition number of $\widetilde{H}$ is used as a measure of improved scaling. This measure is based on the definition of poor scaling in the unconstrained case where a change in the variable vector $\boldsymbol{z}$ in one direction produces a much larger change in the residual $r = f(z)$ than in another direction.

A process model with a large condition number of the first order derivatives will have larger rounding errors. If the matrix of first order derivatives $\frac{\partial f}{\partial z}$ has a high condition number a small change in $\Delta \boldsymbol{z}$, caused by rounding errors, may cause a large change in $\Delta \boldsymbol{r}$.

The objective function scaling factor, $S_o$, has a large influence on the solution path of the solver during the iterations. A large scaling factor gives large deviations in the model equations in the solution path and rapid decrease in the objective. In case of numerical problems, like temporarily negative values of flows and compositions, the scaling factor of the objective function should be reduced.

## 2.4 Case study 1: "Pipe model"

A simple model of a pipe, as described in section 2.3.2, demonstrates the use of the suggested modeling procedures. This model has two process streams, one inlet stream

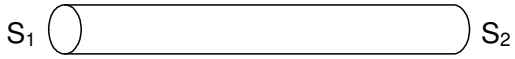


Figure 2.3: Pipe

and one outlet stream. The fluid is a mixture of two components, propane and butane ($NC = 2$). The variables are the composition, flow, temperature and pressure of the two process streams. The variable vector organized as $z^{\mathrm{T}} = [S_1^{\mathrm{T}} \; S_2^{\mathrm{T}}]$ where $S_i^{\mathrm{T}} = [\boldsymbol{x}_i^{\mathrm{T}} \; F_i \; T_i \; P_i]$. There are no internal variables in this model.

The equations of the pipe model are written as

$$\begin{aligned} F_1 \boldsymbol{x}_1 - F_2 \boldsymbol{x}_2 &= 0 \\ \sum \boldsymbol{x}_2 - 1 &= 0 \\ F_1 h(T_1, \boldsymbol{x}_1) - F_2 h(T_2, \boldsymbol{x}_2) &= 0 \\ P_1 - P_2 &= 0 \end{aligned} \tag{2.21}$$

These equations represent the mass balance, mole fraction summation, energy balance and pressure-flow relation (with no pressure drop in this case).

The pipe model is in this case unit model number 1 and is in short-hand notation written as $f_1(z) = 0$.

The number of variables in the variable vector $z$ is $2(NC + 3) = 10$, with $NC = 2$ and the number of equations in the pipe model is $NC + 3 = 5$. In order to solve the model equations, as in the simulation case, $NC + 3 = 5$ variables have to be specified. In this case the inlet stream molar fraction, flow, temperature and outlet stream pressure are

specified.

$$\boldsymbol{x}_1 = \boldsymbol{x}_s \tag{2.22}$$
$$F_1 = F_s \tag{2.23}$$
$$T_1 = T_s \tag{2.24}$$
$$P_2 = P_s \tag{2.25}$$

The specifications are implemented as linear constrains $A_s z = b_s$, where $A_s$ has $n_z$ columns and $n_s = 5$ rows, one row for each specification. $A_s$ is written as

$$A_s = \begin{bmatrix} 1 & 0 & 0 & 0 & 0 & 0 & 0 & 0 & 0 & 0 \\ 0 & 1 & 0 & 0 & 0 & 0 & 0 & 0 & 0 & 0 \\ 0 & 0 & 1 & 0 & 0 & 0 & 0 & 0 & 0 & 0 \\ 0 & 0 & 0 & 1 & 0 & 0 & 0 & 0 & 0 & 0 \\ 0 & 0 & 0 & 0 & 0 & 0 & 0 & 0 & 0 & 1 \end{bmatrix} \tag{2.26}$$

The values of the specific variables are collected in $b_s$ and $b_s^{\mathrm{T}} = [\boldsymbol{x}_s^{\mathrm{T}}\ F_s\ T_s\ P_s]$. The specification values $F_s = 0.27$kmol/s, $T_s = 285$K, $P_s = 30$bar and $x_s = [0.5\ 0.5]^{\mathrm{T}}$ which gives $b_s = [0.5\ 0.5\ 0.27\ 285\ 30\ ]^{\mathrm{T}}$

| Description | Equation | Pairing |
|---|---|---|
| Unit model MB Eq. 1 | $x_1(1)F_1 - x_2(1)F_2 = 0$ | $F_2$ |
| Unit model MB Eq. 2 | $x_1(2)F_1 - x_2(2)F_2 = 0$ | $x_2(2)$ |
| Sum of compositions | $\sum \boldsymbol{x}_2 - 1 = 0$ | $x_2(1)$ |
| Energy balance | $F_1 h(T_1, \boldsymbol{x}_1) - F_2 h(T_2, \boldsymbol{x}_2) = 0$ | $T_2$ |
| Pressure-flow rel. | $P_1 - P_2 = 0$ | $P_1$ |
| Specification no. 1 | $A(1)z = b_1$ | $x_1(1)$ |
| Specification no. 2 | $A(2)z = b_2$ | $x_1(2)$ |
| Specification no. 3 | $A(3)z = b_3$ | $F_1$ |
| Specification no. 4 | $A(4)z = b_4$ | $T_1$ |
| Specification no. 5 | $A(5)z = b_5$ | $P_2$ |

Table 2.2: Equation variable assignment for the pipe unit model

The selected equation-variable pairings are listed in table 2.2. The equation-variable pairing is not unique and other valid combinations exist. An obvious requirement is that, if an equation is paired with a variable, this variable must exist in the actual equation. In the pipe model this leaves two choices for pairing of the outlet stream $F_2$, component balance one (propane) or component balance two (butane). In this case the recommendation is to pair $F_2$ with the component balance of the component with the largest molar fraction. This will in fact simplify the variable and equation scaling and remove the need for "extreme" scaling factors.

The first order derivatives of the pipe unit model, $\frac{\partial f_1(z)}{\partial z}$, is written as a $n_{f_1} \times n_z$ matrix where $n_{f_1}$ is the number of equations in unit model number 1 and $n_z$ the total number of variables in the process model.

$$\frac{\partial f_1(z)}{\partial z} =$$

$$\begin{bmatrix} F_1 & 0 & x_1(1) & 0 & 0 \\ 0 & F_1 & x_1(2) & 0 & 0 \\ 1 & 1 & 0 & 0 & 0 \\ F_1\frac{\partial h(x_1,T_1)}{x_1(1)} & F_1\frac{\partial h(x_1,T_1)}{x_1(2)} & h(x_1,T_1) & F_1\frac{\partial h(x_1,T_1)}{T_1} & 0 \\ 0 & 0 & 0 & 0 & 1 \end{bmatrix} \tag{2.27}$$

$$\begin{matrix} -F_2 & 0 & -x_2(1) & 0 & 0 \\ 0 & -F_2 & -x_2(2) & 0 & 0 \\ 0 & 0 & 0 & 0 & 0 \\ -F_2\frac{\partial h(x_2,T_2)}{x_2(1)} & -F_2\frac{\partial h(x_2,T_2)}{x_2(2)} & -h(x_2,T_2) & -F_2\frac{\partial h(x_2,T_2)}{T_o} & 0 \\ 0 & 0 & 0 & 0 & -1 \end{matrix} \Bigg]$$

A simple verification of the model equations and calculation of first order derivatives is recommended.

- Compare $\frac{\partial f_i(z)}{\partial z}$ with numerically calculated derivatives.
- Verify that equations are linearly independent. The rank of the first order derivative $\frac{\partial f_i(z)}{\partial z}$ must equal the number of equations $n_{f_i}$.
- Specifications added in $A$ (ref. equation (2.1-2.4)) must be linearly independent of any unit model equation. I.e. the matrix $[\frac{\partial f_i(z)}{\partial z}^{\mathrm{T}} \; A^{\mathrm{T}}]^{\mathrm{T}}$ must have full rank

The matrix of the first order derivatives of the specifications and pipe model, where $\frac{\partial f(z)}{\partial z} = \frac{\partial f_1(z)}{\partial z}$, are shown in equation (2.28).

$$H = \begin{bmatrix} \frac{\partial f(z)}{\partial z} \\ A_s \end{bmatrix} =$$

$$\left[\begin{array}{cccccccccc} 0.27 & 0 & 0.50 & 0 & 0 & -0.27 & 0 & \mathbf{-0.50} & 0 & 0 \\ 0 & 0.27 & 0.50 & 0 & 0 & 0 & \mathbf{-0.27} & -0.50 & 0 & 0 \\ 0 & 0 & 0 & 0 & 0 & \mathbf{1} & 1 & 0 & 0 & 0 \\ 9203 & 10190 & 35913 & 34 & 0 & -9203 & -10190 & -35913 & \mathbf{-34} & 0 \\ 0 & 0 & 0 & 0 & \mathbf{1} & 0 & 0 & 0 & 0 & -1 \\ \hdashline \mathbf{1} & 0 & 0 & 0 & 0 & 0 & 0 & 0 & 0 & 0 \\ 0 & \mathbf{1} & 0 & 0 & 0 & 0 & 0 & 0 & 0 & 0 \\ 0 & 0 & \mathbf{1} & 0 & 0 & 0 & 0 & 0 & 0 & 0 \\ 0 & 0 & 0 & \mathbf{1} & 0 & 0 & 0 & 0 & 0 & 0 \\ 0 & 0 & 0 & 0 & 0 & 0 & 0 & 0 & 0 & \mathbf{1} \end{array}\right] \tag{2.28}$$

The condition number of $H$ is $8.13 \cdot 10^7$. The main cause of the high condition number is the energy balance equation. This equation has large values compared to the other equation and changes in the paired variable, $T_2$, has the least significant influence on the equation residual.

In order to reduce the condition number, the model is scaled according to the proposed method (method 4 in section 2.3.4).

The matrix of equation and variable pairing, $P$, is derived from Table 2.2 and the pairing is shown in equation (2.28) using bold font.

The values of flow, temperature and pressure variables are approximately 0.25kmol/s, 280K and 30bar and the variable scaling matrix
$S_v = \text{diag}([1\ 1\ 0.25\ 280\ 30\ 1\ 1\ 0.25\ 280\ 30])$.

The equation scaling matrices $S_n$ and $S_l$ are computed according to step three in the proposed scaling procedure. This gives $S_n = \text{diag}([10.0\ 2.0\ 1.0\ 0.000056\ 0.033])$ and $S_l = \text{diag}([1.0\ 1.0\ 4.0\ 0.0036\ 0.033])$.

The matrix of specifications and first order derivatives are written as:

$$\widetilde{H} = \begin{bmatrix} \widetilde{\frac{\partial f(z)}{\partial z}} \\ A_s \end{bmatrix} = \begin{bmatrix} S_n & 0 \\ 0 & S_l \end{bmatrix} \begin{bmatrix} \frac{\partial f(z)}{\partial z} \\ A_s \end{bmatrix} S_v =$$

$$\left[\begin{array}{cccccccccc} 2.0 & 0 & 1.75 & 0 & 0 & -5.0 & 0 & \mathbf{-1.0} & 0 & 0 \\ 0 & 0.4 & 0.15 & 0 & 0 & 0 & \mathbf{-1.0} & -0.3 & 0 & 0 \\ 0 & 0 & 0 & 0 & 0 & \mathbf{1.0} & 1.0 & 0 & 0 & 0 \\ 0.37 & 0.41 & 0.48 & 0.39 & 0 & -0.91 & -1.0 & -0.48 & \mathbf{-1.0} & 0 \\ 0 & 0 & 0 & 0 & \mathbf{1.0} & 0 & 0 & 0 & 0 & -1.0 \\ \hdashline \mathbf{1.0} & 0 & 0 & 0 & 0 & 0 & 0 & 0 & 0 & 0 \\ 0 & \mathbf{1.0} & 0 & 0 & 0 & 0 & 0 & 0 & 0 & 0 \\ 0 & 0 & \mathbf{1.0} & 0 & 0 & 0 & 0 & 0 & 0 & 0 \\ 0 & 0 & 0 & \mathbf{1.0} & 0 & 0 & 0 & 0 & 0 & 0 \\ 0 & 0 & 0 & 0 & 0 & 0 & 0 & 0 & 0 & \mathbf{1.0} \end{array}\right] \tag{2.29}$$

As a result of the applied scaling the condition number of $\widetilde{H}$ is reduced from $8.1 \cdot 10^7$ to 6.8.

The pipe model is solved using Matlabs `fsolve` and `fmincon`. `fsolve` is based on a nonlinear least squares algorithm and `fmincon` is an SQP algorithm with BFGS Hessian update (Matlab, 2000). The initial value $z_0 = [0.7\ 0.3\ 0.2\ 278\ 20\ 0.4\ 0.6\ 0.5\ 270\ 25]^{\mathrm{T}}$ is used as a starting point for both solvers..

The unscaled model was solved using 14 iterations using `fsolve` and the scaled model was solved using 4 iterations. The scaled and unscaled model where both solved in 3 iterations using `fmincon` and scaling does not seem to have any significant effect in this case. Still, when a unit model becomes part of a larger model the condition number will increase further and the effect of scaling will be significant. To compare, the three

| | Iterations | | Condition number of |
|---|---|---|---|
| Scaling | `fsolve` | `fmincon` | $\widetilde{H}$ |
| Unscaled | 14 | 3 | $8.1 \cdot 10^7$ |
| Method 1 | 5 | 3 | $4.3 \cdot 10^3$ |
| Method 2 | * | 3 | $3.7 \cdot 10^6$ |
| Method 3 | 5 | 3 | 30 |
| Method 4 | 4 | 3 | 6.8 |

Table 2.3: Comparison of scaling procedures

scaling methods presented in section 2.3.4 where also applied to the pipe model. The results are summarized in table 2.3. The condition number for the unscaled model was $8.1 \cdot 10^7$. The smallest condition number for the scaled model, 6.8, was obtained using scaling method 4. Note that `fsolve` did not converge to a valid solution using scaling method 2. The solver terminated (successfully) in 3 iterations at a solution where there was a 2.5K difference in inlet and outlet temperature. The scaled variables had values in the order of $1 \cdot 10^4$ which may have caused the failure of convergence.

## 2.5 Case study 2: Flash process with preheating

A simple flash process is here studied in order to demonstrate the use of the above modeling guidelines in simulation, data reconciliation and optimization. The process, shown in figure 2.4, has three unit models, a heat exchanger, a heater and a flash drum (see Appendix A for details). The three unit models are connected using six process streams.

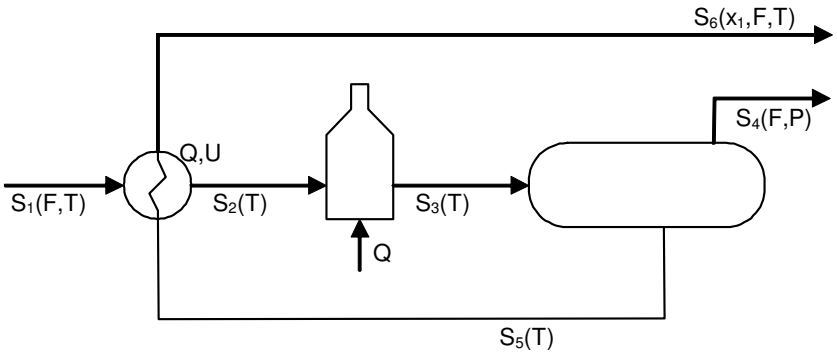


Figure 2.4: Flash process

The model has three chemical components, propane, butane and pentane ($NC = 3$).

The process operating constraints are $S_1$ (flow) $< 0.3$kmol/s, $S_4$ (pressure) $> 28$ bar and $< 40$ bar, $H_1$ (heat duty) $< 5500$ kW, $S_3$ (temperature) $< 485K$ and $S_6$ (propane content) $< 0.2$ mol/mol. The feed and energy price are respectively 100\$/kmol and 0.001\$/kW and the product price are 50\$/kmol for vapor product and 200\$/kmol for liquid product.

The variables in the model include $6(NC+3) = 36$ process stream variables ($6(NC+3)$), two internal variables in the heat exchanger (duty and heat transfer coefficient) and one internal variable in the heater (duty). This gives a total number of $n_z = 39$ variables.

The heat exchanger unit model has $2NC+7 = 13$ equations, the heater has $NC+3 = 6$ equations and the flash drum has $2NC+6 = 12$ equations. This gives the total number of $n_f = 31$ equations. The number of degrees of freedom is then $n_z - n_f = 8$.

There are ten measurements; the propane composition, three flows, five temperatures and pressure. The measurements are shown on the figure using the symbols $x_1$, $F$, $T$ and $P$. The measurements are generated by adding normal distributed noise to a simulation result, $y = Uz_y + e_y$ where $e_y = \mathcal{N}(0, \sigma)$.

In the simulation problem, as defined by equation (2.1), eight variables have to be specified. In this case feed composition (three variables), feed flow, feed temperature, heater outlet temperature, vapor product pressure and heat transfer coefficient are specified.

In data reconciliation, as defined by equation (2.3), only the feed composition is specified.

The objective of operation is to maximize the profit within constraints. In process optimization, as defined by equation (2.4), feed composition, feed temperature and the heat transfer coefficient are specified. The specification values are set equal to the reconciled values. Table 2.4 shows the optimization results. Only variables related to

| Var. | $y$ | $\sigma$ | $p$ | $z_{min}$ | $z_{max}$ | Init. $z_0$ | Sim. $z_s$ | Rec. $z_r$ | Opt. $z_{opt}$ |
|---|---|---|---|---|---|---|---|---|---|
| $F_1$ | 0.20 | 0.025 | 100 | | 0.30 | 0.20 | 0.25 | 0.20 | 0.28 |
| $T_1$ | 289.92 | 0.250 | | | | 280.00 | 280.00 | 289.97 | 289.97 |
| $T_2$ | 308.06 | 0.250 | | | | 320.00 | 301.77 | 308.02 | 302.78 |
| $T_3$ | 474.53 | 0.250 | | | 485.00 | 370.00 | 480.00 | 474.51 | 438.52 |
| $F_4$ | 0.11 | 0.025 | -50 | | | 0.10 | 0.14 | 0.10 | 0.09 |
| $P_4$ | 31.45 | 0.500 | | **28.00** | 40.00 | 30.00 | 31.50 | 30.22 | 28.00 |
| $T_5$ | 418.29 | 0.250 | | | | 400.00 | 417.18 | 418.36 | 405.81 |
| $x_6(1)$ | 0.15 | 0.005 | | | **0.20** | 0.20 | 0.18 | 0.15 | 0.20 |
| $F_6$ | 0.10 | 0.025 | -200 | | | 0.20 | 0.11 | 0.10 | 0.20 |
| $T_6$ | 383.90 | 0.250 | | | | 380.00 | 369.75 | 383.88 | 387.92 |
| $U_{HX}$ | | | | | | 0.010 | 0.015 | 0.010 | 0.010 |
| $Q_{HT}$ | | | 0.001 | | **5500** | 2000 | 6264 | 4856 | 5500 |
| $J_{opt}(z)$ | | | | | | | 2.48 | -0.206 | -9.848 |

Table 2.4: Results for flash process

measurements and constraints are shown.

The optimal solution has three active constraints; minimum pressure (28.00), maximum

liquid product propane content (0.20) and maximum heater duty (5500). The operational profit was increased from a starting point of 0.2\$/s (reconciled) to an optimal of 9.8\$/s.

To compare the results of solving the scaled (method 4) and unscaled data reconciliation problem, the relative estimation error, $d_{est} = \Sigma_{j=1}^{n_y}|((Uz_r - y)_j/y_j|$, is used. Ten different sets of normal distributed measurement error where generated and for each set the unscaled and scaled data reconciliation and optimization problem was solved.

In eight of ten runs the unscaled data reconciliation problem converges to a local optimum where $d_{est} \approx 3$. In these runs the scaled problem converges with an average of ten iterations and an average estimation error $d_{est} \approx 0.3$. In the other two runs the scaled and unscaled problem converge to the same solution. In this case the unscaled problem converged using 45 and 50 iterations and the scaled problem 9 and 10 iterations respectively.

The optimization problem was solved using the reconciled values as described above. In ten of ten runs the scaled optimization problem converged to the optimal solution with pressure, product composition and heater duty as active constraints. In ten of ten runs the unscaled optimization problem failed to converge to the optimal solution and converged to a solution where only the product composition constraint was active. In this case the average objective was $J_{opt} \approx -9.3$.

| | Cond.no. | Number of iterations | | | | | Active |
|---|---|---|---|---|---|---|---|
| | $\widetilde{H}$ | Sim. | Rec. | Opt. | $d_{est}$ | $J_{opt}$ | Constraints |
| Unscaled | 5.0E+09 | 5 | 23 | 11 | 2.99 | -9.34 | $x_6(1)$ |
| Method 1 | 4.8E+05 | 4 | 14 | 7 | 0.30 | -9.85 | $P_4$,$x_6(1)$,$Q_{HT}$ |
| Method 2 | 7.0E+09 | 4 | 9 | 3 | 3.49 | -5.84 | $Q_{HT}$ |
| Method 3 | 4.0E+03 | 4 | 28 | 10 | 0.30 | -9.85 | $P_4$,$x_6(1)$,$Q_{HT}$ |
| Method 4 | 5.1E+01 | 4 | 12 | 5 | 0.30 | -9.85 | $P_4$,$x_6(1)$,$Q_{HT}$ |

Table 2.5: Scaling methods applied to flash process

To compare the four scaling methods presented in section 2.3.4 the simulation, data reconciliation and optimization problem is solved for the flash process. The results are summarized in table 2.5.

A valid solution of the data reconciliation and optimization problem are found using scaling method 1, 3 and 4. A common property of these methods is a reduction of the condition number of the constraint first order derivatives, $\widetilde{H}$. The smallest condition number (5.1) is achieved using method 4 which also solves these problems using the fewest number of iterations. The condition number of a model increases with the model size and large models will benefit more from the use of scaling methods that gives a large reduction in condition number.

## 2.6 Discussion

Multiple steady states are not handled by this method. Rather, the scaling is performed at the desired steady-state.

Nonlinear inequality constraints can be added in this framework by introduction of slack variables according to Luenberger (1984). As a simple example we have that $g(x) < c$ is equivalent to $g(x) - v = 0$, $v < c$ where $v$ is a slack variable.

The simplified thermodynamic relations used in the case studies are all explicit functions and have explicit functions for their first order derivatives. For example, specific enthalpy is calculated as $h = C_p x^{\mathrm{T}}$. The specific heat of a component, $C_{pi}$, is a fixed value for the liquid phase and a function of temperature for the vapor phase (sixth order polynomial fitted to data from NIST (2005)). Vapor-liquid equilibrium is based on Raoult's law and Antoine vapor pressure with parameters from the same source.

The described unit model structure is well suited for object oriented programming. A model written in C++ or similar programming language, most commonly used in applications, will be far more effective than the Matlab code used in the examples.

The use of sparse matrices and sparse math in the model and solver code will also give a significant reduction in computational load. In the flash process case study the matrix $H$ has 1521 elements of which only 169 are nonzero.

## 2.7 Conclusions

A procedure for building steady state models has been presented. The procedure is based on unit models which interact through a shared variable vector. The unit models and specifications form an "open equation" set, well suited as nonlinear constrains in an optimization problem. In the suggested structure each unit model can be developed, tested and scaled before it is added to the overall process model. This simplifies the modeling work and saves a lot of troubleshooting.

The scaling procedure, which is applied at unit model level, results in a significant improvement in the overall numerical properties of the model. The numerical examples of the flash process optimization shows that proper scaling reduces the number of iterations used for solving each case. More important though, it makes the results more reliable. In both data reconciliation and optimization, the solver failed in finding the optimal solution when using an unscaled model.

## 2.8 Acknowledgement

The first author acknowledges Statoil Mongstad for the financial support. The authors are grateful to Professor Terje Hertzberg at the Norwegian University of Science and

Technology (NTNU) in Trondheim, for his interest in this work, encouragement and helpful comments. The authors are also grateful to Dr. Stig Strand at the Statoil Research Center in Trondheim for many stimulating discussions and helpful comments.

# Chapter 3

# Data Reconciliation


## Abstract

*Process measurements are contaminated with random and possibly systematic errors. For this reason, they do not obey the conservation laws of the process, like the mass and energy balance. Data reconciliation is a method of optimally adjusting these measurements, such that they obey the conservation laws or process model. The process model is incorporated as a set of equality constraints in an optimization problem where the objective is to minimize the deviation between the measurement and the corresponding variable values in the process model. As a basis for the adjustments or estimation, each process and its measurement should be analyzed. The measurements are classified as redundant or nonredundant, the process model variables as measured or unmeasured, the unmeasured variables as observable or unobservable. The above classification and the computation of the estimate uncertainty give valuable information of the quality of the estimate. If systematic errors also named gross errors are present, they are removed or a robust objective function is used. These methods are applied to a small stream mixing process as an example.*


## 3.1 Introduction

Estimation of the current state of the process is the basis for economical optimization and performance monitoring. The process state is the collection of measured and unmeasured variables describing the mass and energy balance, reactions, vapor-liquid equilibrium and so forth. The constrained estimation problem is in chemical engineering called data reconciliation.

> Data reconciliation is the procedure of optimally adjusting measured data so that the adjusted values obey the conservation laws and other constraints (Crowe, 1996).

In this chapter some of the methods of data reconciliation are evaluated using a small two stream mixing process. The objective is to gain some "hands on" experience, and insight in what is actually gained, by the use of these methods.

Process measurements do not obey the conservation laws (mass and energy balance) due to measurement errors. The measurement errors are caused by measurement noise, process variability due to disturbances and dynamic variance. The conservation laws are given as a process model ($f(z) = 0$) where the variable vector $z$ holds both measured and unmeasured variables.

The reconciled values are the solution of

$$\begin{aligned} \min_{z} \quad & J(y - y_m) \\ \text{s.t.} \quad & f(z) = 0 \end{aligned} \tag{3.1}$$

where $y_m$ are the measured values and $y$ the corresponding values in the variable vector $z$. The objective is to adjust the variables $z$, given the process model $f(z) = 0$, such that the deviation from the measured values are minimized.

In addition to the estimated process state, information describing uncertainty in the estimate, observability of unmeasured values and a measurement redundancy analysis should be present.

The local error in the estimate is calculated using a linearized process model (Britt and Luecke, 1973) and the estimated variables are classified as observable or unobservable (Stanley and Mah, 1981). The measured variables are classified as redundant or nonredundant (Crowe, 1989).

For some measurements the mean of the measurement error is different from zero. In this case the measurement is said to have a systematic error, to be biased or to have a gross error. This error may be due to instrument malfunction, miscalibration or drift, poor sampling or possible a leakage. If some measurements have gross errors, precautions have to be taken to avoid biased measurement adjustments or estimate. Gross errors is detected and identified using statistical tests (Romagnoli and Stephanopoulos, 1981) or by the use of robust objective functions (Johnston and Kramer, 1995; Tjoa and Biegler, 1991; Chen et al., 1998).

This section does not cover the use of dynamic models or multiple data sets.

## 3.2 Example process and model

A process where two process streams are mixed into one process stream is used as an example. A simple example is preferable in order to get an understanding of what is achieved using these methods and their advantages and disadvantages. The process model of the mixing process, shown in figure 3.1, are a simple mass and energy balance.

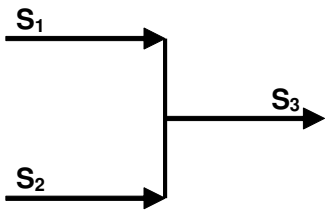


Figure 3.1: Simple mix process

Assuming equal specific heat capacity of the inlet streams the process model (mass and energy balance) can be written as

$$f(\boldsymbol{z}) = \begin{bmatrix} F_1 + F_2 - F_3 \\ F_1T_1 + F_2T_2 - F_3T_3 \end{bmatrix} = 0 \tag{3.2}$$

where the variable vector $\boldsymbol{z} = [F_1\ T_1\ F_2\ T_2\ F_3\ T_3]^{\mathrm{T}}$.

The measured values are the process values with some measurement noise added

$$\boldsymbol{y}_m = U\boldsymbol{z}^* + \omega \tag{3.3}$$

where $z^*$ is a valid solution of the process model, $\omega$ is normal distributed $\mathcal{N}(0, \sigma_\omega)$ measurement noise and $U$ is a measurement mapping matrix. Each measured value is defined by a row in $U$ where $U(i, j) = 1$ defines measurement $i$ as a measurement of variable number $j$.

The variables, values and measurement uncertainty are shown in table 3.1.

| Description | Variable | Unit | $z^*$ | $\sigma_\omega$ |
|---|---|---|---|---|
| Inlet flow 1 | $F_1$ | kg/s | 10 | 0.3 |
| Inlet temperature 1 | $T_1$ | K | 300 | 1.0 |
| Inlet flow 2 | $F_2$ | kg/s | 20 | 0.3 |
| Inlet temperature 2 | $T_2$ | K | 350 | 1.0 |
| Inlet flow 3 | $F_3$ | kg/s | 30 | 0.3 |
| Inlet temperature | $T_3$ | K | 333.3 | 1.0 |

Table 3.1: Variable values and measurement uncertainties.

## 3.3 Data reconciliation

The data reconciliation problem is defined as

$$\begin{aligned} \min_{z} \quad & J(Uz, y_m) \\ \text{s.t.} \quad & f(z) = 0 \\ & Az = b \end{aligned} \tag{3.4}$$

where the objective function $J(Uz, y_m)$ is selected based on the measurement error characteristics. The measured values are collected in the measurement vector $y_m$ and the matrix $U$ is a mapping of the variables $z$ into the measurements $y$ ($y = Uz$). The constraints are the process model equations $f(z) = 0$. If some of the variables are known or unobservable their values must be specified using a set of linear constraints, $Az = b$. For each row in a we have $A(i, j) = 1$ if variable $j$ is to be set equal to the value of $b(i)$, all other elements in row $i$ equals zero.

There are $n_z$ variables in $z$ and $n_y$ measurement values in $y_m$. The dimension of $f(z)$ is $n_f \times 1$, $A$ is $n_s \times n_z$ and $b$ is $n_s \times 1$.

### 3.3.1 Variable classification

Classification of variables gives valuable information about the data reconciliation results. Is the solution to problem 3.4 unique? In case of measurement failure, is the failed measurement redundant? If the failed measurement is removed from the set of measurements, are the unmeasured variables still observable? Answers to these questions are found by the following variable classification.

The variables in $z$ are classified into three groups, measured ($y$), unmeasured ($x$) and known variables ($v$).

The measured variables, corresponding to the measurements in $y_m$, are classified as redundant or non-redundant. The definition of a redundant measurement is stated as

> A measured quantity is redundant if it would be observable if that quantity were not measured. (Crowe, 1989)

The unmeasured variables are classified as observable, barely observable or unobservable where the definition of an observable variables is stated as

> An unmeasured quantity in a steady state process is observable, if it can be uniquely determined from a fixed set of values, corresponding to the measurements, which are consistent with all of the given constraints. Any unmeasured quantity which is not so determinable is unobservable (Crowe, 1989).

It is important to recognize that, if one ore more of the unmeasured variables are unobservable, then the solution $z^*$ of the data reconciliation problem in equation 3.4 is not unique. A barely observable variable is defined by

> An observable unmeasured variable is barely observable if there is a nonredundant measurement whose removal makes the observable variable unobservable (Crowe et al., 1983).

In order to make the above variable classification the process model is linearized around $z^*$ where $z^*$ is a valid solution of the data reconciliation problem in equation 3.4. Since the variable classification is based on a linearized process model the results are valid only locally.

The linearized process model is written as

$$f(z) \approx f(z^*) + H(z - z^*) = 0 \tag{3.5}$$

where $H = \frac{\partial f(z)}{\partial z}\Big|_{z=z^*}$. The linearized process model and the linear constraints in the data reconciliation problem, in equation 3.4, are rewritten in terms of the differential variable $\tilde{z} = z - z^*$

$$H\tilde{z} = -f(z^*) \tag{3.6}$$
$$A\tilde{z} = b - Az^* \tag{3.7}$$

where by definition $f(z^*) = 0$ and $b - Az^* = 0$ given $z^*$ as a solution of equation 3.4. The data reconciliation problem, with linear constraints, is now written in terms of $\tilde{z}$ as

$$\begin{aligned} \min_{\tilde{z}} \quad & J(U\tilde{z}, y_m) \\ \text{s.t.} \quad & H\tilde{z} = 0 \\ & A\tilde{z} = 0 \end{aligned} \tag{3.8}$$

There are two methods for variable classification. The first are from Stanley and Mah (1981) and the second from Crowe et al. (1983). They are both based on linear analysis of the linearized data reconciliation problem in equation 3.8.

Using the results from Stanley and Mah (1981), the observability for unmeasured variables is verified using the first order local observability sufficient condition. That is, if $\text{rank}(\mathbb{D}) = n_z$ then the system is locally observable. The matrix $\mathbb{D}$ is defined as

$$\mathbb{D} = \begin{bmatrix} H \\ A \\ U \end{bmatrix} \tag{3.9}$$

A requirement is that the process model constraints are continuously differentiable close to $z^*$.

Redundancy of a measured value is verified by a similar test where one measurement is removed at a time. A new measurement mapping matrix $U_i$ is created by removal of row $i$ in the measurement matrix $U$ .

$$\mathbb{D}_i = \begin{bmatrix} H \\ A \\ U_i \end{bmatrix} \tag{3.10}$$

Based on the definition in Crowe et al. (1983) the removed measurement is redundant if $\text{rank}(\mathbb{D}_i) = n_z$.

If a nonredundant measurement is removed from $U$ the resulting unobservable variables is said to be barely observable.

Using the results from Crowe et al. (1983) the variables are separated into three groups; measured variables $y$, unmeasured variables $x$ and known or fixed variables $v$. The linearized process model in equation 3.8 is rewritten as

$$H_1\tilde{y} + H_2\tilde{x} + H_3\tilde{v} = 0 \tag{3.11}$$

where $H_1$, $H_2$ and $H_3$ are the columns of $H$ corresponding to the measured, unmeasured and specified variables respectively.

In addition we have from equation 3.8 that $A\tilde{z} = 0$. Since the nonzero elements of $A$ are located in the columns corresponding to the fixed variables $A\tilde{z} = 0 \Leftrightarrow A_3\tilde{v} = 0$. $A_3$ are the columns of $A$ corresponding to the fixed variables. $A_3$ is an $n_v \times n_v$ matrix with full rank and $A_3\tilde{v} = 0 \Rightarrow \tilde{v} = 0$. By insertion of $v = 0$ the fixed variables are removed from the equation. The unmeasured variables are removed by pre-multiplying equation 3.11 by a matrix $Y$, defined such that

$$\tilde{A}_2^{\mathrm{T}} Y = 0 \tag{3.12}$$

The matrix $Y$ spans the null space of $\tilde{A}_2^{\mathrm{T}}$ and pre-multiplication with $Y$ projects the measured variables into the subspace defined by $H_2$. The reduced process model is written as

$$Y^{\mathrm{T}} H_1 \tilde{y} = 0 \tag{3.13}$$

and using $y = Uz$ the linearized data reconciliation problem from equation 3.8 is rewritten in the terms of the measured values only

$$\begin{aligned} &\min_{\tilde{y}} \; J(\tilde{y}, y_m) \\ \text{s.t.} \quad &Y^{\mathrm{T}} H_1 \tilde{y} = 0 \end{aligned} \tag{3.14}$$

Given the solution of equation 3.14, $\tilde{y}^*$ the values of the unmeasured variables $\tilde{x}^*$ are calculated, using $H_1\tilde{y} + H_2\tilde{x} = 0$, as

$$\tilde{x}^* = (H_2^{\mathrm{T}} H_2)^{-1} H_2^{\mathrm{T}} H_1 \tilde{y}^* \tag{3.15}$$

Using equation 3.15 the unmeasured values can be calculated from the values of the measured variables if $H_2^{\mathrm{T}} H_2$ is invertible. That is, the columns of $H_2$ must be independent ($\mathrm{rank(H_2) = n_x}$). If the rows of $H_2$ are dependent, the unobservable variables correspond to the dependent columns, and can be identified by column reduction of $H_2$.

A variable $x_i$ is barely observable if the removal of a nonredundant measurement $y_j$ would make $x_i$ unobservable. Such a variable corresponds to a column of $H_2$ which is linearly independent of other columns of $H_2$ but is dependent of those columns together with the column of $H_1$ corresponding to the nonredundant measurement.

The nonredundant measurements correspond to zero columns of $Y^{\mathrm{T}} H_1$ and do not contribute to the calculation of the unmeasured values. If the weighting matrix $Q$ is diagonal we also have that $y_i^* = y_{m_i}$ for the nonredundant measurements.

As a example, the two methods of variable classification are applied to the stream mix process. In this case there are no fixed values which makes $A$ an empty matrix. The linearized model at $z^* = [10\ 300\ 20\ 350\ 30\ 333]$ is given as

$$H = \begin{bmatrix} 1 & 0 & 1 & 0 & -1 & 0 \\ 300 & 10 & 350 & 20 & -333 & -30 \end{bmatrix} \tag{3.16}$$

Using the first method (Stanley and Mah, 1981) the matrix $\mathbb{D}$ is, in the case where all variables are measured, written as

$$\mathbb{D} = \begin{bmatrix} 1 & 0 & 1 & 0 & -1 & 0 \\ 300 & 10 & 350 & 20 & -333 & -30 \\ 1 & 0 & 0 & 0 & 0 & 0 \\ 0 & 1 & 0 & 0 & 0 & 0 \\ 0 & 0 & 1 & 0 & 0 & 0 \\ 0 & 0 & 0 & 1 & 0 & 0 \\ 0 & 0 & 0 & 0 & 1 & 0 \\ 0 & 0 & 0 & 0 & 0 & 1 \end{bmatrix} \tag{3.17}$$

where the measurement mapping matrix $U = I$ and $I$ is a $6 \times 6$ identity matrix. The columns of $\mathbb{D}$ correspond to the variable vector $\boldsymbol{z} = [F_1\ T_1\ F_2\ T_2\ F_3\ T_3]^{\mathrm{T}}$.

When all six variables are measured they are all observable ($\mathrm{rank}(\mathbb{D}) = 6$) and all measurements are redundant ($\mathrm{rank}(\mathbb{D}_i) = 6$ for $i = 1...6$).

If five process variables are measured, all variables are observable but not all measurements are redundant. Computation of $\mathrm{rank}(\mathbb{D}_i)$, using only five measurements, shows that if one temperature is unmeasured the two remaining temperature measurements are nonredundant. By inspection of $\mathbb{D}$, we see that removal of two rows in $U$ corresponding to two temperature measurements, makes the columns corresponding the

same measurements dependent. With two dependent columns $\text{rank}(\mathbb{D}_i) < n_z$. If one flow is unmeasured all measurements will be redundant, given different inlet temperatures.

If one of the temperatures is unmeasured, the temperatures are defied as "barely observable". According to the definition, removal of one of the temperature measurements which are nonredundant, will make the temperatures unobservable.

If four process variables are measured all variables are observable as long as at least two of the temperatures are measured. There are no redundant measurements in this case and all variables are "barely observable".

The second variable classification method is applied to the stream mix process using five measurements. The measurements are $\boldsymbol{y} = [F_1\ F_2\ T_2\ F_3\ T_3]^{\mathrm{T}}$ and unmeasured variables are $\boldsymbol{x} = T_1$. The matrices $H_1$, $H_2$ are written as

$$H_1 = \begin{bmatrix} 1 & 1 & 0 & -1 & 0 \\ 300 & 350 & 20 & -333 & -30 \end{bmatrix} \qquad H_2 = \begin{bmatrix} 0 \\ 10 \end{bmatrix} \tag{3.18}$$

which gives

$$P^{\mathrm{T}}H_1 = \begin{bmatrix} -1 & -1 & 0 & 1 & 0 \end{bmatrix} \qquad \text{where} \qquad P = \begin{bmatrix} -1 \\ 0 \end{bmatrix} \tag{3.19}$$

The nonredundant measurements,$T_2$ and $T_3$, are identified by the zero columns of $P^{\mathrm{T}}H_1$. The columns (one column only in this case) of $H_2$ are independent and the unmeasured variable $T_1$ is observable. The variables $T_2$ and $T_3$ are "barely observable" since the corresponding columns of $H_1$ are linearly dependent of the column in $H_2$.

### 3.3.2 Error in the estimates

In the case where the measurement errors have a Gaussian distribution with zero mean ($\mathcal{N}(0, \sigma)$) the estimate in 3.14 is obtained by minimization of the negated probability density function. The gaussian probability density function is given as

$$\Phi = \frac{1}{\sigma\sqrt{2\pi}} \exp\left(-\frac{1}{2}\frac{(y - y_m)^2}{\sigma^2}\right) \tag{3.20}$$

The minimization of $J = -\Phi$ has the same solution as the minimization of $J = \log(1/\Phi)$. Using the later, the objective function $J$ reduces to the well known least squares objective function $J = (y - y_m)^2/\sigma^2$. Normally there are more than one measurement and the objective function based on the sum of the probability density functions is written as

$$J = (y - y_m)^{\mathrm{T}}\Sigma^{-1}(y - y_m) \tag{3.21}$$

where $\Sigma(i,i) = \sigma_i^2$. The data reconciliation problem as written in equation 3.14 with a least squares objective function has a known solution. In this case the uncertainty of the estimated values can be calculated analytically.

The propagation of error rule states that if $y = f(x_1, x_2...x_n)$ and the uncertainty of the variables $x_1, x_2...x_n$ are known, described by the standard deviation $\sigma_{x_1}, \sigma_{x_2}, ...\sigma_{x_n}$, then

$$\sigma_y^2 = \left(\frac{\partial f}{\partial x_1}\right)^2 \sigma_{x_1}^2 + \left(\frac{\partial f}{\partial x_2}\right)^2 \sigma_{x_2}^2 + ... + \left(\frac{\partial f}{\partial x_n}\right)^2 \sigma_{x_n}^2 \tag{3.22}$$

In the case where $y = Ax$ and $\Sigma_x$ the covariance matrix of $x$ the propagation of error rule gives $\Sigma_y = A\Sigma_x A^{\mathrm{T}}$.

The least squares objective function is expanded and terms with fixed values are removed (constant values in the objective function do not contribute to the solution). The objective is then multiplied by $\frac{1}{2}$ and finally written as

$$J = \frac{1}{2}\tilde{y}^{\mathrm{T}} Q \tilde{y} + (y^* - y_m) Q \tilde{y} \tag{3.23}$$

where $Q = \sum_m^{-1}$ and the measurement error covariance matrix $\sum_m(i,i) = \sigma_\omega^2(i)$. The known solution of the QP problem with linear equality constraints is written as Luenberger (1984)

$$\tilde{y} = -Q^{-1}\left[I - A^{\mathrm{T}}(AQ^{-1}A^{\mathrm{T}})^{-1}AQ^{-1}\right]Q(y_o - y_m) \tag{3.24}$$

where $A = P^{\mathrm{T}}H_1$. Applying the propagation of error rule and substituting $Q = \Sigma_m^{-1}$, where $\Sigma_m$ is the diagonal measurement covariance matrix, the covariance matrix if the estimation error $\Sigma_y$ is computed as

$$\Sigma_y = \Sigma_m - \Sigma_m A^{\mathrm{T}}(A\Sigma_m A^{\mathrm{T}})^{-1}A\Sigma_m \tag{3.25}$$

When the measured values are known, the values of the unmeasured variables are calculated as

$$\tilde{x} = (A_2^{\mathrm{T}}A_2)^{-1}A_2^{\mathrm{T}}A_1\tilde{y} \tag{3.26}$$

and the covariance matrix of the estimation error is calculated as

$$\Sigma_x = (A_2^{\mathrm{T}}A_2)^{-1}A_2^{\mathrm{T}}A_1\Sigma_y A_1^{\mathrm{T}}A_2(A_2^{\mathrm{T}}A_2)^{-1} \tag{3.27}$$

As an example, the uncertainty of the estimates of the mixing process variables using four, five and six measurements are computed using the method outlined above and the results are shown in table 3.2.

| Description | Variable | $y_t$ | Unit | $\sigma_m$ | $\sigma$ $n_y = 4$ | $\sigma$ $n_y = 5$ | $\sigma$ $n_y = 6$ |
|---|---|---|---|---|---|---|---|
| Inlet flow 1 | $F_1$ | 10 | kg/s | 0.30 | 0.30* | 0.24* | 0.24* |
| Inlet temperature 1 | $T_1$ | 300 | K | 1.0 | 1.0* | 1.0* | 0.97* |
| Inlet flow 2 | $F_2$ | 20 | kg/s | 0.30 | 0.30* | 0.24* | 0.24* |
| Inlet temperature 2 | $T_2$ | 350 | K | 1.0 | 1.0* | 1.0* | 0.85* |
| Inlet flow 3 | $F_3$ | 30 | kg/s | 0.30 | 0.42 | 0.24* | 0.24* |
| Inlet temperature | $T_3$ | 333 | K | 1.0 | 0.83 | 0.83 | 0.63* |
| $\sum \sigma_i$ | | | | 3.9 | 3.85 | 3.55 | 3.17 |

Table 3.2: Uncertainty of the estimated values. (True value $y_t$. Measured variables are marked with an asterisk *)

Using four measurements, there are no redundant measurements and the uncertainty of the estimated measured values $y$ are equal to the uncertainty of the measurements. An observation is that the uncertainty of the reconciled outlet temperature is less than the uncertainty of the measurement value.

The uncertainty in the estimates are further reduced when using five and six measurements. The "interaction" between the mass and energy balance is in this case less than expected. The addition of a temperature measurement gives a significant reduction of the uncertainty in the estimate of temperatures but close to zero reduction of the uncertainty estimates of the flows. Similar with the addition of a flow measurement, the uncertainty of the flow estimates is reduced but this gives only an insignificant reduction in the error of the temperature estimates.

### 3.3.3 Gross error detection

If the mean value of the measurement error is different from zero a systematic error, also named a gross error, is present. The estimate using data reconciliation will be biased due to the gross error. There are several methods dealing with this problem where one solution is to detect and remove the measurements containing the gross error. The estimate is then computed based on the remaining measurements. The variable, corresponding to the biased measurement, which is currently defined as a measured value is redefined as an unmeasured value. A second method is to use an objective function less sensitive to large errors. The estimate computed using these robust functions will still result in a biased estimate but the bias will be reduced. The use of robust objective functions is described in section 3.4.

The first method for gross error detection (Crowe et al., 1983) uses a statistical test which detects the presence of a gross error. When the gross error detection test is true the measurement containing the gross error is identified using a second test.

The imbalance in the model equations, due to measurement error, is written in terms of the measured values as

$$\delta = Y^{\mathrm{T}} B_1(\tilde{y} + \omega) = Y^{\mathrm{T}} B_1 \omega \tag{3.28}$$

where $\tilde{y}$ is the vector with the measured variables and the measurement error $\omega = y_m - \tilde{y} - y^*$ . The estimate of the measured variables obeys the model equations and we have that $Y^{\mathrm{T}} B_1 \tilde{y} = 0$. The covariance matrix of the imbalance in the model equations, due to measurement error, is written as

$$\Sigma_\delta = Y^{\mathrm{T}} B_1 \Sigma_m B_1^{\mathrm{T}} Y \tag{3.29}$$

A gross error test function based on this imbalance is defined (Romagnoli and Stephanopoulos, 1981)

$$h = \delta^{\mathrm{T}} \Sigma_\delta \delta \tag{3.30}$$

which is $\chi^2(k)$ distributed with $k = \mathrm{rank}(Y)$ degrees of freedom. The gross error detection test is defined by

$$h > \chi^2_{(1-\alpha)}(k) \tag{3.31}$$

If the condition above is true a gross error is present with the probability of $\alpha$.

The measurement containing a gross error is identified as the measurement with the largest contribution to the objective function (Crowe et al., 1983). For each measurement $(y_m - y)/\sigma$ is calculated and the largest absolute value identifies the measurement containing a gross error.

| | $y_t$ | $y_m$ $\mu = 0$ | $y$ $\mu = 0$ | $y$ $\mu_{F_1} = 2$ | $y$ $\mu_{T_1} = 10$ | $y$ $\mu_{F_3} = 2$ | $y$ $\mu_{T_3} = 10$ |
|---|---|---|---|---|---|---|---|
| $F_1$ | 10.0 | 9.7 | 9.9 | 11.2* | 10.0 | 10.6 | 9.4 |
| $T_1$ | 300.0 | 300.6 | 300.2 | 300.5 | 309.5* | 300.2 | 302.0 |
| $F_2$ | 20.0 | 20.2 | 20.2 | 19.6 | 20.1 | 20.9 | 20.6 |
| $T_2$ | 350.0 | 351.7 | 350.8 | 351.5 | 349.4 | 350.9 | 354.8 |
| $F_3$ | 30.0 | 30.2 | 30.1 | 30.7 | 30.1 | 31.4* | 30.0 |
| $T_3$ | 333.3 | 332.7 | 334.1 | 333.0 | 336.1 | 333.9 | 338.2* |
| h | | | 3.6 | 10.5 | 19.5 | 22.4 | 34.8 |

Table 3.3: Gross error detection. The true value $y_t$, measured value $y_m$ and estimated value $y$ (Gross error is present if $h > 4.6$ and identified gross errors are marked with an asterisk *)

In order to verify this gross error detection test, gross errors are added sequentially to the following measured values, $F_1$, $T_1$, $F_3$ and $T_3$. The results are shown in table 3.3.

In this case the $\mathrm{rank}(P) = 2$ and the cumulative $\chi^2(2)$ distribution is shown in figure 3.2. The probability of a gross error $\alpha = 0.1$. The $\chi^2$ cumulative distribution where $\chi^2_{(0.9)}(2)$ gives $h > 4.6$ as the threshold for the gross error detection test.

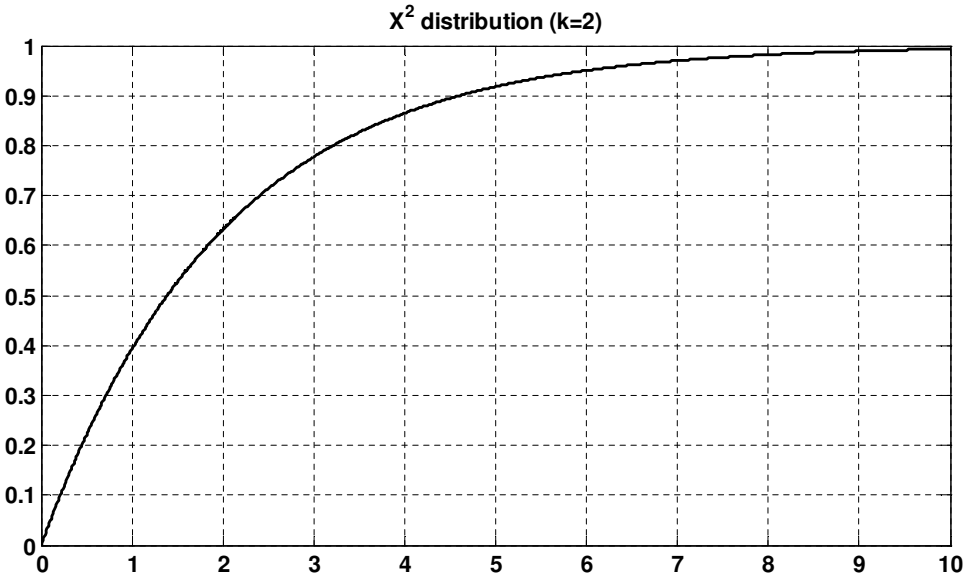


Figure 3.2: $\chi^2$ cumulative distribution

As shown in table 3.3 all four gross errors are correctly detected and the measurement containing the gross errors are identified. The final estimate is computed using the remaining measurements.

## 3.4 Data reconciliation using data containing gross errors

In the presence of gross errors the estimate of the process states is biased using the least squares objective function in the data reconciliation. This bias may be reduced using an objective function less sensitive to large errors. In this case the measurements containing a gross error are not removed prior to solving the data reconciliation problem. As a compensation, an objective function less sensitive to gross errors is applied in the data reconciliation.

The error sensitivity is described by the influence function $IF = \partial J/\partial e$ where $J$ is the objective function and $e$ the measurement error $e = (y_m - y)$. In the case of the quadratic objective function ,$J = (y_m - y)^{\mathrm{T}} Q(y_m - y)$, the influence function $IF = 2Q(y_m - y)$ increases linearly with the size of the error. In presence of gross error this objective function is not robust and its ability to ignore the contribution of extreme data is poor.

In the following sections some of the objective functions less sensitive to gross errors are evaluated. These are the contaminated Gaussian function, Fair function and the Lorentzian or Cauchy function. The Gaussian distribution is used for reference only.

### 3.4.1 Gaussian distribution

The quadratic objective function is derived from the assumption of normal distributed measurement errors with zero mean $\mu = 0$ and variance $\sigma^2$.

The probability density function of the Gaussian distribution of a single measurement error $e \sim \mathcal{N}(0, \sigma)$ is written

$$p_G(e) = \frac{1}{\sigma\sqrt{2\pi}} \exp\left(-\frac{1}{2}\frac{e^2}{\sigma^2}\right) \tag{3.32}$$

The maximum likelihood estimate is obtained by maximizing

$$p_G(e_1, e_2, ..., e_{n_y}|\mu_i, \sigma_i) = \prod_{i=1}^{n_y} \frac{1}{\sigma_i\sqrt{2\pi}} \exp\left(-\frac{1}{2}\frac{e_i^2}{\sigma_i^2}\right) \tag{3.33}$$

subject to the process model equality constraints. Minimization of the log reciprocal of the likelihood function yields the same minima and simplifies the computation of the estimates

$$\psi_G(e) = \ln\left(\frac{1}{p_G(e)}\right) = \sum_{i=1}^{n_y} \frac{1}{2}\frac{e_i^2}{\sigma_i^2} - \sum_{i=1}^{n_y} \ln(\sigma_i) - n_y \ln(\sqrt{2\pi}) \tag{3.34}$$

Fixed value terms have no influence on the solution and are removed from the data reconciliation objective function

$$J_G = \sum_{i=1}^{n_y} \frac{e_i^2}{\sigma_i^2} \tag{3.35}$$

The objective function can also be written as $J_G = e^{\mathrm{T}}Qe$ where the weighting matrix $Q$ is diagonal with $Q(i,i) = \sum_m^{-1} = 1/\sigma_i^2$.

The error sensitivity or influence function is given as

$$IF_G = \frac{\partial J_G}{\partial e} = 2\sum_{i=1}^{n_y} \frac{e_i}{\sigma_i^2} = 2Qe \tag{3.36}$$

The objective and influence function are shown in figure 3.3. The influence function is unbounded for large errors.

### 3.4.2 Combined Gaussian distribution

In presence of gross errors a linear combination of two normal distribution functions, based on their likelihood, is used (Tjoa and Biegler, 1991). With the probability of a

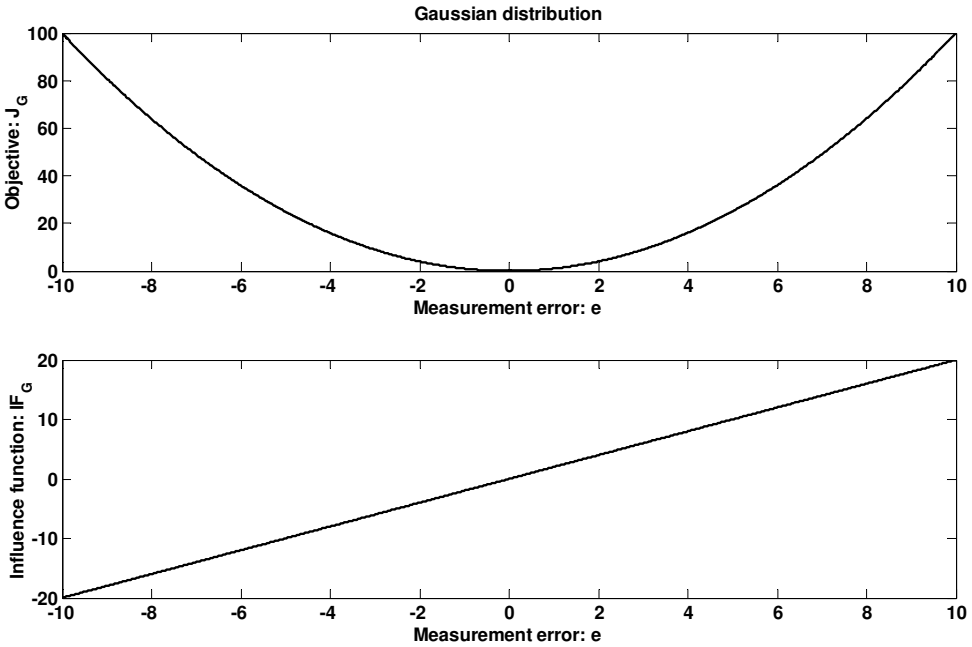


Figure 3.3: Objective function and influence function.

gross error in the measurements $p$ ($p < 0.5$) and the ratio of the standard deviations of the gross errors to that of the random errors is $b$ ($b > 1$), then the frequency function for the combined Gaussian distribution of a single measurement error is written

$$p_{CG}(e) = \frac{1}{\sigma\sqrt{2\pi}}\left[(1-p)\exp\left(-\frac{1}{2}\frac{e^2}{\sigma^2}\right) + \frac{p}{b}\exp\left(-\frac{1}{2}\frac{e^2}{\sigma^2 b^2}\right)\right] \tag{3.37}$$

In figure 3.4 we can see that the probability of a measurement error in the range of $2 - 8 \times \sigma$ has increased, compared with the Gaussian distribution. This makes the estimates less sensitive to large errors in this area. The maximum likelihood estimate is obtained by maximizing

$$p_{CG}(e_1, e_2, ..., e_{n_y}|\mu_i, \sigma_i) = \prod_{i=1}^{n_y} \frac{1}{\sigma_i\sqrt{2\pi}}\left[(1-p)\exp\left(-\frac{1}{2}\frac{e_i^2}{\sigma_i^2}\right) + \frac{p}{b}\exp\left(-\frac{1}{2}\frac{e_i^2}{\sigma_i^2 b^2}\right)\right] \tag{3.38}$$

subject to the process model equality constraints. Minimization of the log reciprocal of the likelihood function yields the same minima and simplifies the computation of the estimates. The resulting objective function is written as

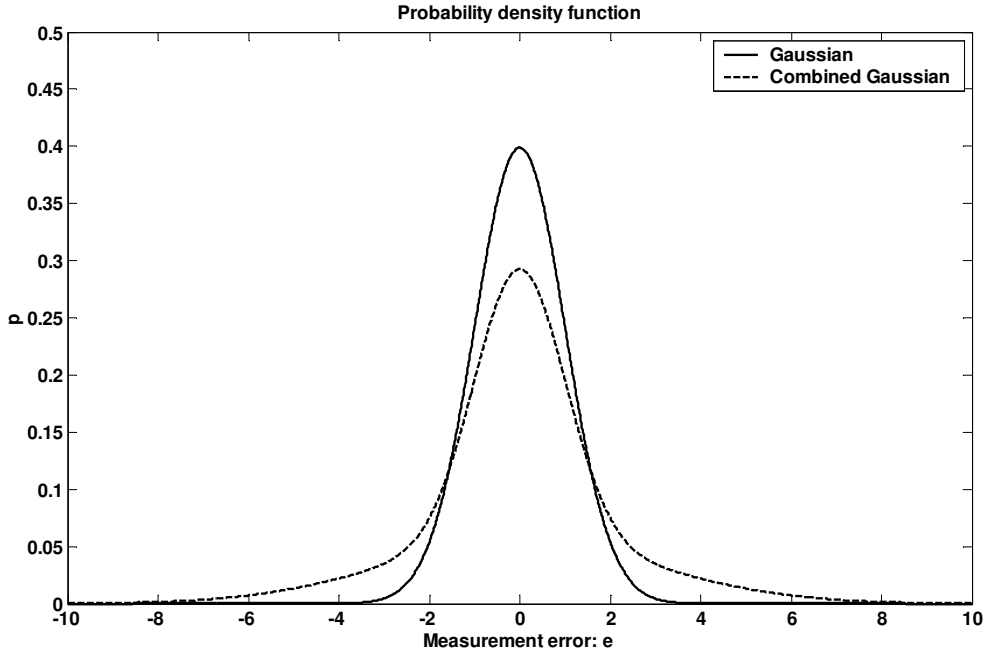


Figure 3.4: Gassian and combined Gaussian frequency function. The standard deviation $\sigma = 1$, probability for an outlier $p = 0.4$ and ratio of the standard deviations $b = 3$.

$$J_{CG}(e) = \ln\left(\frac{1}{p_{CG}}\right) = -\sum_{i=1}^{n_y} \ln\left[(1-p)\exp\left(-\frac{1}{2}\frac{e^2}{\sigma^2}\right) + \frac{p}{b}\exp\left(-\frac{1}{2}\frac{e^2}{\sigma^2 b^2}\right)\right] \quad (3.39)$$

The influence function $\partial J_{CG}/\partial e$

$$IF_{CG}(e) = \frac{\partial J_{CG}}{\partial e} = \frac{e}{\sigma^2}\left[1 + \frac{1}{b^2}\frac{p(b^2-1)\exp(\frac{e^2}{2\sigma^2})}{b(p-1)\exp(\frac{e^2}{2b^2\sigma^2}) - p\exp(\frac{e^2}{2\sigma^2})}\right] \quad (3.40)$$

Figure 3.5 and 3.6 show the objective function and the influence function for a single measurement with different values of $p$ and $b$. In figure 3.5 we can see how an increase in the standard deviation ratio gives a reduction in the influence function for large errors.

In figure 3.5 we can see how an increase in the probability $p$ for a gross error reduces the penalty for a large error. The sensitivity to large errors is almost unchanged.

Each measurement error can be tested against the combined distribution. If the probability associated with an error is greater than the probability of a random error, then the measurement error is identified as a gross error. The distribution function may be used as a rational gross error detection test. That is, if

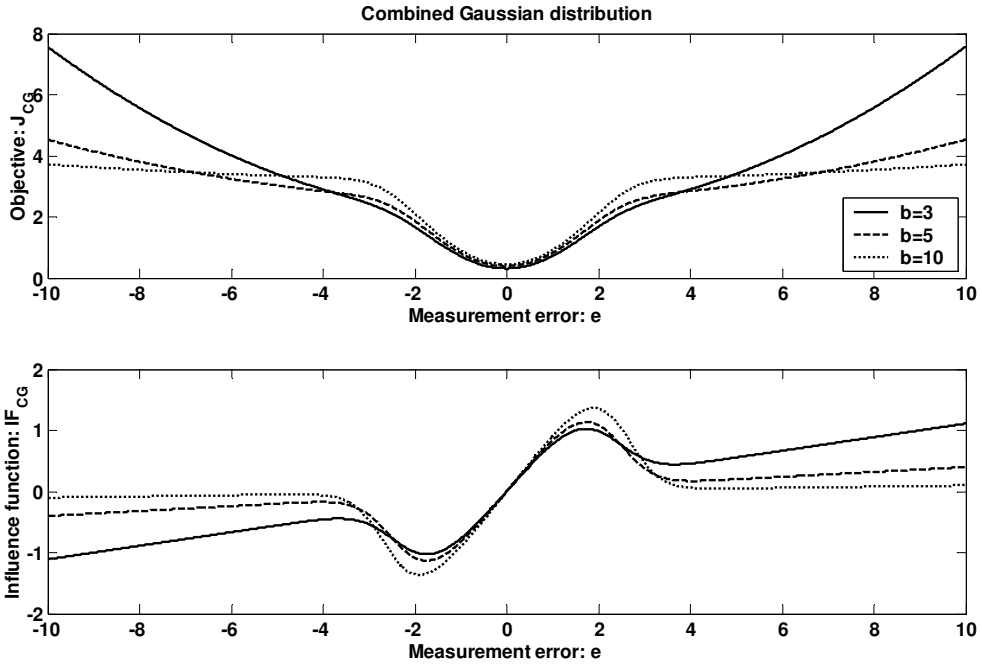


Figure 3.5: Combined Gaussian frequency function with different values of $b$. $\sigma = 1$ and $p = 0.4$.

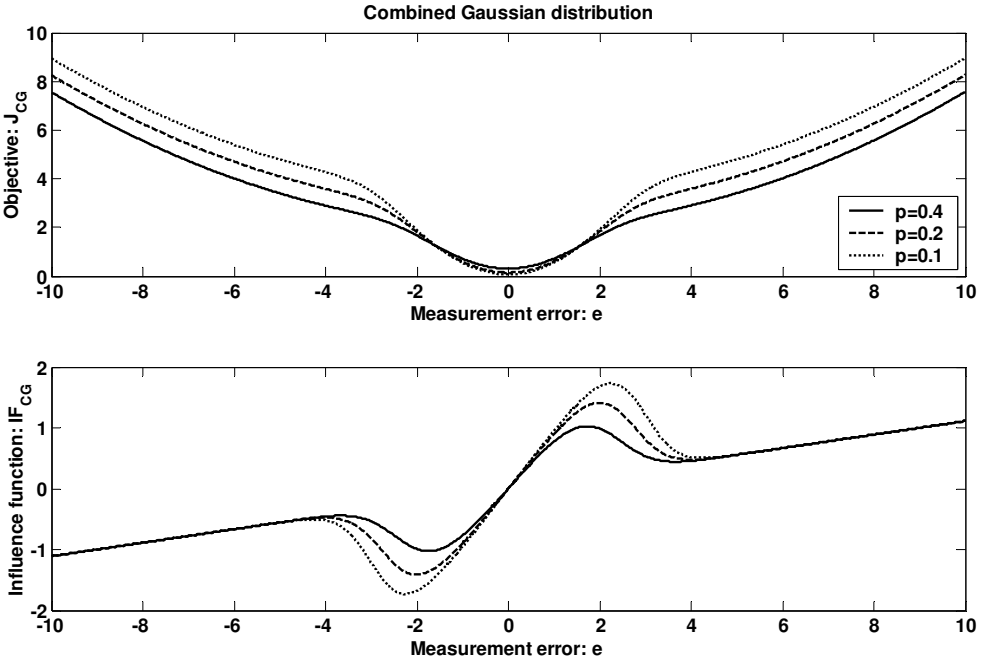


Figure 3.6: Combined Gaussian frequency function with different values of $p$. $\sigma = 1$ and $b = 3$.

$$\frac{p}{b}\exp\left(-\frac{1}{2}\frac{e^2}{\sigma_i^2 b^2}\right) > (1-p)\exp\left(-\frac{1}{2}\frac{e^2}{\sigma_i^2}\right) \tag{3.41}$$

or if

$$\mid e_i \mid > \sigma_i\sqrt{\frac{2b^2}{b^2-1}\ln\left(\frac{b(1-p)}{p}\right)} \tag{3.42}$$

a gross error in measurement $i$ is present.

### 3.4.3 Cauchy distribution

The probability density function of the Cauchy distribution, also called the Lorentzian distribution or Lorentz distribution, is written as

$$p_C(e) = \frac{1}{\pi\gamma\left[1+\frac{e^2}{\gamma^2}\right]} \tag{3.43}$$

where $\gamma$ is a "half width at half maximum" parameter. An objective function, corresponding to the maximum likelihood estimate, is obtained from the log reciprocal of $p_C(e_1, e_2, ..., e_{ny})$ where

$$\grave{J}_C = n_y \ln(\pi\gamma_i) + \sum_{i=1}^{n_y}\ln\left(1+\frac{e_i^2}{\gamma_i^2}\right) \tag{3.44}$$

removing fixed value terms and selecting $\gamma_i = \sigma_i$

$$J_C = \sum_{i=1}^{n_y}\ln\left(1+\frac{e_i^2}{\sigma_i^2}\right) \tag{3.45}$$

The influence function of the Cauchy distribution $IF_C$ is written as

$$IF_C = \frac{\partial J_C}{\partial e} = \frac{2}{\sigma^2}\frac{e}{\left(1+\frac{(e)^2}{\sigma^2}\right)} \tag{3.46}$$

The influence function, using the Cauchy distribution approaches zero for large values of $e$ .

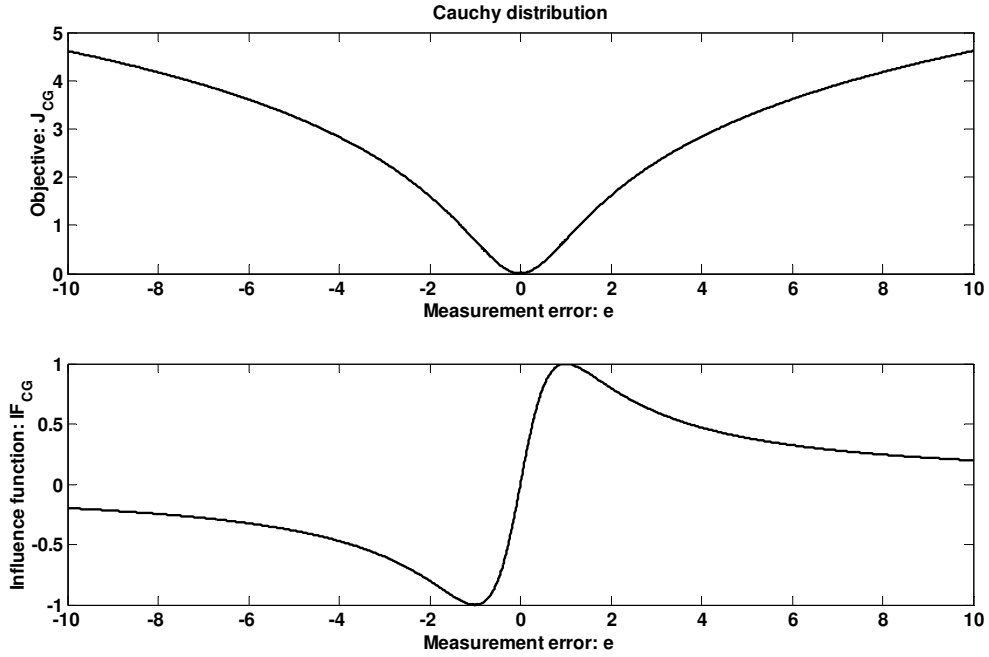


Figure 3.7: Cauchy function and influence function

### 3.4.4 The Fair function

The Fair function for a single measurement error is given as (Özyurt and Pike, 2004)

$$\psi_F = c^2 \left[ \frac{|\ e\ |}{c\sigma} - \ln\left(1 + \frac{|\ e\ |}{c\sigma}\right)\right] \tag{3.47}$$

where $c$ is a tuning parameter. In data reconciliation the sum of the Fair function of each measurement is used as the objective function

$$J_F = c^2 \left[ \frac{|\ e_i\ |}{c\sigma_i} - \ln\left(1 + \frac{|\ e_i\ |}{c\sigma_i}\right)\right] \tag{3.48}$$

The influence function is written as

$$IF_F = \frac{\partial J_F}{\partial e} = \text{sign}(e_i)\frac{1}{\sigma}\left(c - \frac{c^2}{\frac{|e_i|}{\sigma} + c}\right) \tag{3.49}$$

The Fair function and its influence function is shown in figure 3.8. The influence function of large values is bounded by the tuning parameter $c$ such that $-c < IF_F(e) < c$. This gives a close to linear penalty on large errors.

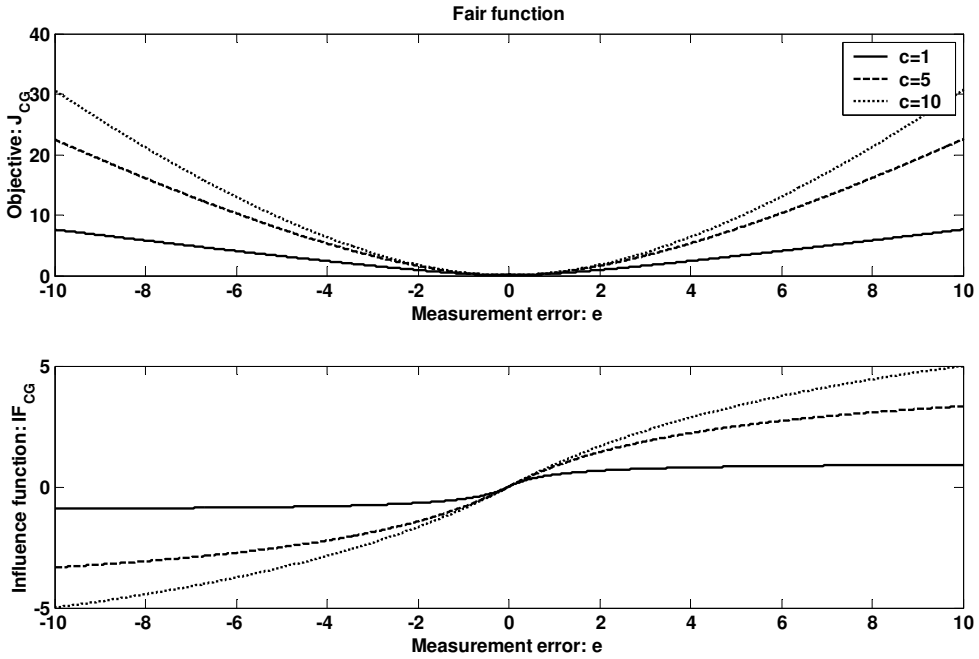


Figure 3.8: Fair function and influence function with different values of $c$

### 3.4.5 Case study

The objective functions described above are applied to the stream mixing process. The objective is to compare the effects of gross errors added to the measured values. Figure 3.9 shows the value of the objective functions and the influence functions in the range $-20 < e < 20$ with the measurement error standard deviation $\sigma = 1$.

In order to compare the behavior of the objective functions the measurement error is separated into three ranges; $|e| < 1$, $1 < |e| < 5$ and $5 < |e| < 10$. The tuning parameters are $p = 0.4$, $b = 3$ and $c = 1$. In the range of $|e| < 1$, the Combined Gaussian, Cauchy and Fair function have similar behavior, by a scale factor, and are in this range similar to the gaussian function (see figure 3.9). In the error range of $1 < |e| < 5$ the Combined Gaussian and the Cauchy function have similar behavior and the Fair function has a lower "penalty". In the range of $5 < |e| < 10$ the Combined Gaussian and Fair function have similar behavior and the Cauchy function has a lower "penalty".

The data reconciliation problem is solved using the Gaussian, Combined Gaussian, Cauchy and Fair objective functions when a gross error is sequentially added to the variables $F_1$, $T_1$, $F_3$ and $T_3$. The gross error detection method, as described in section 3.3.3 is also applied to this example for comparison.

The results are shown in the tables 3.4 to 3.7. The columns contain the results for each method where the subscripts identify the methods as follows

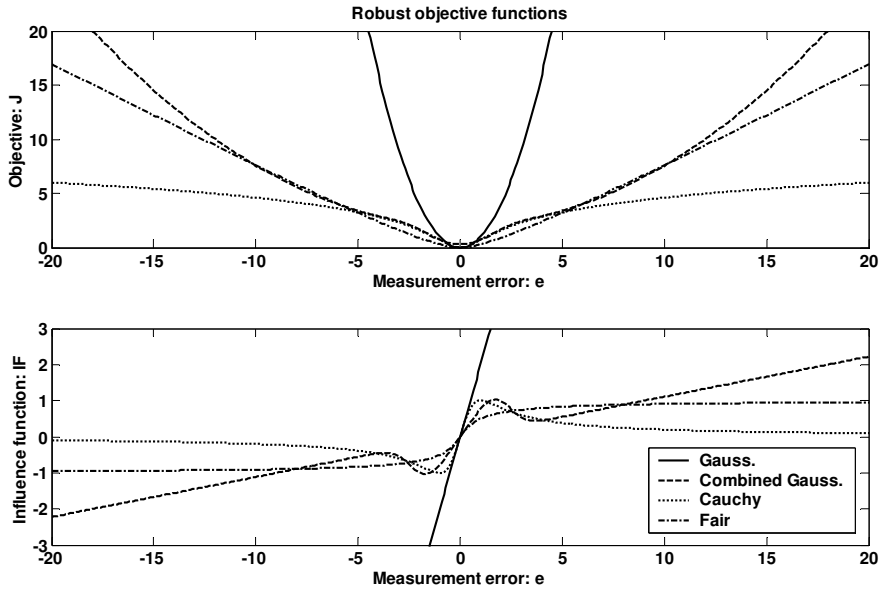


Figure 3.9: Gaussian, Combined Gaussian, Cauchy and Fair objective functions

- **GED**: Gross error detection, identification and removal of measurement containing gross error. Finally, data reconciliation using a Gaussian objective function as described in section 3.4.1. (The parameters p=0.1, b=12)
- **G**: Data reconciliation using a Gaussian objective function with no removal of gross errors.
- **CG**: Data reconciliation using a Combined Gaussian objective function
- **C**: Data reconciliation using the Cauchy function
- **F**: Data reconciliation using the Fair function

The estimation error is computed as the absolute value of the difference between the estimate and the true value. The overall estimation error is computed as the sum of all individual estimation errors.

Table 3.4 shows the results where a gross error ($\mu_{F_1} = 2$) is added to the variable $F_1$. The GED method has the best performance followed by the G method. An observation is that the G method performs better than the CG, C and F methods in this case.

Table 3.5 shows the results where a gross error ($\mu_{T_1} = 10$) is added to the variable $T_1$. In this case the CG method has the best performance and the C method a close number two. The G and F methods has significantly poorer performance. The CG and C methods have an estimation error of $T_1 \approx 5$ but the C and F methods have an estimation error of $T_1 \approx 10$. That is, they both fail to reduce the gross error.

| | True value | $y_m$ $\mu_{F_1} = 2$ | $y_{GED}$ | $y_G$ | $y_{CG}$ | $y_C$ | $y_F$ |
|---|---|---|---|---|---|---|---|
| $F_1$ | 10.0 | 11.7 | 10.3 | 11.2 | 11.7 | 11.7 | 11.2 |
| $T_1$ | 300.0 | 300.6 | 300.3 | 300.5 | 300.6 | 300.6 | 300.5 |
| $F_2$ | 20.0 | 20.2 | 20.0 | 19.6 | 20.1 | 20.1 | 19.5 |
| $T_2$ | 350.0 | 351.7 | 351.0 | 351.5 | 351.6 | 351.6 | 351.6 |
| $F_3$ | 30.0 | 30.2 | 30.3 | 30.7 | 31.8 | 31.7 | 30.7 |
| $T_3$ | 333.3 | 332.7 | 333.8 | 333.0 | 332.8 | 332.9 | 332.9 |
| $\sum \lvert y_t - y \rvert$ | | | 2.24 | 4.69 | 6.31 | 6.11 | 5.04 |

Table 3.4: Data reconciliation of mixing process where a Gross Error is added to the measured inlet flow $F_1$. ($\mu_{F_1} = 2$)

| | True value | $y_m$ $\mu_{T_1} = 10$ | $y_{GED}$ | $y_G$ | $y_{CG}$ | $y_C$ | $y_F$ |
|---|---|---|---|---|---|---|---|
| $F_1$ | 10.0 | 9.7 | 9.8 | 10.0 | 9.8 | 9.8 | 9.9 |
| $T_1$ | 300.0 | 310.6 | 293.4 | 309.5 | 295.1 | 294.4 | 310.2 |
| $F_2$ | 20.0 | 20.2 | 20.3 | 20.1 | 20.2 | 20.2 | 20.2 |
| $T_2$ | 350.0 | 351.7 | 351.7 | 349.4 | 351.5 | 351.6 | 350.5 |
| $F_3$ | 30.0 | 30.2 | 30.1 | 30.1 | 30.1 | 30.1 | 30.1 |
| $T_3$ | 333.3 | 332.7 | 332.7 | 336.1 | 333.0 | 332.9 | 337.2 |
| $\sum \lvert y_t - y \rvert$ | | | 9.43 | 13.06 | 7.17 | 8.05 | 14.97 |

Table 3.5: Data reconciliation of mixing process where a Gross Error is added to the measured inlet flow $T_1$. ($\mu_{T_1} = 10$)

| | True value | $y_m$ $\mu_{F_3} = 2$ | $y_{GED}$ | $y_G$ | $y_{CG}$ | $y_C$ | $y_F$ |
|---|---|---|---|---|---|---|---|
| $F_1$ | 10.0 | 9.7 | 9.8 | 10.6 | 9.8 | 9.8 | 11.0 |
| $T_1$ | 300.0 | 300.6 | 300.1 | 300.2 | 300.4 | 300.5 | 300.4 |
| $F_2$ | 20.0 | 20.2 | 20.1 | 20.9 | 18.2 | 20.2 | 20.6 |
| $T_2$ | 350.0 | 351.7 | 350.7 | 350.9 | 351.2 | 351.4 | 351.3 |
| $F_3$ | 30.0 | 32.2 | 29.9 | 31.4 | 28.0 | 30.0 | 31.6 |
| $T_3$ | 333.3 | 332.7 | 334.1 | 333.9 | 333.4 | 334.8 | 333.6 |
| $\sum \lvert y_t - y \rvert$ | | | 1.98 | 4.50 | 5.57 | 3.77 | 5.06 |

Table 3.6: Data reconciliation of mixing process where a Gross Error is added to the measured inlet flow $F_3$. ($\mu_{F_3} = 2$)

Table 3.6 shows the results where a gross error ($\mu_{F_3} = 2$) is added to the variable $F_3$. The GED method has again the best performance with the C method as number two. The G, CG and F methods has similar performance and all fails to significantly reduce the gross error in $F_3$. Also in this case the G method has surprisingly good performance.

| | True value | $y_m$ $\mu_{T_3} = 10$ | $y_{GED}$ | $y_G$ | $y_{CG}$ | $y_C$ | $y_F$ |
|---|---|---|---|---|---|---|---|
| $F_1$ | 10.0 | 9.7 | 9.8 | 9.4 | 9.8 | 9.8 | 9.7 |
| $T_1$ | 300.0 | 300.6 | 300.6 | 302.0 | 300.6 | 300.7 | 301.0 |
| $F_2$ | 20.0 | 20.2 | 20.3 | 20.6 | 20.3 | 20.3 | 20.4 |
| $T_2$ | 350.0 | 351.7 | 351.7 | 354.8 | 351.7 | 351.8 | 353.1 |
| $F_3$ | 30.0 | 30.2 | 30.1 | 30.0 | 30.1 | 30.1 | 30.1 |
| $T_3$ | 333.3 | 342.7 | 335.0 | 338.2 | 335.1 | 335.1 | 336.3 |
| $\sum \lvert y_t - y \rvert$ | | | 4.53 | 12.85 | 4.63 | 4.79 | 7.83 |

Table 3.7: Data reconciliation of mixing process where a Gross Error is added to the measured inlet flow $T_3$. ($\mu_{T_3} = 10$)

Table 3.7 shows the results where a gross error ($\mu_{T_3} = 10$) is added to the variable $T_3$. In this case the GED, CG and C methods have similar and good performance. The G and F methods have less reduction in the estimation error of $T_3$ and in this case the G method has significantly poorer performance.

## 3.5 Conclusion

The application of methods for measurement redundancy analysis, observability analysis and uncertainties of the estimates gives valuable understanding of the process and its measurements. It also levels the expectations of what can be achieved by the use of data reconciliation methods.

If only random measurement errors are present the least squares objective function, based on a Gaussian error distribution, results in a maximum likelihood estimate of the process state. The standard deviation of the measured values can be based on data from the instrument installed or general guidelines regarding measurement uncertainty. It may also be possible to estimate from the measured values (Keller et al., 1992).

When systematic or gross errors are present, the data reconciliation problem is more challenging. The simple evaluation in section 3.4 does not give a clear indication of which method or objective function to select. The preferred method is dependent of its numerical properties and the error characteristics. The gross error detection method with measurement removal is a sequential method where one measurement is removed as long as a gross error is detected. For each iteration, the data reconciliation problem has to be solved. The Cauchy function has good performance but has poor numerical properties. The influence function approaches zero for large values of $e$

and the probability of converging to a local minimum is high, compared to the other methods. The Gauss, Combined Gaussian and Fair function are all numerically robust and the Combined Gaussian gives the overall best performance.

The method selected will also depend on the problem to be solved. If data reconciliation is used to fit a model to some plant data, it may be solved only a few times and the numerical robustness and required computational time is not that important. If data reconciliation is part of an on-line application, the same problem may be solved thousands of times. The results may be used with no human interaction and the requirements for numerical robustness and computational load will be higher. In an on-line application measurement maintenance will also be an important part of the handling of gross errors. If a gross error is detected, the first actions should be verification and maintenance of the instrument in question.

Based on the above the Combined Gaussian method is used in the data reconciliation problems in this thesis. The Combined Gaussian is not a clear "winner" but has stable performance and good numerical properties.

# Chapter 4

# Data reconciliation and optimal operation of a catalytic naphtha reformer

*Submitted to Journal of Process Control*
*Authors: Tore Lid and Sigurd Skogestad*

## Abstract

*The naphtha reforming process converts low-octane gasoline blending components to high-octane components for use in high-performance gasoline fuels. The reformer also has an important function as the producer of hydrogen to the refinery hydrotreaters. There are large seasonal variations in the reformer product price and two operational cases are studied. In case 1, the product price is high and throughput is maximized with respect to process and product quality constraints. In case 2, the product price is low and the throughput is minimized with respect to a low constraint on the hydrogen production. A process model based on a unit model structure, is used for estimation of the process condition using data reconciliation. Measurements are classified as redundant or nonredundant and the model variables are classified as observable, barely observable or unobservable. The computed uncertainty of the measured and unmeasured variables shows that even if a variable is observable it may have a very large uncertainty and may thereby be practically unobservable. The process condition at 21 data points, sampled from two years of operation, is estimated and operation is optimized. Based on the characteristics of the optimal operation a "self optimizing" control structure is suggested for each of the two operational cases.*

## 4.1 Introduction

The naphtha reforming process converts low-octane gasoline blending components to high-octane components for use in high-performance gasoline fuels. "Octane" or, more precisely the octane number, is the measure or rating of the gasoline fuels antiknock properties. "Knocking" occurs in an engine when the fuel self detonates due to high pressure and temperature before it is ignited by the engine spark. Permanent damage of the engine cylinder and piston parts is a likely result of persistent "knocking". The most common measure of the octane number is the RON (Research Octane Number). By definition iso-octane (2,2,4 trimethyl pentane) is given an octane number (RON) of 100 and n-heptane an octane number of 0. A fuel with 95 RON has, by use of this measure, equal anti knock properties to a mixture of 95% of iso-octane and 5% n-heptane.

A simplified process model of a semiregenerative catalytic naphtha reformer, involving five pseudo components, was presented by Smith (1959) and validated against plant data. The same model was used in Bommannan et al. (1989), where reaction parameters were estimated from two sets of plant data, and in Lee et al. (1997) where a process with continuous catalyst regeneration was modeled. In all three cases above, good agreement with plant data was reported. These models are used for simulation and design purposes except in Taskar and Riggs (1997) where optimal operation during a catalyst cycle, is considered. Taskar and Riggs (1997) developed a more detailed model of a semiregenerative catalytic naphtha reformer, involving 35 pseudo components. They claimed that the simplified model is an oversimplification of the process but no details of the practical consequences of the discrepancies where presented.

In this paper the simplified model of Smith (1959) is used for modeling a catalytic naphtha reformer with continuous catalyst regeneration. The model uses the unit model structure of Lid and Skogestad (2007). Scaling is applied to the process model variables and equations to improve its numerical properties. The process model is compared to 21 data sets from the naphtha reformer at the Statoil Mongstad refinery. These data where collected in a two year period and include feed and product analysis and process measurements. The current state of the process is estimated using data reconciliation (Tjoa and Biegler, 1991), where redundancy of measurements, observability of variables and uncertainty of the estimate are examined. The same model is also used for computation of optimal operation and economical analysis of operational cases. Based on this analysis, a model predictive control (MPC) structure for "optimal" operation of the process is suggested.

## 4.2 Data reconciliation

Data reconciliation is used to estimate the actual condition of the process and is obtained as the solution of

$$\begin{aligned} \min_{z} \quad & J(y_m, z) \\ \text{s.t.} \quad & f(z) = 0 \\ & A_r z = b_r \\ & z_{r\,\min} \leq z \leq z_{r\,\max} \end{aligned} \tag{4.1}$$

where $J(y_m, z)$ is the objective function for data reconciliation. The $n_y$ measured values are collected in the measurement vector $y_m$.

If the measurement error is normally distributed $\mathcal{N}(\mu, \sigma)$ and a zero mean measurement error ($\mu = 0$) is assumed the maximum likelihood estimate is achieved using a quadratic objective function $J_G = (y_m - Uz)^{\mathrm{T}} Q (y_m - Uz)$. The weighting matrix $Q$ is set equal to the inverse of the measurement error covariance matrix $\Sigma_m$ where $\Sigma_m(i,i) = \sigma(i)^2$ (Crowe et al., 1983).

The matrix $U$ gives a mapping of the variables $z$ into the measurements where $y = Uz$ represents the estimated values of the measurements $y_m$. The matrix $U$ has $n_y$ rows and in each row one nonzero value, equal to one, in element $U(i,j)$ where variable $j$ corresponds to measurement $i$ in the measurement vector $y_m$.

If the measurement error is normally distributed $\mathcal{N}(\mu, \sigma)$ with mean $\mu$ and variance $\sigma^2$ the quadratic objective function will result in a biased estimate. In data reconciliation, a mean measurement error $\mu \neq 0$, is called a gross error.

The bivariate distribution from Tjoa and Biegler (1991) describes both gross and random errors using two parameters, $p$ and $b$. The frequency function of measurement $i$ is written as

$$\varphi_i = \frac{1}{\sigma_i \sqrt{2\pi}} \left[ (1-p) \exp\left( -\frac{1}{2} \frac{(y_m(i) - U(i)z)^2}{\sigma_i^2} \right) + \frac{p}{b} \exp\left( -\frac{1}{2} \frac{(y_m(i) - U(i)z)^2}{\sigma_i^2 b^2} \right) \right] \tag{4.2}$$

where $U(i)$ is row number $i$ of the measurement matrix $U$. The parameter $p$ describes the probability of a gross error in a measurement $p < 0.5$ and the parameter $b$ the ratio of the standard deviation of a gross error to that of the random error $b > 1$.

In figure 4.1 we can see that the probability of a measurement error in the range of $2 - 8 \times \sigma$ has increased. This makes the objective less sensitive to large errors. We define $\psi$ as the log reciprocal of the error likelihood ($\varphi_i$) for each measurement and for a set of $n_y$ measurements the objective function

$$J_{CG} = -\sum_{i=1}^{n_y} \ln \left[ (1-p) \exp\left( -\frac{1}{2} \frac{(y_m(i) - U(i)z)^2}{\sigma_i^2} \right) + \frac{p}{b} \exp\left( -\frac{1}{2} \frac{(y_m(i) - U(i)z)^2}{\sigma_i^2 b^2} \right) \right] \tag{4.3}$$

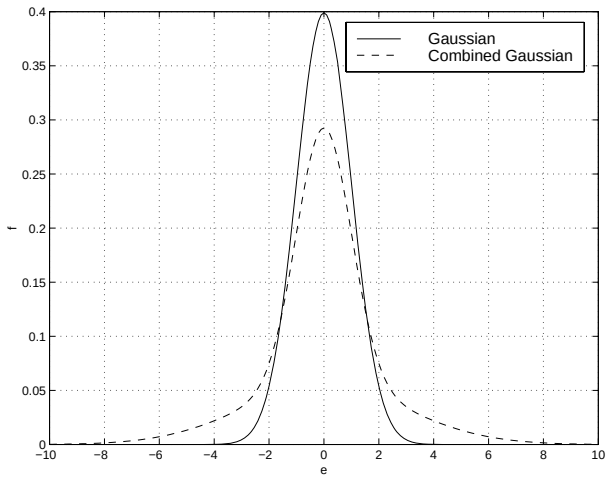


Figure 4.1: Gassian and combined Gaussian frequency function. The standard deviation $\sigma = 1$, probability for an outlier $p = 0.4$ and ratio of the standard deviations $b = 3$.

is minimized subject to process constraints.

A measurement is defined to have to have a gross error if the probability of the measurement error in the gross error distribution is larger than the probability of the random error distribution (Tjoa and Biegler, 1991). According to this definition a measurement has a gross error if

$$|y_m(i) - U(i)z| > \sigma_i \sqrt{\frac{2b^2}{b^2 - 1} \ln \left[ \frac{b(1-p)}{p} \right]} \tag{4.4}$$

### 4.2.1 Observability and redundancy

Observability for unmeasured variables can be verified using the first order local observability sufficient condition from Stanley and Mah (1981). If

$$\text{rank} \begin{bmatrix} H_r(z^*) \\ U \end{bmatrix} = n_z \tag{4.5}$$

then the system is locally observable close to $z^*$ where $z^*$ is a solution of the data reconciliation problem in equation 4.1. The linearized model equations $H_r(z^*)r$ are defined as

$$H_r(z^*) = \begin{bmatrix} \frac{\partial f}{\partial z}\Big|_{z=z^*} \\ Ar \end{bmatrix} \tag{4.6}$$

and U is the measurement matrix, $y = Uz$. A requirement is that the process model constraints should be continuously differentiable close to $z^*$

Redundancy for a measured value can be verified by removal of the row, corresponding actual measurement in $U$, making a new measurement mapping matrix $U_{n_y-1}$.

$$\text{rank} \begin{bmatrix} H_r(z^*) \\ U_{n_y-1} \end{bmatrix} = n_z \tag{4.7}$$

If the removed measurement is redundant then the rank of the matrix in equation 4.7 still has rank equal the total number of variables $n_z$.

### 4.2.2 Uncertainty of estimates

The uncertainty of a measured value is assumed to be normally distributed with zero mean and standard deviation $\sigma$. In order to give an indication of what is ideally gained using data reconciliation, the uncertainty of the reconciled variable is calculated.

The calculation of the error in the estimate is outlined as follows. The data reconciliation problem is linearized around the solution $z_o$ with the measured values $y_m$. Then, variables in $z$ are separated into measured variables $y$, unmeasured variables $x$ and known or specified variables $v$. The specified and unmeasured variables are then removed from the problem. The data reconciliation problem is rewritten as a QP (quadratic programming) problem containing only the measured variables $y$ and linear equality constraints. The QP problem has a known solution which can be written as $y = Gy_m$. The covariance of the measured values $\Sigma_m$ is assumed to be known and the uncertainty of the estimate is computed, using the propagation of error rule, which in the linear case gives $\Sigma_y = G\Sigma_m G^{\mathrm{T}}$.

The linearized data reconciliation problem from equation 4.1 is written as

$$\begin{aligned} \min_{\tilde{z}} \ & (y_m - U\tilde{z} - Uz_0)^{\mathrm{T}} Q (y_m - U\tilde{z} - Uz_0) \\ \text{s.t.} \quad & \left.\frac{\partial f(z)}{\partial z}\right|_{z=z_0} \tilde{z} + f(z_0) = 0 \\ & A_{r1}\tilde{z} = b_{r1} - A_{r1}z_0 \\ & A_{r2}\tilde{z} = b_{r2} - A_{r2}z_0 \end{aligned} \tag{4.8}$$

where $\tilde{z} = z - z_0$. The linear constraints are separated into two sets of linear constraints where $A_{r1}$ and $b_{r1}$ are the rows in $A_r$ corresponding to the reactor equal efficiency constraints (according to equation 4.39). $A_{r2}$ and $b_{r2}$ are the constraints added to specify the values of known or specified values.

Using that $f(z_0) = 0$ and $A_{r1}z_0 = b_{r1}$ and $A_{r2}z_0 = b_{r2}$ the linearized data reconciliation problem is rewritten as

$$\begin{aligned} \min_{\tilde{z}} \ & (y_m - U\tilde{z} - Uz_0)^{\mathrm{T}} Q (y_m - U\tilde{z} - Uz_0) \\ \text{s.t.} \quad & H\tilde{z} = 0 \\ & A_{r2}\tilde{z} = 0 \end{aligned} \tag{4.9}$$

where

$$H = \begin{bmatrix} \frac{\partial f(z)}{\partial z}\Big|_{z=z_0} \\ A_{r1} \end{bmatrix} \tag{4.10}$$

The variables in $\tilde{z}$ are separated into measured variables $\tilde{y}$, unmeasured variables $\tilde{x}$ and specified variables $\tilde{v}$. Using that $y = Uz$ the data reconciliation problem is written

$$\begin{aligned} \min_{z} \ & (y_m - \tilde{y} - \tilde{y_0})^{\mathrm{T}} Q (y_m - \tilde{y} - \tilde{y_0}) \\ \text{s.t.} \quad & H_1\tilde{y} + H_2\tilde{x} + H_3\tilde{v} = 0 \\ & \widetilde{A}_{r2}\tilde{v} = 0 \end{aligned} \tag{4.11}$$

where $H_1$ are the columns of $H$ corresponding to the measured values, $H_2$ are the columns of $H$ corresponding to the unmeasured values and $H_3$ are the columns of $H$ corresponding to the specified values. $\widetilde{A}_{r2}$ is the columns of $A_{r2}$ corresponding to the specified values

The matrix $\widetilde{A}_{r2}$ has full rank and the specifications $\widetilde{A}_{r2}\tilde{v} = 0$ give the solution $\tilde{v} = 0$.

Using that $\tilde{v} = 0$ and pre multiplying the linearized model equations $H_1\tilde{y} + H_2\tilde{x} + H_3\tilde{v}$ with a matrix $P^{\mathrm{T}}$, defined such that $H_2^{\mathrm{T}}P = 0$, the unmeasured and specified variables are removed from the linear equality constraints. The resulting QP problem with linear equality constraints is written as

$$\begin{aligned} \min_{z} \ & (y_m - \tilde{y} - \tilde{y_0})^{\mathrm{T}} Q (y_m - \tilde{y} - \tilde{y_0}) \\ \text{s.t.} \quad & P^{\mathrm{T}} H_1 \tilde{y} = 0 \end{aligned} \tag{4.12}$$

Expanding the objective function, removing terms with fixed value, and multiplying by $\frac{1}{2}$ gives

$$J = \frac{1}{2}\tilde{y}^{\mathrm{T}} Q \tilde{y} + (y_0 - y_m) Q \tilde{y} \tag{4.13}$$

using the known solution of a QP problem with linear equality constraints the solution of equation 4.12 is written as

$$\tilde{y} = -Q^{-1}\left[I - A^{\mathrm{T}}(AQ^{-1}A^{\mathrm{T}})^{-1}AQ^{-1}\right] Q(y_o - y_m) \tag{4.14}$$

where $A = P^{\mathrm{T}}H_1$. Applying the propagation of error rule and substituting $Q = \Sigma_m^{-1}$ the covariance matrix if the estimation error $\Sigma_y$ is computed as

$$\Sigma_y = \Sigma_m - \Sigma_m A^{\mathrm{T}}(A\Sigma A^{\mathrm{T}})^{-1} A\Sigma_m \tag{4.15}$$

When the measured values are known, values of the unmeasured variables are

$$\tilde{x} = (A_2^{\mathrm{T}} A_2)^{-1} A_2^{\mathrm{T}} A_1 \tilde{y} \tag{4.16}$$

and similarly the covariance matrix of the estimation error

$$\Sigma_x = (A_2^{\mathrm{T}} A_2)^{-1} A_2^{\mathrm{T}} A_1 \Sigma_y A_1^{\mathrm{T}} A_2 (A_2^{\mathrm{T}} A_2)^{-1} \tag{4.17}$$

In summary observability of variables is verified using equation 4.5, the measurements are grouped into redundant and non-redundant measurements using equation 4.7. Finally the uncertainty of the measured and unmeasured variables are computed using equation 4.15 and 4.17.

## 4.3 Scaling of the variables and model

The process model $f(z) = 0$ is scaled according to the scaling procedure proposed in Lid and Skogestad (2007).

First, every equation is paired with one variable. The equation-variable pairing may be regarded as "equation $i$ is used for computation of the value of variable $j$". It is written in a matrix P, where $P(i,j) = 1$ if variable $j$ is paired with equation number $i$. All other values equal zero. This is done both for the linear specifications $A_s$ and the nonlinear process model $f(z)$.

Second, all variables $z$ are scaled $z = S_v * \bar{z}$ such that the scaled variable $\bar{z}$ has a value close to one. $S_v$ is a $n_z \times n_z$ fixed diagonal variable scaling matrix.

Finally, the equation scaling matrices of the process model and the linear constraints, $S_f$ and $S_l$, are computed as

$$S_f = \left| \left[ I \times \left( \frac{\partial f_i(z)}{\partial z} S_v P_{nl}^{\mathrm{T}} \right) \right]^{-1} \right| \tag{4.18}$$

$$S_l = \left| [I \times (A_s S_v P_l^{\mathrm{T}})]^{-1} \right| \tag{4.19}$$

where $\times$ denotes element by element multiplication so that $S_f$ and $S_l$ are diagonal matrices. The scaled model is written as

$$\widetilde{f}(\tilde{z}) = 0 \tag{4.20}$$

$$\widetilde{A}s\tilde{z} = \tilde{b} \tag{4.21}$$

$$\tag{4.22}$$

where $\tilde{z} = S_v^{-1} z$, $\widetilde{f}(\tilde{z}) = S_f f(S_v \tilde{z})$, $\widetilde{A}s = S_l A_s S_v$, and $\tilde{b} = S_l b$. If the model equations are properly scaled, the condition number of

$$H = \begin{bmatrix} \widetilde{\mathbb{F}}(\tilde{z}) \\ \widetilde{A}_r \end{bmatrix} \tag{4.23}$$

should be reasonable low ($< 1 \times 10^6$).

It should be noted that the variable scaling has some pitfalls. A simple input-output mass balance of a two component ($j = 1, 2$) process stream is used as an example. The resulting model has six variables and three equations. To solve the model three variable values have to be specified . The model equations are the component mass balance and sum of outlet molar fractions. The equations are written as

$$f(z) = \begin{bmatrix} \boldsymbol{x}_i F_i - \boldsymbol{x}_o F_o \\ \sum_j \boldsymbol{x}_o(j) - 1 \end{bmatrix} = 0 \tag{4.24}$$

The variable vector $\boldsymbol{z} = [\boldsymbol{x}_i^{\mathrm{T}}\ Fi\ \boldsymbol{x}_o^{\mathrm{T}}\ F_o]^{\mathrm{T}}$. Three specifications are added in $A_r z = b_r$ . They are feed composition and feed flow ($\boldsymbol{x}_i = [0.5\ 0.5]^{\mathrm{T}}$ and $F_i = 1$) which gives

$$A_r = \begin{bmatrix} 1 & 0 & 0 & 0 & 0 & 0 \\ 0 & 1 & 0 & 0 & 0 & 0 \\ 0 & 0 & 1 & 0 & 0 & 0 \end{bmatrix} \quad \text{and} \quad \boldsymbol{b}_r = \begin{bmatrix} 0.5 \\ 0.5 \\ 1 \end{bmatrix} \tag{4.25}$$

In this case the first order derivatives of the process model $f(\boldsymbol{z})$ and the specification matrix $A_s$ are written as

$$H = \begin{bmatrix} \mathbb{F}(z) \\ A_s \end{bmatrix} = \begin{bmatrix} F_i & 0 & x_i(1) & F_o & 0 & x_o(1) \\ 0 & F_i & x_i(2) & 0 & F_o & x_o(2) \\ 0 & 0 & 0 & 1 & 1 & 0 \\ 1 & 0 & 0 & 0 & 0 & 0 \\ 0 & 1 & 0 & 0 & 0 & 0 \\ 0 & 0 & 1 & 0 & 0 & 0 \end{bmatrix} \tag{4.26}$$

The condition number of $H(\boldsymbol{z}^*) \approx 5.3$, where $z^*$ is a solution of the process model, i.e. $f(\boldsymbol{z^*}) = 0$ and $A_s \boldsymbol{z^*} = \boldsymbol{b}_s$. If the feed composition specifications are changed to $\boldsymbol{x}_i = [0.01\ 0.99]^{\mathrm{T}}$ the condition number of $H(\boldsymbol{z}^*) \approx 6.7$. This shows that, in this case, small values of the variables $x_i(1)$ and $x_o(1)$ are not a problem. However, if variable scaling is added, such that the scaled variables have a value equal to one the condition number of $\widetilde{H} \approx 7.4 \times 10^3$. I.e. we have by improper variable scaling created an "ill conditioned" model.

On the other hand, if the molar flow $Fi$ is increased from 1 to 100 the condition number of $H \approx 2.8 \times 10^4$. If the flow variables are scaled such that the scaled variable has a value equal to one, and the equations are scaled according to the procedure above,

the condition number of the scaled model is reduced to $\widetilde{H}(z^*) \approx 8.2$. The "rule of thumb", which was applied to this model, is: be careful by assigning large variable scaling factors to variables with values close to zero. Typically, all molar fractions are by definition close to one ([0 1]) and are scaled by a factor equal to one.

The reformer model is scaled according to the procedure above and the condition number of $H$ is reduced from $2.3 \times 10^{12}$ to $3.6 \times 10^4$. The maximum absolute value of the elements in $H$ is reduced from $4.8 \times 10^5$ to 7.6 and the values of $\widetilde{H}$ corresponding to the equation-variable pairing has a value equal to one.

## 4.4 Case study: Naphtha reformer

### 4.4.1 Process description

The feed to the naphtha reformer is a crude oil fraction from the refinery crude unit with a boiling range of $\approx 100 - 180°\text{C}$ and a density of $\approx 763\text{kg/m}^3$. The products are a high-octane naphtha, also called "reformate", "Gas" ($C_2 - C_4$) and hydrogen.

The overall reaction is endothermic and there is a significant temperature drop from the inlet to the outlet of the reactors. In order to compensate for this temperature drop, the reactor is separated into four sections with intermediate reheating, see figure 4.2. The fresh feed is mixed with hydrogen rich recycle gas and is preheated in the reactor effluent heat exchanger (E1). The feed is further heated in heater number one (H1) before it enters reactor number one (R1), and so on. The hot reactor product enters the feed pre-heater (E1) and is further cooled with cooling water before it enters the separator. Hydrogen rich gas is compressed, except for a small purge stream, and recycled. The liquid product from the separator (D1), a mixture of reformate and gas, is separated in a downstream distillation column.

The amount of catalyst in the four reactors is approximately in the ratio of 1:1:2:3. The reactor inlet temperatures are in the range of 770-800K. The increase in octane number is due to a conversion of paraffins and naphthenes in the feed into aromatics.

The components in the process are lumped into five pseudo components. These are hydrogen (H), "Gas" $C_2 - C_4$ (G), paraffines (P), naphthenes (N) and aromatics (A). The thermodynamic properties of these pseudo components are described in appendix 4.A.

The justification for this simplification is that the carbon number of the molecules does not change in the two reactions (4.27) and (4.28). For example, a $C_7$ naphthene is converted to a $C_7$ aromatic and a $C_7$ paraffin is converted to a $C_7$ naphthene.

This conversion is described by four main reactions (Smith, 1959):

1. Dehydrogenation of naphthenes to aromatics
2. Dehydrocyclization of paraffins to naphthenes

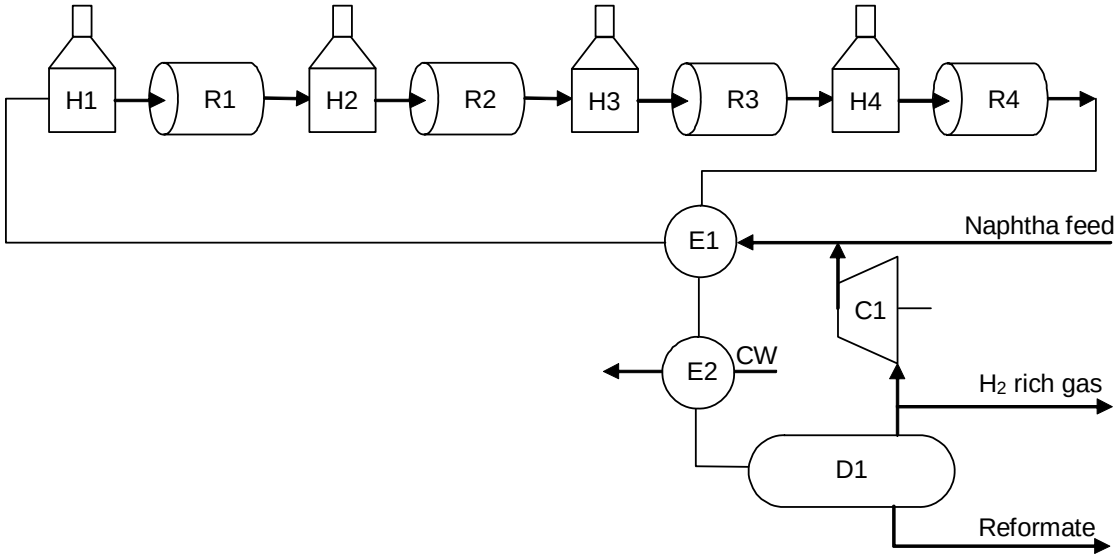


Figure 4.2: Naphtha reformer

3. Hydrocracking of naphthenes to light ends
4. Hydrocracking of paraffins to light ends

The simplified naphtha reforming kinetics, as described in Smith (1959), are written as

$$\mathrm{N} \overset{r_1}{\rightleftharpoons} \mathrm{A} + 3\mathrm{H_2} \tag{4.27}$$

$$\mathrm{N} + \mathrm{H_2} \overset{r_2}{\rightleftharpoons} \mathrm{P} \tag{4.28}$$

$$\mathrm{N} + 2\mathrm{H_2} \overset{r_3}{\rightarrow} 2\mathrm{G} \tag{4.29}$$

$$\mathrm{P} + \mathrm{H_2} \overset{r_4}{\rightarrow} 2\mathrm{G} \tag{4.30}$$

with the stoichiometric matrix $\boldsymbol{N}$

$$\boldsymbol{N} = \begin{bmatrix} 3 & 0 & 0 & -1 & 1 \\ -1 & 0 & 1 & -1 & 0 \\ -2 & 2 & 0 & -1 & 0 \\ -1 & 2 & -1 & 0 & 0 \end{bmatrix} \tag{4.31}$$

where the columns refer to the components H, G, P, N and A. The reaction rates are,

$$r_1 = k_{f_1} p_N - k_{r_1} p_A p_{H_2}^3 \tag{4.32}$$

$$r_2 = k_{f_2} p_N p_{H_2} - k_{r_2} p_P \tag{4.33}$$

$$r_3 = k_{f_3} p_N / p \tag{4.34}$$

$$r_4 = k_{f_4} p_P / p \tag{4.35}$$

where $p_x$ is the partial pressure of component $x$ and $p$ is the overall reactor pressure.

For the forward and reverse rate constants, $k_f$ and $k_r$, an Arrhenius type of rate expression is assumed

$$k_f = k_{0f} e^{\left(\frac{-E_f}{RT}\right)} \qquad k_r = k_{0r} e^{\left(\frac{-E_r}{RT}\right)} \tag{4.36}$$

where the activation energy $E$ is dependent on the catalyst and $k_{0f}$ is dependent of the molarity of the reaction (Bommannan et al., 1989). $R$ is the universal gas constant. Reaction 1 is endothermic and reaction 2-4 are exothermic. Reaction 1 dominates such that the overall reaction is endothermic.

The model equations are organized in unit models. Appendix A gives a detailed description of all unit models used in this paper. A description of the modeling framework, with case studies, can be found in Lid and Skogestad (2007).

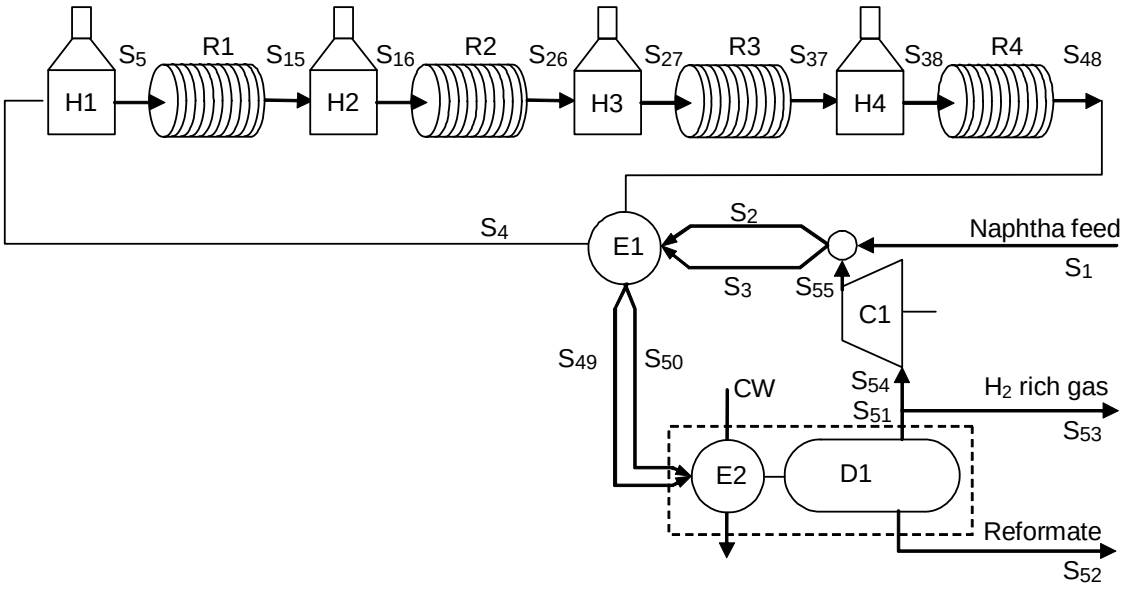


Figure 4.3: Model details of the naphtha reformer

The details of the reformer model are shown in figure 4.3. The liquid feed $S_1$ is mixed with recycle gas $S_{55}$. The resulting vapor $S_2$ and a liquid $S_3$ outlet stream enters the reactor effluent heat exchanger E1. The E1 outlet streams $S_4$ then enters the first heater and reactor section. The heaters are modeled as a direct heat input and each of the four reactors is modeled using ten CSTRs in series with even distribution of catalyst. Heat exchanger E2 and separator D1 is modeled using the same flash unit model . The reason is that the flash calculation is needed in the heat exchanger to compute the enthalpy of the outlet streams.

In addition variables and equations for Reformate octane number (RON), feed hydrogen to hydrocarbon ratio, and some mass flows are added as internal variables in a "dummy"

unit model. The mass flows are the feed mass flow, Reformate, gas and hydrogen product mass flow and the recycle gas mass flow

### 4.4.2 Process model

The mass balance of a reactor element is written as

$$F_i\boldsymbol{x}_i - F_o\boldsymbol{x}_o + \boldsymbol{N}A_c^{\mathrm{T}}\boldsymbol{r}(T_o, P_o)m_c = 0 \tag{4.37}$$

where $F_i$,$\boldsymbol{x}_i$ and $F_o$,$\boldsymbol{x}_o$ is the inlet and outlet stream molar flow and molar component fractions, $m_c$ is the mass of catalyst, and $A_c$ is the catalyst activity parameter, which is expected to be close to one.

The resulting model and specifications are written

$$\begin{aligned} f(z) &= 0 \\ A_s z &= b_s \end{aligned} \tag{4.38}$$

There are $n_z = 501$ variables $z$ and $n_f = 442$ equations in the reformer process model $f(z) = 0$. These are listed in table 4.1 and the equations 4.2.

The remaining $n_z - n_f = 59$ variables need to be specified and are added as $n_s = 59$ rows in $A_s$ with the corresponding specification values in $b_s$.

The catalyst efficiency factors for all CSTRs within one reactor were constrained to have equal values. This is incorporated as 36 linear constraints in $A_s$.

$$A_{c_i} - A_{c_{i+1}} = 0 \text{ for } i = 1...9, 10...19, 20...29, 30...39 \tag{4.39}$$

Values for feed condition, reactor temperatures, recycle rate, heat transfer coefficients and compressor efficiency are also specified by addition of rows in $A_s$ and corresponding values in $b_s$. The specified variables with corresponding values for the 23 remaining degrees of freedom are shown in table 4.3.

The selection of specification variables is not unique and other valid variable combinations exist. In order to have a unique solution, the matrix of first order derivatives of the nonlinear constraints and the linear constraint matrix must have full rank.

In order to reduce the computational load in solving the model, the first order derivatives are calculated analytically.

$$\mathbb{F}(z) = \frac{\partial f(z)}{\partial z} \tag{4.40}$$

| | | | |
|---|---|---|---|
| Process streams | | | |
| $x$ | | Molar fraction | $NC$ |
| $F$ | kmol/s | Molar flow | 1 |
| $T$ | K | Temperature | 1 |
| $P$ | bar | Pressure | 1 |
| | | Total: $(NC+3)\times 55$ | 440 |
| Heaters | | | |
| $Q$ | kW | Duty | 1 |
| | | Total: $1\times 4$ | 4 |
| Reactors | | | |
| $A_c$ | | Catalyst efficiency factor (one for each CSTR) | 10 |
| | | Total: $4\times 10$ | 40 |
| Heat exchanger E1 | | | |
| $Q$ | kW | Duty | 1 |
| $U_1$ | kW/m$^2$/K | Heat transfer coefficient | 1 |
| Heat exchanger E2 and condenser | | | |
| $Q$ | kW | Duty | 1 |
| $U_2$ | kW/m$^2$/K | Heat transfer coefficient | 1 |
| $F_{CW}$ | kmol/s | Cooling water molar flow | 1 |
| $T_{CW_i}$ | K | Cooling water inlet temperature | 1 |
| $T_{CW_o}$ | K | Cooling water outlet temperature | 1 |
| Compressor | | | |
| $W$ | kW | Work | 1 |
| $\psi$ | | Efficiency | 1 |
| $T_s$ | K | Reversible compression outlet temperature | 1 |
| Additional constraints | | | |
| RON | | Reformate octane number | 1 |
| $H_2/HC$ | | Hydrogen to hydrocarbon ratio | 1 |
| $\widetilde{F}_1$ | t/h | Feed mass flow | 1 |
| $\widetilde{F}_{55}$ | t/h | Recycle mass flow | 1 |
| $\widetilde{F}_{53}$ | t/h | Vapor product mass flow | 1 |
| $\widetilde{F}_{52}$ | t/h | Reformat product mass flow | 1 |
| $\widetilde{F}_{53}(H_2)$ | t/h | Hydrogen product mass flow | 1 |
| | | Total: | $n_z = 501$ |

Table 4.1: Reformer model variables

| Unit model | $n_{fi}$ | Total |
|---|---|---|
| Heater | $NC+3$ | $(NC+3)\times 4$ |
| CSTR | $NC+3$ | $(NC+3)\times 40$ |
| Heat exchanger E1 | $3NC+10$ | $3NC+10$ |
| Heat exchanger E2 and condenser | $2NC+8$ | $2NC+8$ |
| Compressor | $NC+4$ | $NC+4$ |
| Vapor/liquid feed mixer | $2NC+6$ | $2NC+6$ |
| Stream split | $2NC+5$ | $2NC+5$ |
| Additional constraints | 7 | 7 |
| Total | $54NC+172=$ | $n_f = 442$ |

Table 4.2: Reformer model equations

| Description | Variable | Value |
|---|---|---|
| Catalyst efficiency factor reactor 1 | $A_{c1}$ | 1 |
| Catalyst efficiency factor reactor 2 | $A_{c11}$ | 1 |
| Catalyst efficiency factor reactor 3 | $A_{c21}$ | 1 |
| Catalyst efficiency factor reactor 4 | $A_{c31}$ | 1 |
| E1 heat transfer coefficient | $U_1$ | 560 |
| E2 heat transfer coefficient | $U_2$ | 200 |
| E2 cooling water flow | $F_{CW}$ | 5 |
| E2 cooling water inlet temperature | $T_{CW_i}$ | 288 |
| Compressor efficiency | $\psi$ | 0.75 |
| Feed component molar fraction | $x_1(H)$ | 0 |
| Feed component molar fraction | $x_1(G)$ | 0 |
| Feed component molar fraction | $x_1(P)$ | 0.32 |
| Feed component molar fraction | $x_1(N)$ | 0.56 |
| Feed component molar fraction | $x_1(A)$ | 0.12 |
| Feed mass flow | $\widetilde{F}_1$ | 85 |
| Feed temperature | $T_1$ | 358 |
| Reactor 1 inlet temperature | $T_5$ | 790 |
| Reactor 2 inlet temperature | $T_{16}$ | 790 |
| Reactor 3 inlet temperature | $T_{27}$ | 790 |
| Reactor 4 inlet temperature | $T_{38}$ | 790 |
| Compressor recycle mass flow | $\widetilde{F}_{55}$ | 8.0 |
| Vapor product pressure | $P_{53}$ | 7.9 |
| Liquid product pressure | $P_{52}$ | 8.0 |

Table 4.3: Simulation variable specifications

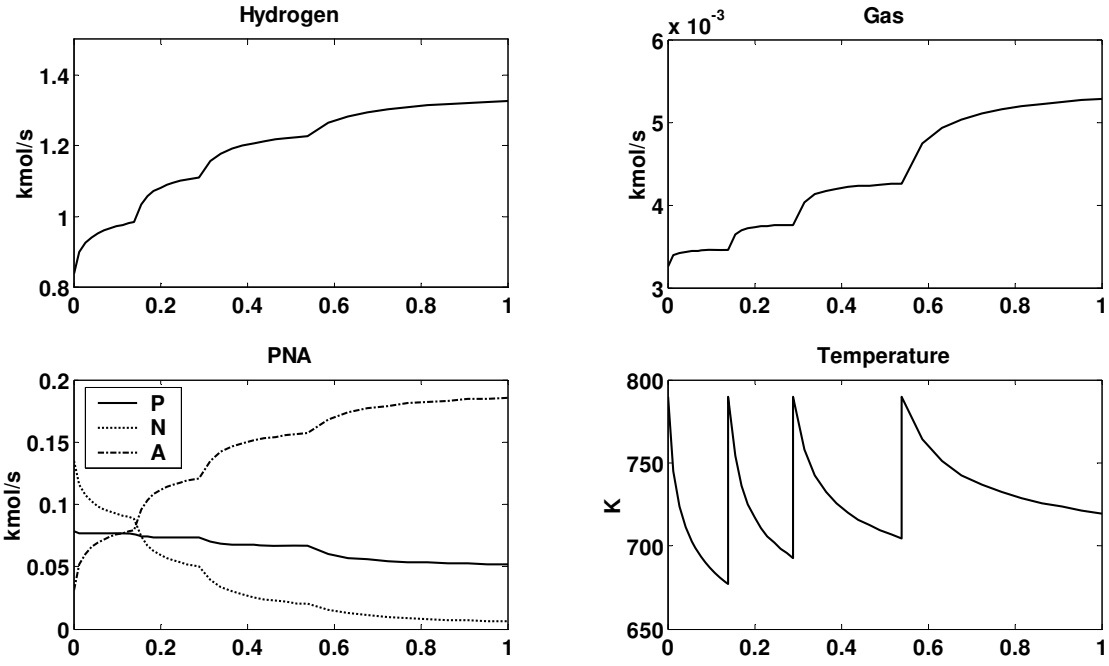


Figure 4.4: Nominal flows and temperature in reactors

### 4.4.3 Nominal operation

Figure 4.4 shows the molar flows of each component trough the four reactors as a function of normalized catalyst mass. The figure shows a net production of hydrogen and gas. The largest amount of hydrogen is produced in reactor one and the largest amount of gas is produced in reactor four. The dominating reaction in reactor number one is conversion of naphthenes to aromatics. The dominating reaction in reactor number four is conversion of paraffines to naphthenes. The large temperature drop in reactor one is due to the large heat of reaction for the conversion of naphthenes to aromatics.

Other key variables like heater duties and product yields are listed in table 4.4. The ref-

| Variable | | Value | Unit |
|---|---|---|---|
| Heater 1 duty | $Q_{H_1}$ | 8818 | kW |
| Heater 2 duty | $Q_{H_2}$ | 11865 | kW |
| Heater 3 duty | $Q_{H_3}$ | 10350 | kW |
| Heater 4 duty | $Q_{H_4}$ | 9196 | kW |
| Compressor duty | $W_C$ | 682 | kW |
| Heat exchanger E1 duty | $Q_{E_1}$ | 37596 | kW |
| Heat exchanger E2 duty | $Q_{E_2}$ | 6865 | kW |
| Feed $H_2$/HC ratio | $H_2/HC$ | 3.48 | |
| Reformate octane number | $RON$ | 102.4 | |
| Reformate product flow | $\widetilde{F}_{52}$ | 80.4 | t/h |
| Vapor product flow | $\widetilde{F}_{53}$ | 4.6 | t/h |

Table 4.4: Simulation results

ormate and vapor yields are 94.57% and 5.43% respectively. If the vapor stream is split into hydrogen and gas the hydrogen and gas yield are 4.13% and 1.30% respectively.

## 4.5 Data reconciliation results

The naphtha reformer process has in total $n_y = 26$ measured values. These are feed, product and recycle gas analyzers, feed product and recycle gas mass flow measurements and various temperature measurements. All the measurements are listed in table 4.6

The limitation of equal catalyst efficiency factor within each reactor added as rows in $A_r$. The feed hydrogen and gas content is known to be practically equal to zero and specifications for $x_1(1) = 0$ and $x_1(2) = 0$ are added in $A_r$. The remaining degrees of freedom then equal 21.

For the reformer model we have that

$$\text{rank}\begin{bmatrix} H_r(z^*) \\ U \end{bmatrix} = 498 \tag{4.41}$$

using equation 4.6. This indicates three unobservable variables.

The condenser liquid outlet pressure is not specified and the liquid stream is not connected to any downstream unit. This variable is not present in any of the model equations and is clearly unobservable.

There are no measurements of the cooling water inlet or outlet flow or temperature.

In order to make all variables observable the values of $P_{52}$, $F_{CW}$ and $T_{CW_i}$ are specified by adding three linear constraints in $A_r$ and the corresponding values in $b_r$. The matrix in equation 4.41, with the addition of three new rows in $A_r$, has rank equal to $n_z$ and all variables are now, by definition in the equation 4.5, observable. The degrees of freedom are now reduced from 21 to 18.

It is verified, using equation 4.7, that all measurements in the reformer process are redundant.

The standard deviation if the estimated values $\sigma_{y_i} = \sqrt{\Sigma_y(i,i)}$ is shown in table 4.6.

There is almost no reduction of uncertainty in the estimate of the reactor inlet or outlet temperatures, compared with the uncertainty of the measured values. The feed and product mass flow uncertainty is reduced by approximately 30%. The compressor inlet temperature, separator outlet temperature and recycle gas hydrogen content has a large reduction of uncertainty. This is probably due to oversimplification in the modeling of the separator and recycle gas system (i.e. model error).

The values and uncertainties of the heat exchangers heat transfer coefficient, reactor and compressor efficiency are shown in table 4.5. On average the uncertainty in these

| Description | Variable | Estimate | $\sigma$ |
|---|---|---|---|
| Catalyst efficiency factor reactor one | $A_{c1}$ | 1.30 | 0.16 |
| Catalyst efficiency factor reactor one | $A_{c2}$ | 0.59 | 0.17 |
| Catalyst efficiency factor reactor one | $A_{c3}$ | 1.36 | 0.21 |
| Catalyst efficiency factor reactor one | $A_{c4}$ | 0.93 | 0.20 |
| E1 heat transfer coefficient [W/m$^2$/K] | $U_1$ | 515 | 165 |
| E2 heat transfer coefficient [W/m$^2$/K] | $U_2$ | 200 | 1362100 |
| Compressor efficiency | $\psi$ | 0.76 | 0.10 |

Table 4.5: Estimates of unmeasured variables for data set no. 12

variables are 10-35% of the actual value except for the estimate of $U_2$. The estimated uncertainty in $U_2$ shows that this variable is not practically observable and indeed the estimate of $U_2 = 200\text{W/m}^2\text{/K}$ is equal to its initial value.

The reconciliation problem was solved for 21 different data sets, sampled during a period of two years of operation. The reconciled solution shown in table 4.6 is from data set number 12. Gross errors are detected for the measured values marked with $^*$. The outlet temperatures of reactor four and of heat exchanger E1 have a gross error detected in all 21 data sets. The outlet temperatures of reactors one and two have gross errors detected in data sets 13 and 14 , respectively. The compressor mass flow has a gross error detected in three data sets and the feed temperature has a gross error

| Measurement | Variable | Meas. $y_m$ | Std. $\sigma_m$ | Estimate $y = Uz_r$ | Std. $\sigma_y$ | Unit |
|---|---|---|---|---|---|---|
| Feed P molar fraction | $x_1(3)$ | 0.32 | 0.01 | 0.32 | 0.01 | |
| Feed N molar fraction | $x_1(4)$ | 0.56 | 0.01 | 0.56 | 0.01 | |
| Feed A molar fraction | $x_1(5)$ | 0.12 | 0.01 | 0.12 | 0.01 | |
| Feed temperature | $T_1$ | 358.5 | 3.0 | 360.8 | 2.72 | K |
| E1 cold side inlet temperature | $T_2$ | 344.5 | 3.0 | 338.2 | 1.49 | K |
| E1 cold side outlet temperature | $T_4$ | 706.6 | 3.0 | 706.6 | 2.71 | K |
| Heater 1 outlet temperature | $T_5$ | 794.0 | 3.0 | 794.3 | 2.96 | K |
| Reactor 1 outlet temperature | $T_{15}$ | *649.1 | 3.0 | 670.0 | 2.97 | K |
| Heater 2 outlet temperature | $T_{16}$ | 788.6 | 3.0 | 788.9 | 2.96 | K |
| Reactor 2 outlet temperature | $T_{26}$ | 704.0 | 3.0 | 703.8 | 2.96 | K |
| Heater 3 outlet temperature | $T_{27}$ | 798.4 | 3.0 | 798.8 | 2.96 | K |
| Reactor 3 outlet temperature | $T_{37}$ | 698.6 | 3.0 | 698.4 | 2.96 | K |
| Heater 4 outlet temperature | $T_{38}$ | 797.8 | 3.0 | 798.2 | 2.96 | K |
| Reactor 4 outlet temperature | $T_{48}$ | *763.6 | 3.0 | 722.8 | 2.71 | K |
| E1 hot side outlet temperature | $T_{50}$ | *385.4 | 3.0 | 353.5 | 1.98 | K |
| Separator D1 pressure | $P_{51}$ | 7.93 | 0.2 | 7.89 | 0.16 | bar |
| Separator D1 outlet temperature | $T_{52}$ | 292.2 | 3.0 | 294.1 | 0.51 | K |
| Recirculation gas H molar frac. | $x_{54}(1)$ | 0.90 | 0.1 | 0.99 | 0.0002 | |
| Compressor inlet temperature | $T_{54}$ | 294.2 | 3.0 | 294.1 | 0.51 | K |
| Compressor outlet temperature | $T_{55}$ | 323.0 | 3.0 | 324.4 | 2.92 | K |
| Compressor outlet pressure | $P_{55}$ | 10.3 | 0.2 | 10.3 | 0.14 | bar |
| Reformate product octane number | $RON$ | 103.9 | 1.0 | 103.7 | 0.72 | |
| Feed mass flow | $\widetilde{F}_1$ | 88.0 | 3.0 | 87.1 | 2.13 | t/h |
| Compressor outlet mass flow | $\widetilde{F}_{55}$ | 10.1 | 1.0 | 9.78 | 0.67 | t/h |
| Vapor product mass flow | $\widetilde{F}_{53}$ | 6.54 | 1.0 | 4.96 | 0.17 | t/h |
| Reformate product mass flow | $\widetilde{F}_{52}$ | 80.3 | 3.0 | 82.1 | 2.02 | t/h |

Table 4.6: Estimates of measured variables for data set no. 12

detected in one data set.

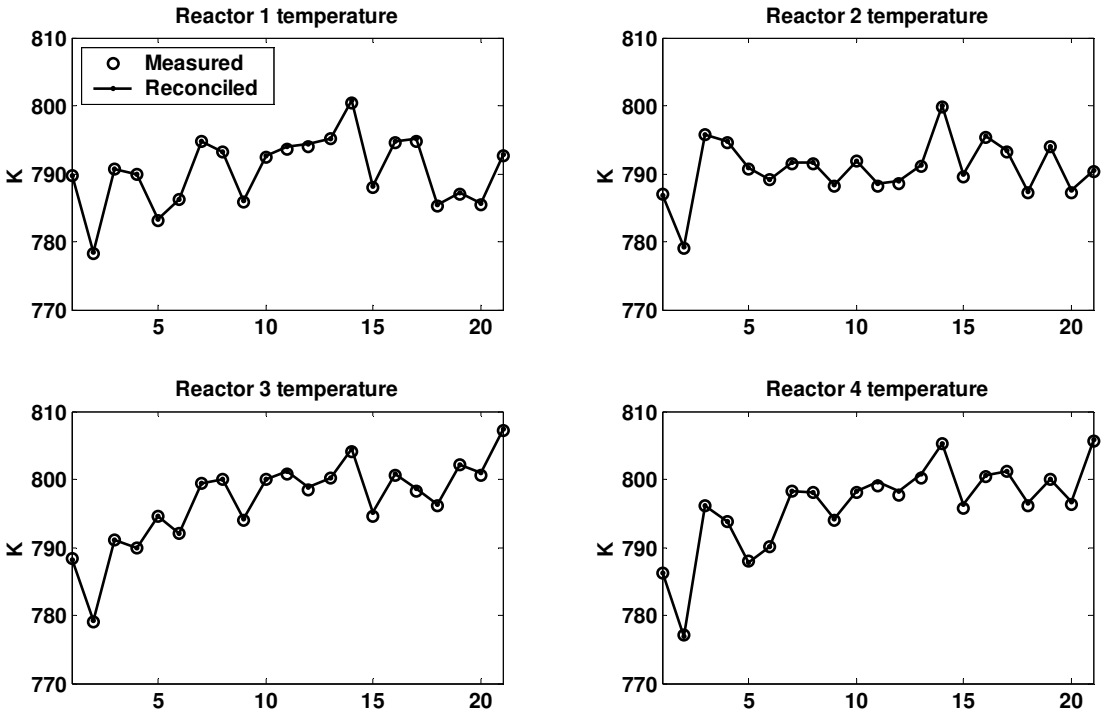


Figure 4.5: Reconciled reactor inlet temperatures for the 21 data sets

Figure 4.5 shows the measured and reconciled reactor inlet temperatures. The adjustments of the catalyst efficiency factors contributes to an almost perfect fit to the measured data. We have the highest reaction rate, and influence on the other measured values, at the inlet of the reactor and this may be the reason why the error in temperature drop over each reactor is assigned to the reactor outlet temperatures.

There are large measurement errors in the reactor outlet temperatures, as shown in figure 4.6. The outlet temperature of reactor one and two have gross errors in most data sets but some data points have almost zero measurement error. The outlet temperature of reactor number four has an almost fixed bias in all data sets. As a curiosity, the outlet temperature of reactor three, which has an almost zero measurement error in all data points is "accepted" as an untrustworthy measurement at the refinery.

The estimated catalyst efficiencies for all data sets are shown in figure 4.7.

Ideally, the catalyst efficiency factors $A_c$ should be close to one in all data sets but due to variation in the catalyst circulation some changes in $A_c$ are expected. In periods, where the catalyst regenerator is shut down, the unit may run for several days with no catalyst circulation . In these periods the catalyst efficiency will decrease due to coke build up on the catalyst.

The values of $A_c$ have large variations in data points 5, 10, 17 and 19. There is no clear reason for this and the data at these points does not differ significantly from the

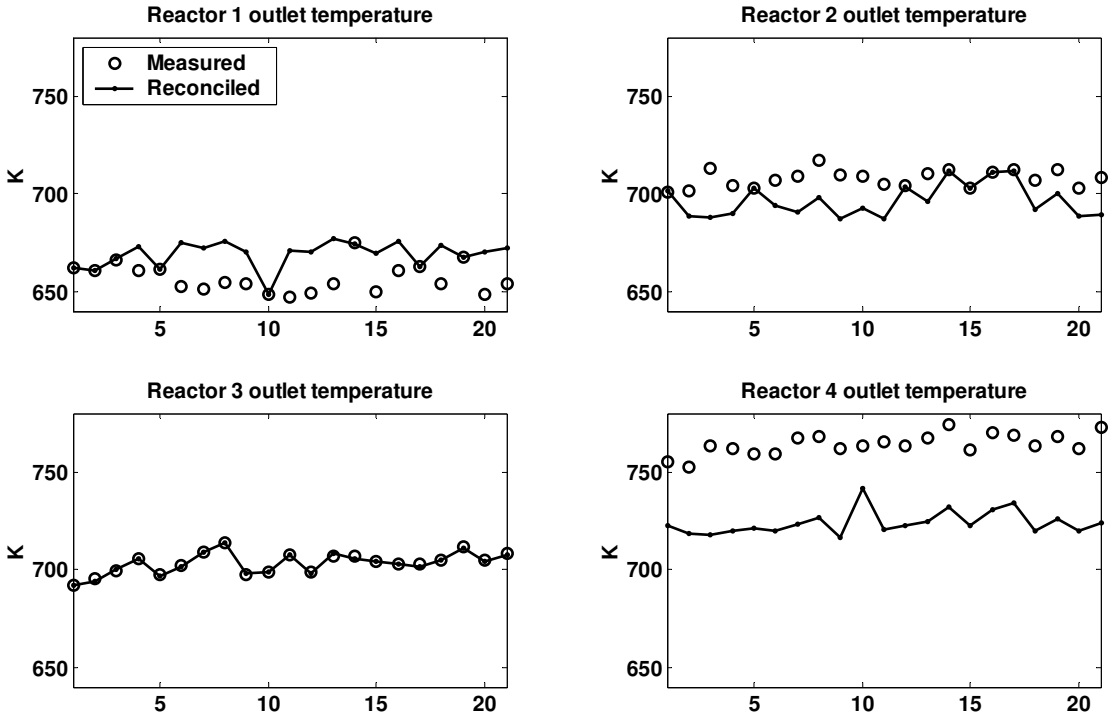


Figure 4.6: Reconciled reactor outlet temperatures for the 21 data sets

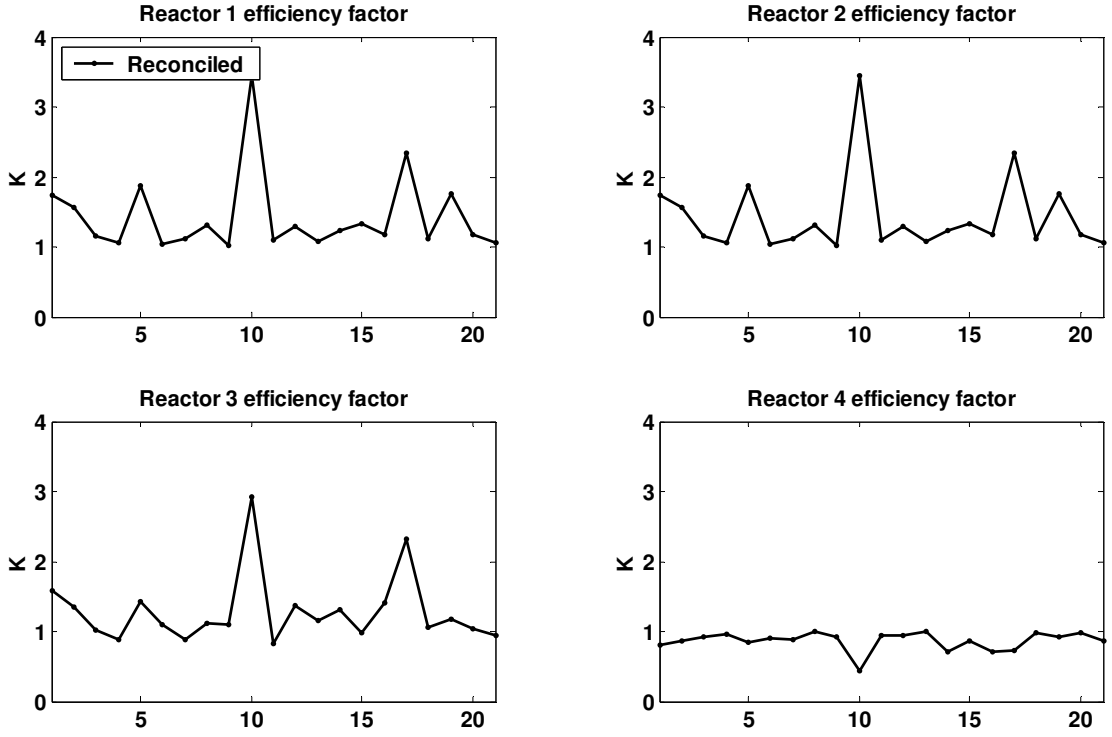


Figure 4.7: Reactor efficiencies $A_c$ for the 21 data sets

others. An observation is that the measurement error of reactor one outlet temperature is almost zero at these points but this is also true for data point 1, 2, 3 and 14.

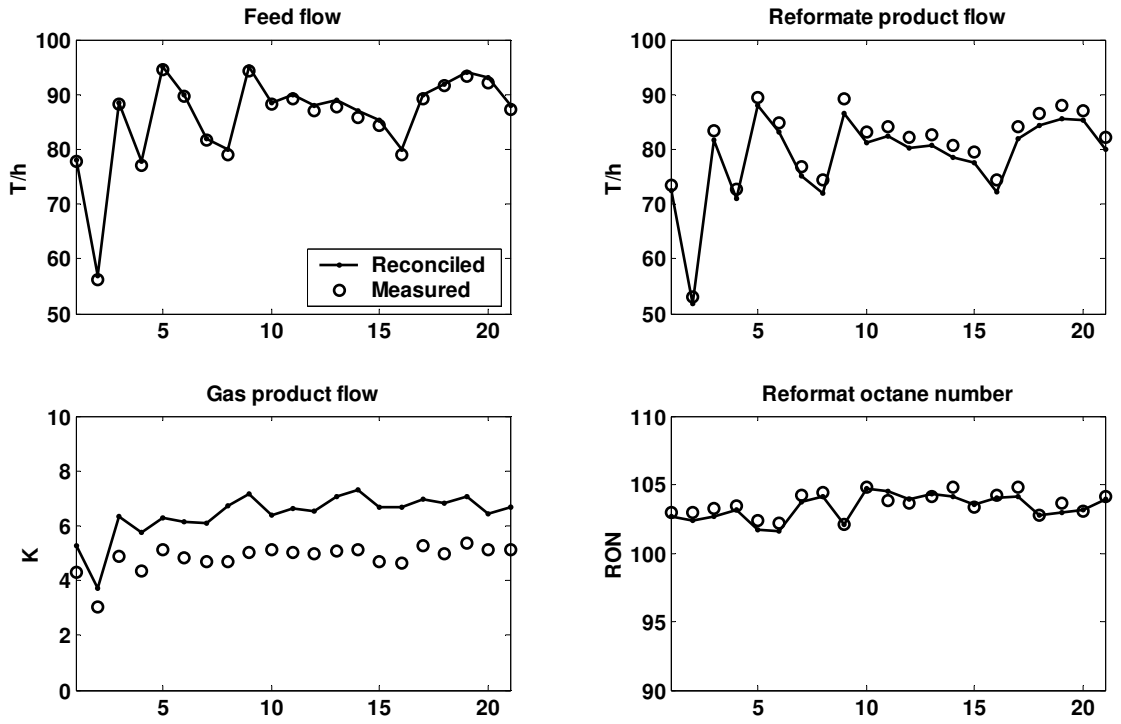


Figure 4.8: Reconciled mass flows and product quality

The average deviation of measured and reconciled feed, reformate and gas mass flows, as shown in figure 4.8, are 0.7t/h, -1.93t/h and 1.59t/h respectively. The octane reconciled and measured value deviation is -0.25. The reconciled gas mass flow is persistently lower than the measured value and even if no gross errors where detected in the measured value the presence of a systematic error is clear.

## 4.6 Optimal operation

Optimal operation is defined as the operation which maximizes the profit, given the current process condition and operating constraints. The current process condition is estimated using data reconciliation, $\boldsymbol{z}_r$ and the optimal operation is calculated by minimization of a cost or negated profit function subject to the process model, fixed

variables and operating constrains. The optimization problem is written as

$$\begin{aligned} \min_{z} \quad & J(z) \\ \text{s.t.} \quad & f(z) = 0 \\ & A_{opt} z = b_{opt} \\ & z_{opt\,\min} \leq z \leq z_{opt\,\max} \end{aligned} \tag{4.42}$$

where $J(z) = -p(z)^{\mathrm{T}} z$. In most cases $p$ is a vector of fixed prices of feed, products and energy.

Values for variables describing feed conditions like composition and temperature, heat exchanger heat transfer coefficients and compressor efficiency are fixed and set equal to their reconciled values. These values are specified using the linear equality constraints $A_{opt} z = b_{opt}$ in (4.42).

Operating constraints like maximum feed flow, maximum pressure, maximum temperature and minimum product octane are added as upper and lower bounds on the variables in $z_{opt\,\min}$ and $z_{opt\,\max}$.

The number of degrees of freedom $n_z - n_f - n_{opt} = 7$ where the number of variables $n_z = 501$, $n_f = 442$ and the number of rows in $A_{opt}$, $n_{opt} = 52$. The specified or fixed values added in $A_{opt}$ are 40 catalyst efficiency factors, 2 heat exchanger heat transfer coefficients, compressor efficiency, feed temperature and feed composition (NC=5), reformate outlet pressure, cooling water flow and cooling water inlet temperature.

### 4.6.1 Cost function

The feed, product and energy prices in problem 4.42 are shown in table 4.7. The

| Description | Value | Unit | Variable |
|---|---|---|---|
| Feed cost | -60 | \$/t | $\widetilde{F}_1$ |
| Reformate cost | 100 | \$/t | $\widetilde{F}_{52}$ |
| Gas cost | 50 | \$/t | $\widetilde{F}_{53}$ |
| Energy cost | -0.0015 | \$/kW | $Q_{H1}, Q_{H2}, Q_{H3}, Q_{H4}, W$ |

Table 4.7: Economic data

elements of $p$, corresponding with the variables in table 4.7, are updated with their respective price. All other elements of $p$ equals zero. The most important operational constraints are shown in table 4.7 as maximum and minimum variable values.

### 4.6.2 Active constraints

Two operational cases, which both are common operational regimes for a naphtha reformer unit in a refinery, are analyzed.

- Case 1. The product price is high and reformer throughput is maximized.
- Case 2. The product price is low and reformer throughput is minimized subject to meeting production demand on hydrogen.

The naphtha reformer is the main producer of hydrogen at the refinery and may not be shut down even if the product price is low and the unit profit is negative. Thus, to secure the availability of hydrogen a lower bound is added on the reformer unit hydrogen production.

| Description | Variable | Unit | Min. | Max. | Rec. | Case 1 | Case 2 | Price |
|---|---|---|---|---|---|---|---|---|
| Feed flow | $\widetilde{F}_1$ | t/h | | | 89.2 | 95.6 | 84.1 | -60.0 |
| Reformate flow | $\widetilde{F}_{52}$ | t/h | | | 84.2 | 90.6 | 79.7 | **100.0 |
| Gas flow (LPG) | $\widetilde{F}_{53}(G)$ | t/h | | | 1.2 | 1.0 | 0.9 | 50.0 |
| $H_2$ mass flow | $\widetilde{F}_{53}(H)$ | t/h | 3.5 | | 3.8 | 4.0 | *3.5 | |
| Reformat octane | RON | | 103.0 | | 103.9 | *103.0 | *103.0 | |
| Reactor 1 temp. | $T_5$ | K | | 810.0 | 794.0 | 790.7 | 794.1 | |
| Reactor 2 temp. | $T_{16}$ | K | | 810.0 | 788.6 | 782.7 | 788.8 | |
| Reactor 3 temp. | $T_{27}$ | K | | 810.0 | 801.2 | 799.9 | 798.8 | |
| Reactor 4 temp. | $T_{38}$ | K | | 810.0 | 799.6 | 791.6 | 780.4 | |
| Heater 1 duty | $Q_1$ | MW | | 9.5 | 9.3 | *9.5 | 8.6 | -0.015 |
| Heater 2 duty | $Q_2$ | MW | | 13.0 | 12.7 | *13.0 | 12.2 | -0.015 |
| Heater 3 duty | $Q_3$ | MW | | 13.0 | 12.1 | *13.0 | 11.3 | -0.015 |
| Heater 4 duty | $Q_4$ | MW | | 10.0 | 10.0 | *10.0 | 7.6 | -0.015 |
| Compressor duty | $W$ | MW | | | 0.88 | 0.48 | 0.39 | -0.015 |
| Feed $H_2$/HC ratio | H2/HC | | 3.0 | 5.0 | *3.0 | *3.0 | | |
| Separator pres. | $P_{53}$ | bar | 8.0 | 10.0 | 8.0 | *10.0 | *10.0 | |
| Profit | | \$/h | | | 2638 | 2883 | -249 | |

Table 4.8: Optimal operation with conditions from data set 12 (* = active constraint, **= in case 2 the price of reformate is 65\$/t)

The most important variables of the optimal operation for case 1 and 2 are shown in table 4.8.

In case 1, the operation is constrained on reformate RON, heater duty, feed hydrogen to hydrocarbon ratio and pressure. The improvement in profit, compared to the reconciled solution, is in this case 245\$/h ($2.1 \times 10^6$ \$/year). As a result of increased feed flow and a reformate yield improvement (0.43%) 259\$/h is gained. A total increase in energy consumption results in a loss of 14.1 \$/h. The yield improvement is mainly due to reduced temperatures in the reactors and reduced reformate RON.

In case 2, the operation is constrained on reformate RON, hydrogen product mass flow, feed hydrogen to hydrocarbon ratio and pressure.

The marginal values of the active constraints are computed by adding a small change to the constraint value and observe the corresponding change in the profit function at the new optimal conditions.

| Description | Variable | Case 1 | Case 2 |
|---|---|---|---|
| Reformat octane | RON | -124 | -13 |
| Feed $H_2$/HC ratio | H2/HC | -24 | -5.0 |
| Separator pres. | $P_{53}$ | -0.44 | -1.9 |
| $H_2$ mass flow | $\widetilde{F}_{53}(H)$ | - | -79 |
| Heater 1 duty | $Q_1$ | -60 | - |
| Heater 2 duty | $Q_2$ | -60 | - |
| Heater 3 duty | $Q_3$ | -60 | - |
| Heater 4 duty | $Q_4$ | -60 | - |

Table 4.9: Active constraints marginal values with conditions from data set 12 ($/unit)

In order to operate the process the seven degrees of freedom have to be specified or fixed. These specifications are implemented as controlled variables. The degrees of freedom are related to the heat input to the four heaters and the mass flow of feed, recycle and $H_2$ rich gas. The basic control layer includes heater duty control, feed flow control and pressure control.

In case 1, the seven active constraints are selected as controlled variables.

In case 2, the four active constraints are selected as controlled variables. These are reformate RON, hydrogen product mass flow, feed hydrogen to hydrocarbon ratio and pressure. The remaining three control variables have to be selected so that the economic loss is small. The temperature difference of the inlet of the four reactors are three such control variables. If three control loops are implemented such that all reactor have equal inlet temperatures, the economic loss, compared to having optimal inlet temperatures, is small (0.005$/h). This is also consistent with the equal marginal values of the heater duties in case 1 shown in table 4.9. That is "self optimizing control" is achieved by adding the reactor difference temperatures as control variables with a zero set point.

The constraint marginal values also show that in case 1 the reformate RON is the most important variable to keep close to its minimum value. Similar, the hydrogen mass flow is the most important variable in case 2.

| Manipulated variables | Controlled variables Case 1 | Controlled variables Case 2 |
|---|---|---|
| Feed flow | Reformate RON | $H_2$ product flow |
| Heater 1 duty | Maximum* | Reformate RON |
| Heater 2 duty | Maximum* | $T_{R1_i}$-$T_{R2_i}$(=0) |
| Heater 3 duty | Maximum* | $T_{R2_i}$-$T_{R3_i}$(=0) |
| Heater 4 duty | Maximum* | $T_{R3_i}$-$T_{R4_i}$(=0) |
| Pressure | Maximum* | Maximum* |
| Compressor work | $H_2$/HC ratio | $H_2$/HC ratio |

Table 4.10: Proposed control structure with given set points. (*Manipulated variable fixed at maximum value)

Table 4.10 shows the control structure which yields close to optimal operation for the two operational cases.

## 4.7 Discussion

The measured recycle gas hydrogen mole fraction is 0.90 and the reconciled value is 0.99. This error is mainly due to model error and the simplification of the hydrocarbon light end components. In the model, G does not evaporate at the process conditions in the separator. In the real process a molar fraction of 0.04 $C_1$ and $C_2$ hydrocarbons are present in the recycle gas. Also a molar fraction of 0.03 $C_3+$ is present. This indicates a non ideal behavior in the separator with some entrainment of heavier hydrocarbons. The pseudo component G may give a sufficiently accurate description of the reactions but seams to be to simple to give a good description of the separator and recycle system. The uncertainty of the recycle gas analyzer is set at a high value (0.1) since the "measurement error" in this case is mainly due to a modeling error.

The uncertainty of the heat transfer coefficient of heat exchanger two ($U2$) is large and practically not observable despite that the observability test in equation 4.5 shows that it is observable. A singular value decomposition of the matrix may give more practical information of the variable observability.

$$USV^{\mathrm{T}} = \begin{bmatrix} \widetilde{H}_r(z^*) \\ \widetilde{U} \end{bmatrix} \tag{4.43}$$

The singular values $s_i$, along the diagonal of $S$, have values $1.02 \times 10^{-3} < s_i < 23.2$ except for one value which equals $6.0 \times 10^{-7}$. The corresponding right hand side singular vector has all elements close to zero except for the element corresponding to the variable $U_2$, which is close to one ($1 - s(U_2) < 4 \times 10^{-9}$). If $r = USV^{\mathrm{T}}\tilde{z}$ a change in the variable $U_2$ has a small effect on the residual $r$, compared to the other variables. Changes in $U_2$ will also have a small effect on the the data reconciliation objective. This may be the reason that the reconciled value of $U_2$ is not changed and is always close to its initial value in all of 21 data sets.

## 4.8 Conclusions

A refinery naphtha reformer is successfully modeled using a simple unit model structure. Necessary scaling of variables and equations improves the numerical properties of the model. The condition number of the model equations are reduced from $2.3 \times 10^{12}$ to $3.6 \times 10^4$. The model equations are solved using seven iterations using "best guess" initial values.

The model is fitted to 21 different data points using data reconciliation. The results

show significant variation in catalyst efficiency parameters and deviation in reactor outlet temperatures. A good fit in one data set is not sufficient to claim that the model is a good description of the process.

The data reconciliation problem is analyzed and unobservable variables are identified. This example also shows that if a variable is defined as observable, by the observability test, it still may be practically unobservable. This is consistent with the computed uncertainty of the estimate, where the "barely observable variable" has an uncertainty of 6800 times its value.

The computed uncertainty of the measured values shows that the uncertainty in the estimate of reactor inlet and outlet temperatures, compared with the measurement, is typically reduced by 2%. The uncertainty in mass flows is typically reduced by 30%.

Optimal operation is computed for two common operational cases, case 1 and case 2 respectively, defined by a low and a high product price. The optimum operation has in case 1 seven active constraints and in case 2 four active constraints. In both cases active constraints are selected as controlled variables. In case 2, three degrees of freedom are unconstrained. The remaining three degrees of freedom are specified by adding three reactor inlet temperature differences as "self optimizing control variables".

An MPC (Model Predictive Control), with prioritizing of set points and constraints, has the required flexibility for implementation of the proposed control structure. This simple analysis also shows that the benefits of a real time optimizer (RTO), for computation of the set points for the unconstrained variables, are small.

# Appendix

## 4.A Thermodynamics

A set of simplified properties calculations for the five pseudo components, Hydrogen (H), Gas (G), Paraffines (P), Naphthenes (N) and Aromatics (A), are used in the reformer process model. The number of components in the model ($NC$) equals the number of pseudo components, i.e. $NC = 5$.

The properties of H is set equal to the properties of hydrogen ($H_2$). The properties of G is equal to the properties of a mixture with equal amount of Ethane, Propane and Butane ($C_2H_6, C_3H_8, C_4H_{10}$). P has the same properties as Heptane ($C_7H_{16}$), N the same properties as Cycloheptane ($C_7H_{14}$) and A the same properties as Toluene ($C_7H_8$).

The naphtha reformer feed has an average PNA composition of 35%, 52% and 13% respectively. The average liquid density is 763kg/m$^3$ and the average 50% boiling point is 387K.

The properties of a mixture of the above defined pseudo components, with the same PNA ratio has density equal to 777kg/m$^3$ and boiling point equal to 384.5K. This shows that the selected properties for the pseudo components gives a reasonable fit to the properties of the real process stream.

### 4.A.1 Enthalpy

The specific enthalpy of liquid and vapor is calculated using the specific heat capacity. The specific enthalpy of liquid is calculated as

$$h_l(\boldsymbol{x}, T) = \boldsymbol{x}^{\mathrm{T}} \boldsymbol{C}_{p_l}(T - T_r) \tag{4.44}$$

where $\boldsymbol{x}$ is the molar fractions of each component in the mixture and $\boldsymbol{C}_{p_l}$ is a $NC \times 1$ vector holding the value of specific heats of each component. For the liquid phase the specific heat is a constant value. $T$ and $T_r$ is the actual and reference temperature respectively. The reference temperature $T_r = 273.15$K

The specific enthalpy of a vapor is calculated as

$$h_v(\boldsymbol{x}, T) = \boldsymbol{x}^{\mathrm{T}} \boldsymbol{h}_{vl} + \boldsymbol{x}^{\mathrm{T}} \int_{T_r}^{T} \boldsymbol{C}_{p_v}(T) dT \tag{4.45}$$

where the heat of vaporization $\boldsymbol{h}_{vl}$ is a $NC \times 1$ containing the heat of vaporization, at the reference temperature, of each component. The specific heat of each component is described by a fifth order polynomial function.

$$C_{p_v} = a_0 + a_1 T^1 + a_2 T^2 + a_3 T^3 + a_4 T^4 + a_5 T^5 \tag{4.46}$$

where the coefficients $a_0 ... a_5$ are estimated from properties data tables obtained from NIST (2005).

The specific enthalpy of vapor is calculated as

$$\begin{aligned} h_v(\boldsymbol{x}, T) = \boldsymbol{x}^{\mathrm{T}} \boldsymbol{h}_{vl} + \boldsymbol{x}^{\mathrm{T}} \hat{\boldsymbol{a}}_0 (T - T_r) + \frac{1}{2} \boldsymbol{x}^{\mathrm{T}} \hat{\boldsymbol{a}}_1 (T - T_r)^2 \\ + \frac{1}{3} \boldsymbol{x}^{\mathrm{T}} \hat{\boldsymbol{a}}_2 (T - T_r)^3 + \frac{1}{4} \boldsymbol{x}^{\mathrm{T}} \hat{\boldsymbol{a}}_3 (T - T_r)^4 \\ + \frac{1}{5} \boldsymbol{x}^{\mathrm{T}} \hat{\boldsymbol{a}}_4 (T - T_r)^5 + \frac{1}{6} \boldsymbol{x}^{\mathrm{T}} \hat{\boldsymbol{a}}_5 (T - T_r)^6 \end{aligned} \tag{4.47}$$

where $\hat{\boldsymbol{a}}_0 ... \hat{\boldsymbol{a}}_5$ are $NC \times 1$ vectors of polynomial coefficients.

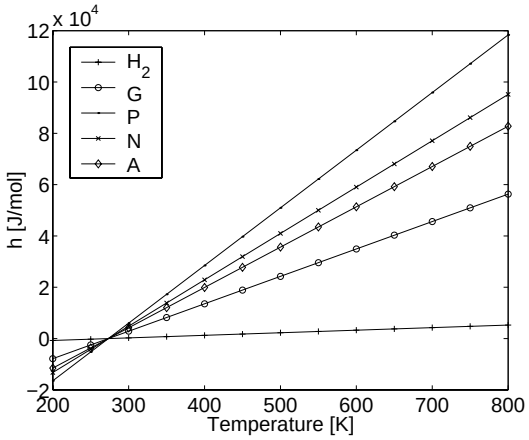


Figure 4.9: Liquid enthalpy plot

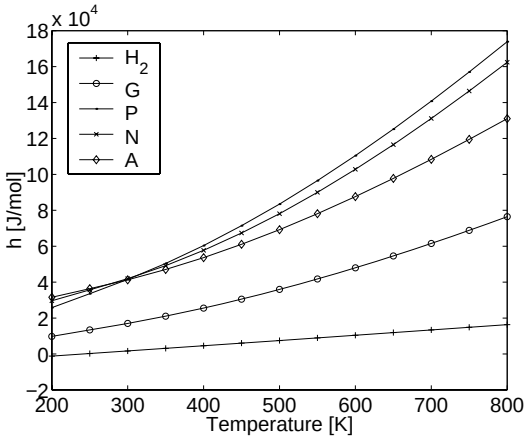


Figure 4.10: Vapor enthalpy plot

Figure 4.9 and 4.10 shows the enthalpy of the five pseudo components in the temperature range of 200-800K.

## 4.A.2 Entropy

The entropy is a function of composition, temperature and pressure. It is used in the compressor unit model and is calculated for the vapor phase only. The entropy of a gas with ideal gas behavior is written as

$$s_v(\boldsymbol{x}, T, P) = \boldsymbol{x}^{\mathrm{T}} \int_{T_r}^{T} \frac{\boldsymbol{C}_{p_v}(T)}{T} dT - R \log(P/P_r) \tag{4.48}$$

and the entropy function is calculated as

$$\begin{aligned} s_v(\boldsymbol{x}, T, P) = \boldsymbol{x}^{\mathrm{T}}\hat{\boldsymbol{a}}_0 \log(\frac{T}{T_r}) + \boldsymbol{x}^{\mathrm{T}}\hat{\boldsymbol{a}}_1(T - T_r) \\ + \frac{1}{2}\boldsymbol{x}^{\mathrm{T}}\hat{\boldsymbol{a}}_2(T - T_r)^2 + \frac{1}{3}\boldsymbol{x}^{\mathrm{T}}\hat{\boldsymbol{a}}_3(T - T_r)^3 \\ + \frac{1}{4}\boldsymbol{x}^{\mathrm{T}}\hat{\boldsymbol{a}}_4(T - T_r)^4 + \frac{1}{5}\boldsymbol{x}^{\mathrm{T}}\hat{\boldsymbol{a}}_5(T - T_r)^5 \\ - R\log(P/P_r) \end{aligned} \tag{4.49}$$

Figure 4.11 shows the entropy of the five pseudo components, at fixed pressure, in

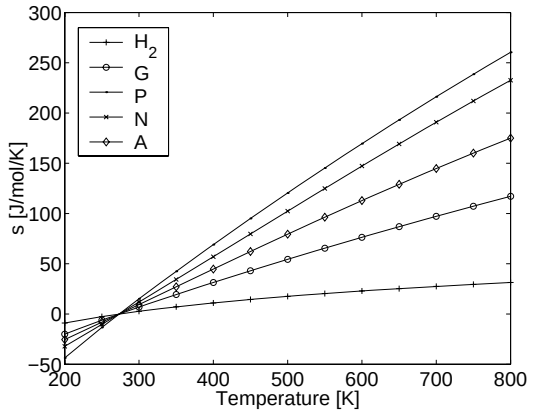


Figure 4.11: Vapor entropy plot at constant pressure, $P = P_r$.

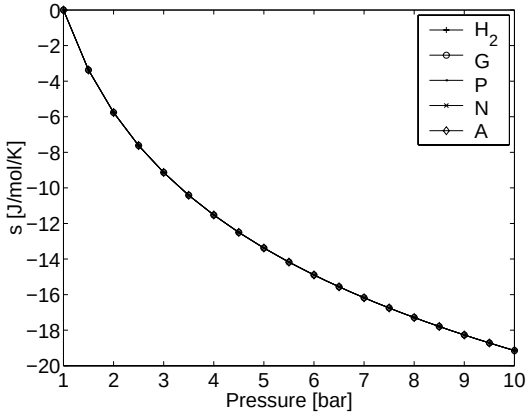


Figure 4.12: Vapor entropy plot at constant temperature, $T = T_r$

the temperature range of 200-800K. Figure 4.12 shows the same entropy, at fixed temperature, in the pressure range of 1-10 bar.

### 4.A.3 Vapor-liquid equilibrium

The equilibrium matrix $K$ relates the compositions of saturated vapor to the composition of saturated liquid at a given temperature $T$ and pressure $P$. This relation is written as

$$y = K(T, P)x \tag{4.50}$$

The relations of vapor and liquid composition is simplified by assuming no component interactions. I.e. the composition of A in the liquid phase does not influence on the composition of P in the vapor phase. This simplification makes $K$ a diagonal matrix. The diagonal elements of $K$ are calculated from the partial pressure of each component and total pressure of the mixture

$$k_{ii} = p_i/P \tag{4.51}$$

where $p_i$ refers to the partial pressure of component $i$ and $P$ is the total pressure. The partial pressure of the components in the mixture is calculated using the Antoine equation

$$p_i = 10^{\left(A_i - \frac{B_i}{T+C_i}\right)} \tag{4.52}$$

where $T$ is the temperature of the mixture. The Antoine equation parameters are specific for each component and its values are obtained from NIST (2005).

G is not a pure component and the partial pressure of G is set equal to the average partial pressure of the components in G ($(p_{C_2H6} + p_{C_3H8} + p_{C_4H10})/3$).

# Chapter 5

# On-line optimization of a crude unit heat exchanger network

*Presented at the CPC6 Conference, Tucson, AZ, Jan 2001*
*Published in the AIChE Symposium Series, Vol 98, No 326*
*Authors: Tore Lid, Sigurd Skogestad and Stig Strand*

## Abstract

*This section describes modeling and on-line optimization of a crude unit heat exchanger network at the Statoil Mongstad refinery. The objective is to minimize the energy input in the gas fired heater by optimally distributing the cold crude oil in the heat exchanger network. The steady state mass and energy balances of the 20 heat exchangers in the network yield the process model. This model is fitted to the measured values using data reconciliation. Unmeasured values like heat exchanger duty and heat transfer coefficients are computed. The fitted model is used to compute the optimal split fractions of crude in the network. This system has been implemented at the refinery and has resulted in a 2% reduction in energy consumption. In operational modes where the unit is constrained on energy input this gives an increased throughput and a significant contribution to the overall refinery profit.*

## 5.1 Introduction

This paper describes the development of a real time optimization system including model development, data reconciliation and on-line optimization. The case studied is a heat exchanger network for pre-heat of feed in a crude oil distillation unit at the Statoil Mongstad Refinery. The system is implemented and is now running in closed loop at the refinery.

The optimal operation is computed using a steady state model which before each run is fitted to the current operation point.

Process measurements contain uncertainties as random errors and possibly gross errors. This may be a result of miscalibration or failure in the measuring devices. This uncertainty is reduced when the current operation point is estimated using a larger number of measurements, than the number of unknowns in the process model, to compute a set of reconciled data.

Model parameters are estimated simultaneously or computed from the reconciled data.

The optimal operation is computed as the maximum of the objective subject to the process model, current process operation and model parameters. The optimal operation is finally implemented as setpoints in the process control system.

A large number of methods for data reconciliation have been suggested. These include robust objective functions (Chen et al., 1998), statistical tests, analysis of measurement redundancy and variable observability (Crowe et al., 1983). However, most examples and case studies presented in the literature are based on simulated processes, and most papers consider the data reconciliation decoupled from the optimization. One noteworthy exception is (Chen et al., 1998) who present an application of data reconciliation to a Monsanto sulfuric acid plant, but the paper is somewhat limited on details on the specific approach they have taken.

The objective of this paper is therefore to present an actual industrial implementation, where we provide details about the data reconciliation approach, model and optimization.

## 5.2 Data reconciliation

Data reconciliation is used to determine the current operation point. If measurement had no uncertainty the current operation point could be determined from $n - m$ independent measurements, where $n$ is the number of variables and $m$ the number of equations in the model.

Since the measurements are uncertain and there are a surplus of measurements, compared to the number of unknown variables in the model, data reconciliation is used to reduce this uncertainty.

The reconciled values minimizes some function of all measurement errors subject to the model equations. This is written as

$$\begin{aligned} \min_x & \sum_{i=1}^{n_m} \psi(\epsilon_i/\sigma_i) \\ \text{s.t.} \quad & Ax = 0 \\ & g(x) = 0 \end{aligned} \tag{5.1}$$

All variables are collected in the vector $x$ of dimension $n \times 1$. The measurement errors

$\epsilon_i = x_i - y_i$ where $y_i$ is a measurement of the variable contained in $x_i$. All measurement errors are scaled by their respective standard deviation $\sigma_i$.

The process model is separated into a set of linear equations, $Ax = 0$, and nonlinear equations, $g(x) = 0$, since most NLP solvers take linear and nonlinear equations as separate arguments.

If the uncertainty in the measurements are normally distributed with zero mean the summed squared measurement error is used as objective function, $\psi$, in equation 5.1. However, in the case of nonzero measurement error mean, also named gross errors, this method gives a biased estimate of the process variables. There are several methods for reducing the effect of gross errors.

In Crowe et al. (1983) and Crowe (1986) collective and individual statistical tests of the measurement errors are used to exclude measurements with gross errors.

In Chen et al. (1998),Tjoa and Biegler (1991) and Johnston and Kramer (1995) objective functions less sensitive to gross errors are used.

In this work the *Combined Gaussian* objective function is selected due to its numerical robustness and promising "small example" results.

In all robust objective functions the measurement error is scaled by its standard deviation. Normally this distribution is not known and the standard deviation has to be estimated from measured data or determined by a reasonable guess based on the actual measurement equipment installed and its measurement range.

The Combined Gaussian function is based on a weighted sum of two Gaussian distributions, one distribution of the random errors and one of the gross errors. The combined Gaussian probability density function is written as

$$f_i = \frac{1}{\sigma_i\sqrt{2\pi}}\left[(1-p)\exp\left(-\frac{1}{2}\frac{\epsilon_i^2}{\sigma_i^2}\right) + \frac{p}{b}\exp\left(-\frac{1}{2}\frac{\epsilon_i^2}{\sigma_i^2 b^2}\right)\right] \tag{5.2}$$

with the probability of a gross error in the measurements $p$ and the ratio of the standard deviations of the gross errors to that of the random errors $b$.

The objective function to be minimized is the negative logarithm of the probability density function, $\sum_{i=1}^{n_m} -\log(1/f_i)$.

The Combined Gaussian objective function is graphed in figure 5.1 with the least squares function for comparison. Compared to the least squares method the combined function gives less penalty for measurement errors larger than $3\sigma$. For the reconciled data this typically gives large measurement errors in few variables and small error in the other variables. At least intuitively this is what one would expect from the process measurements though it is difficult to verify.

In equation 5.1 there is no limitation on the number of measurements and on which variable to measure.

Before the reconciled variables are accepted some analysis has to be made to check if the unmeasured variables are observable. The measurements can also be classified as

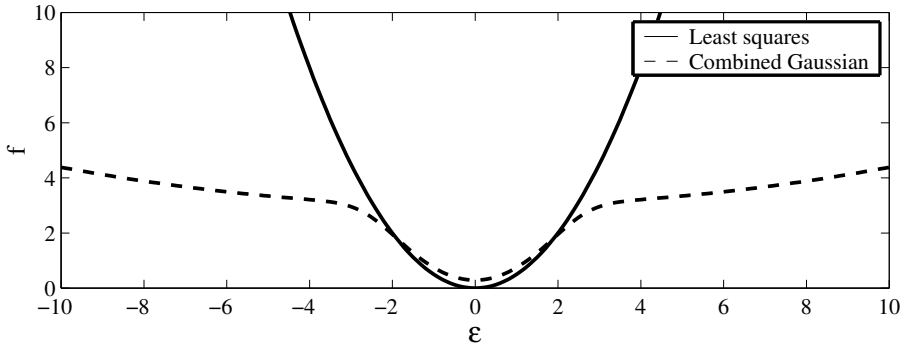


Figure 5.1: Combined Gaussian objective function. The standard deviation $\sigma = 1$, $p = 0.3$ and $b = 6$.

redundant or nonredundant measurements which can be used to evaluate the reconciled variables and decide if data reconciliation can be done when a specific measurement is out of service.

Let $x_r^*$ be a solution to the reconciliation problem in equation 5.1. The nonlinear constraints are linearized at the optimal solution $x_r^*$ such that $g(x) \approx g(x_r^*) + G(x - x_r^*)$, where $G = \partial g(x)/\partial x|_{x=x_r^*}$.

The linear and linearized constraints can now be written as

$$\hat{A}x - \hat{b} = 0 \tag{5.3}$$

where

$$\hat{A} = \begin{bmatrix} A \\ G \end{bmatrix} \qquad \hat{b} = \begin{bmatrix} 0 \\ g(x_r^*) - Gx_r^* \end{bmatrix}$$

The variables in $x$ are separated into measured variables, $y$, and unmeasured variables, $z$.

The matrix $\hat{A}$ is partitioned into $\hat{A}_1$ and $\hat{A}_2$ where $\hat{A}_1$ holds the columns of $\hat{A}$ corresponding to the measured variables and $\hat{A}_2$ the columns of $\hat{A}$ corresponding to the unmeasured variables. Equation 5.3 can now be written as

$$\hat{A}_1 y + \hat{A}_2 z = \hat{b} \tag{5.4}$$

To be able to compute the unmeasured variables, from the measured variables, the matrix $\hat{A}_2$ must have full column rank. If the number of measurements $n_y < n - m$, where $n$ is the number of variables and $m$ the number of equations, the size of $\hat{A}_2$ is $m \times n_z$ where $n_z > m$ and the matrix $\hat{A}_2$ has rank less than $n_z$. This implies that equation 5.4 has no unique solution for $z$ when $y$ is known. A requirement is that the number of measurements $n_y \geq n - m$, which is obvious, and that $\hat{A}_2$ has full column rank.

The measurements can also be separated into redundant and nonredundant measurements. If a measurement of a variable is redundant it still is possible to compute its

value if its measurement is removed. This is not the case for a nonredundant measurement and removing this measurement causes $\hat{A}_2$ to become rank deficient.

A simple test for redundancy is to check if $P^T\hat{A}_1$ has columns with only zero elements, where $P$ is defined as a matrix that spans the null space of $\hat{A}_2^T$. Any zero columns in corresponds to nonredundant measurements. Also note that for a nonredundant measurement $i$ we always have that $y_i - y_{mi} = 0$ and that this measurement does not contribute directly in the calculations of the reconciled values.

## 5.3 Optimization

The typical process optimization problem has a linear objective function like product price times product flow which is to be maximized. For system simplicity the same process model and variable vector are used in both data reconciliation and process optimization.

In the optimization problem some of the variable values are already known. These are typically disturbance variables and connects the data reconciliation with the optimization. The variable values are specified in the optimization problem as a set of linear constraints ($Rx = r$) where $r = Rx_r^*$.

The matrix $R$ has one nonzero element in each row, equal to one, corresponding to the element in $x$, which is set equal to its reconciled value. The optimization problem can now be written as

$$\begin{aligned} \min_x \; & -p^T x \\ \text{s.t.} \quad & Ax = 0 \\ & g(x) = 0 \\ & Rx = r \\ & x_{\min} \geq x \geq x_{\max} \end{aligned} \tag{5.5}$$

Inequality constraints in process optimization are typically bounds on singe variables. Inequality constraints on combinations of variables may be added in this formulation by introducing slack variables.

## 5.4 A case study

In the crude unit the crude feed is separated into suitable components for production of propane, butane, gasoline, jet fuel, diesel and fuel oil. The crude is preheated in a heat exchanger network where heat is recovered from the hot products and circulating refluxes.

As shown in figure 5.2 the cold crude (DCR) is separated into seven parallel streams (A-G) and heated by the hot products (abbreviations are listed in table 5.1). The flow in

each pass and BSR heat exchanger bypasses provides the degrees of freedom necessary for optimization. The optimization objective is to save energy and to recover as much

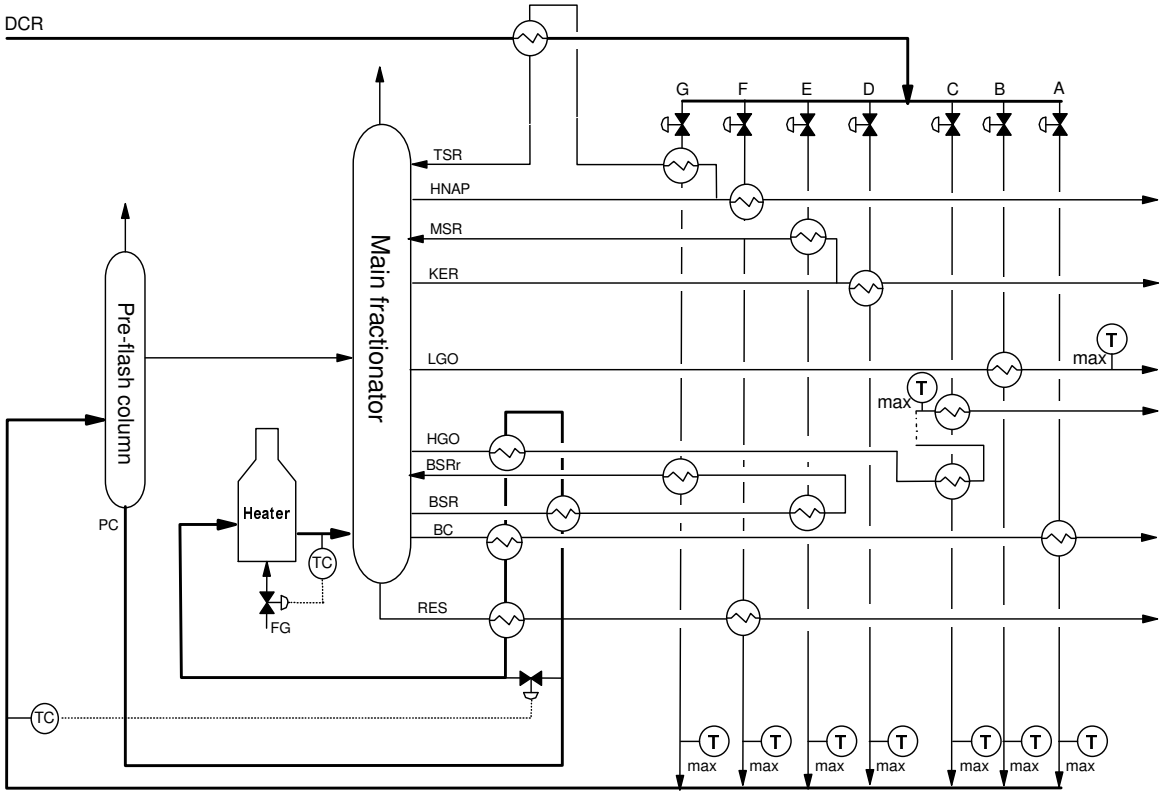


Figure 5.2: Simplified crude unit overview

heat as possible. The heater is the main energy input in the process and heater outlet temperature is held constant. The minimum energy is then achieved by maximizing of the heater inlet temperature.

Both distillation columns have feed conditions independent on the heat exchanger network operation. The inlet temperatures of both columns are assumed to have perfect temperature control. The feed flow and composition are then independent of operation of the heat exchanger network.

With this simplification a model of the distillation columns is not needed and a mass and energy balance of the heat exchanger network is a sufficiently detailed model for optimization. The optimal solution must be within several process operating constraints. The total crude flow or throughput is to be unchanged. At each crude pass outlet there is a maximum temperature constraint to avoid flashing.

The main column LGO and HGO products, exiting the heat exchangers, have a maximum temperature limit as the products are fed to the LGO and HGO driers (the driers are not drawn in figure 5.2).

The preflash column inlet temperature is to be unchanged. Some of the heat exchangers

| Abbreviation | Description |
|---|---|
| DCR | Desalted crude |
| HNAP | Heavy naphtha |
| KER | Kerosine |
| LGO | Light gas oil |
| HGO | Heavy gas oil |
| BC | Buffercut |
| RES | Residue |
| TSR | Top circulating reflux |
| MSR | Middle circulating reflux |
| BSR | Bottom circulating reflux |
| PC | Pre-flash column bottoms product |
| FG | Fuel gas |
| TC | Temperature control |
| Tmax | Temperature constraint |

Table 5.1: Abbreviations used in figure 5.2

are also included in the bottom circulating reflux (BSR) and the total duty in the BSR is to be unchanged.

## 5.5 The process model

The heat exchanger network can be viewed as a set of nodes or unit operations connected by arcs or in this case pipes. A set of balance equations, mass and energy balance, describes the internals of each node. Variables for the arcs or pipes are fluid temperature and mass flow. The nodes in this network are stream mix nodes, stream split nodes and heat exchanger nodes.

This selection of variables makes all nodes independent of all variables exept those included in the input and output arcs. Heat exchanger nodes also have some internal variables like heat transfer coefficient and duty. This variable selection makes the model structure simple and surveyable. It makes it practical possible to compute analytical derivatives of the nonlinear model equations. This reduces the numerical computational load in solving the model. The following describes the simplified balance equations for each type of node.

### 5.5.1 Mixing of streams

In a node where $n$ streams are mixed into one outlet stream the mass and energy balance equations can be written as

$$F_{\text{out}} - \sum_{i=1}^{n} F_{\text{in}_i} = 0 \tag{5.6}$$

$$F_{\text{out}} h(T_{\text{out}}) - \sum_{i=1}^{n} F_{\text{in}_i} h(T_{\text{in}_i}) = 0 \tag{5.7}$$

where $h(T)$ is the specific enthalpy of the fluid. The mass balance results in one linear equation and the energy balance in one nonlinear equation.

### 5.5.2 Splitting of streams

In a node where one inlet stream is separated into $n$ outlet streams the mass and energy balance equations can be written as

$$F_{\mathrm{in}} - \sum_{i=1}^{n} F_{\mathrm{out_i}} = 0 \tag{5.8}$$

$$T_{\mathrm{in}} - T_{\mathrm{out_i}} = 0 \qquad \forall\, i = 1...n \tag{5.9}$$

The mass balance results in one linear equation and the energy balance results in $n$ linear equations.

### 5.5.3 Heat exchanger

For a heat exchanger node hot and cold side mass and energy balance and heat transfer is written as

$$F_{\mathrm{c_{in}}} - F_{\mathrm{c_{out}}} = 0 \tag{5.10}$$

$$F_{\mathrm{h_{in}}} - F_{\mathrm{h_{out}}} = 0 \tag{5.11}$$

$$Q + F_{\mathrm{c_{in}}}(h(T_{\mathrm{c_{in}}}) - h(T_{\mathrm{c_{out}}})) = 0 \tag{5.12}$$

$$Q - F_{\mathrm{h_{in}}}(h(T_{\mathrm{h_{in}}}) - h(T_{\mathrm{h_{out}}})) = 0 \tag{5.13}$$

$$Q - \varepsilon C_{\min}(T_{\mathrm{h_{in}}} - T_{\mathrm{c_{in}}}) = 0 \tag{5.14}$$

where the mass balance results in two linear equations (5.10 ,5.11) and the energy balance results in two nonlinear equations (5.12, 5.13). The heat transfer is described by equation 5.14. The heat exchangers in this unit is of multiple tube and multiple shell pass type and the $\varepsilon$-Ntu method (Mills, 1995) is used for calculation of the heat transfer. In equation 5.14 $\varepsilon$ is the efficiency and $C_{\min}$ is the minimum capacity. $C_{\min}$ is calculated as

$$C_{\min} = \min(C_{\mathrm{c}}, C_{\mathrm{h}}) \tag{5.15}$$

$$C_{\mathrm{c}} = F_{\mathrm{c_{in}}} \mathrm{C_{p_c}} \approx F_{\mathrm{c_{in}}} \frac{h\left(T_{\mathrm{c_{out}}}\right) - h\left(T_{\mathrm{c_{in}}}\right)}{T_{\mathrm{c_{out}}} - T_{\mathrm{c_{in}}}} \tag{5.16}$$

$$C_{\mathrm{h}} = F_{\mathrm{h_{in}}} \mathrm{C_{p_h}} \approx F_{\mathrm{h_{in}}} \frac{h\left(T_{\mathrm{h_{out}}}\right) - h\left(T_{\mathrm{h_{in}}}\right)}{T_{\mathrm{h_{out}}} - T_{\mathrm{h_{in}}}} \tag{5.17}$$

The efficiency, $\varepsilon$, is a function of the number of transfer units, Ntu, and the capacity ratio, $R_C$. $R_C$ and $Ntu$ is calculated as

$$R_C = \frac{C_{\min}}{C_{\max}} \quad Ntu = \frac{UA}{C_{\min}} \tag{5.18}$$

where $C_{\max} = \max(C_c, C_h)$. The efficiency $\varepsilon$ equals $\varepsilon_1$ for heat exchangers with single shell pass ($n = 1$) and a even number of tube passes. $\varepsilon$ equals $\varepsilon_2$ for heat exchangers with even number of tube passes and $n$ shell passes. $\varepsilon_1$ and $\varepsilon_2$ is calculated as

$$\varepsilon_1 = 2\left\{1 + R_C + \sqrt{1+R_C^2}\frac{1+\exp\left(-\frac{Ntu}{n}\left(\sqrt{1+R_C^2}\right)\right)}{1-\exp\left(-\frac{Ntu}{n}\left(\sqrt{1+R_C^2}\right)\right)}\right\}^{-1} \tag{5.19}$$

$$\varepsilon_2 = \left[\left(\frac{1-\varepsilon_1 R_C}{1-\varepsilon_1}\right)^n - 1\right]\left[\left(\frac{1-\varepsilon_1 R_C}{1-\varepsilon_1}\right)^n - R_C\right]^{-1} \tag{5.20}$$

When the equations for $C_{\min}$ and $\epsilon$ is substituted into equation 5.14 each heat exchanger is described by two linear and three nonlinear equations.

### 5.5.4 Model summary

There are totally 85 streams and 20 heat exchangers in the heat exchanger network. There are 9 stream mixes and 7 stream splits. The variables are 85 flows and 85 temperatures from the streams, 20 heat exchanger duties, 20 heat transfer coefficients and adds up to totally 210 variables.

From the heat exchangers we have 40 linear and 60 nonlinear equations. From the stream mixing nodes we have 9 linear and 9 nonlinear equations and from the split nodes we have 29 linear equations.

Coefficients for linear equations are collected in the matrix $A$ where each equation occupy one row. The equation coefficients are placed in the column corresponding to its variable position in $x$. The nonlinear equation residues are collected in the residual vector $g(x)$.

The model is now in the preferred form

$$Ax = 0 \tag{5.21}$$

$$g(x) = 0 \tag{5.22}$$

where $A$ is a $78 \times 210$ matrix with the linear equation coefficients and $g(x)$ is a $1 \times 69$ vector of nonlinear equation residues.

## 5.6 On-line data reconciliation

Data is sampled from the process as one hour averages and reconciled using the Combined Gaussian objective function. Standard deviations for measurements are selected to be 1°C for temperature measurements and 2% of the maximum measuring range for flow measurements.

The Combined Gaussian parameters $p$ and $b$ are set to 0.3 and 6.

To avoid numerical difficulties in the model equations, like reversed flows, appropriate variable bounds are added to the data reconciliation problem in equation 5.1.

There are 88 measurements in the process, which is a surplus of 25 compared to the number of unknowns in the process model. The described analysis shows that all unmeasured variables are observable and that all measurements are redundant. As an

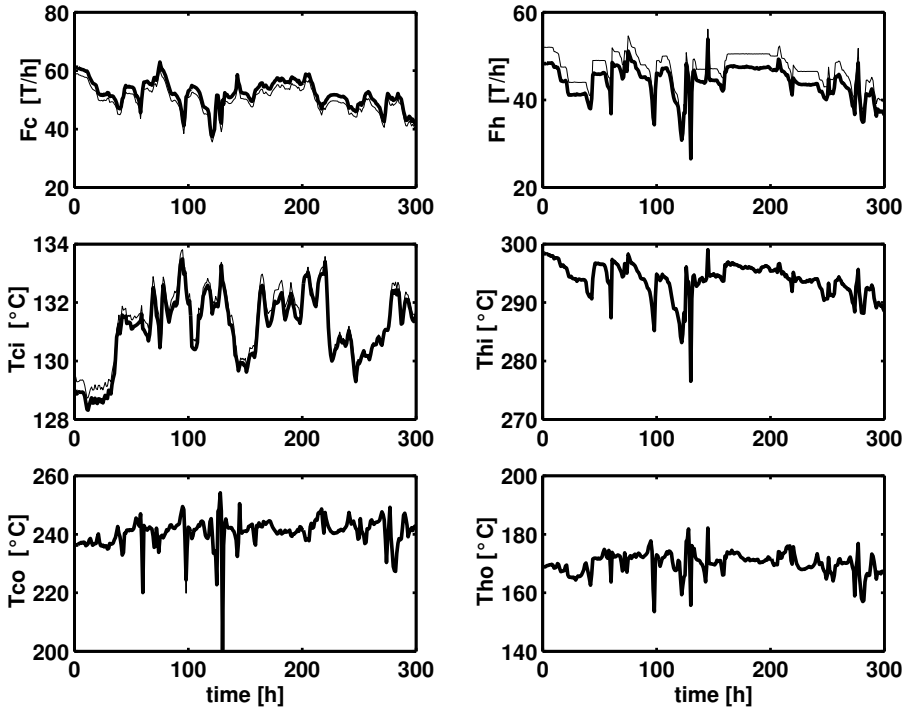


Figure 5.3: Measured (thin lines) and reconciled values (thick lines) for one of the heat exchangers

example figure 5.3 shows measured and reconciled values for 300 successive samples of one hour averages.

The imbalance in the data is most likely caused by a gross error in the flow measurement of the hot stream $F_{\mathrm{h}}$. The average error is 3.1 T/h and is fairly constant in all samples.

## 5.7 On-line optimization

In the optimization problem the number of equality constraints are increased to 205 which leaves 5 degrees of freedom. These degrees of freedom correspond to the flow trough each of the seven passes in the hot train minus two since the total flow and BSR duty is set equal to the reconciled value.

As an example measured data is reconciled and optimum operation computed. Com-

pared to current operation the pass flow (A-G) is changed by [0.0,-9.2,-0.1,+9.0,+0.1,+1.0,-0.8]%.

In addition bypass flows of heat exchangers in the BSR is changed such that more heat is added in each pass while keeping the total duty constant. This increases the heater pre-heat duty by 2.3MW. Compared to the heater duty of $\approx$ 100MW this gives a 2% reduction of energy requirement. Constraints on pass G outlet temperature and LGO drier inlet temperature is active at optimal operation.

Optimal operation is implemented as flow ratio setpoints in the MPC controller.

Both the data reconciliation and optimization problems are solved using a software package for constrained optimization problems (NPSOL from Stanford University). This system runs on a DEC-Alpha computer and the average solution time is 3 minutes.

## 5.8 Conclusion

A process model describing the mass and energy balance is developed and used for data reconciliation and optimization. The model is fitted to the measured values and optimal feed split fractions are computed and implemented in the control system once an hour.

The reconciled values provides valuable information about the current condition of the measurement equipment and of the condition of the heat exchangers. Comparison of reconciled values and measured values revealed several flow measurements with poor performance and also a temperature measurement installed in the wrong pipe. The evolution of heat transfer coefficients during operation is also used to detect fouling and to schedule cleaning of the heat exchangers.

The model is sufficiently detailed for optimization purposes and the predicted optimal heater inlet temperature is achieved in the process.

## 5.9 Acknowledgement

The authors acknowledge the support of the process control staff at the Statoil Mongstad Refinery and the Statoil Research Centre for all help in implementing this system as a Septic MPC and RTO application.

# Chapter 6

# Implementation issues for real-time optimization of a crude unit heat exchanger network

*Presented at the European Symposium On Computer Aided Process Engineering-11*
*Escape-11, Kolding, Denmark, 27-30 May 2001*
*Authors: Tore Lid and Sigurd Skogestad*

## Abstract

*This section provides a case study on the selection of controlled variables for the implementation of real time optimization in a crude unit heat exchanger network. Two different control strategies with 22 different control structures are evaluated. The idea is to select the controlled variables that give the best plant economic performance (smallest loss) when there are disturbances (self-optimizing control). The disturbances are correlated and a simple principal component analysis is used to generate a more realistic set of disturbance variations for evaluation of the different control structures. This analysis shows a large variation of loss for different control structures and proves that a control structure evaluation is necessary to collect the benefits from a RTO system.*

## 6.1 Introduction

A real time optimization system (RTO) can be described as a sequence of three separate functions, (White, 1997).

1. Data reconciliation and parameter estimation to establish the current operation point.

2. Optimization to find optimal operation.

3. Implementation of the optimal result (which variables to control).

Estimated parameters and reconciled process variables are the basis for operations optimization. The optimal operation is computed by maximization of some objective subject to the process model and operating constraints.

The objective can be a direct measure of the profit or some function of the variables that when maximized drives the process towards the optimal operation. Finally the computed optimal operation is implemented in the process as setpoints of the control system.

The selection of these variables is the main focus of this paper. In the RTO "loop" there is a loss related to uncertainty in the process measurements, inaccuracy of the estimated parameters and model errors (Forbes and Marlin, 1996; Zhang and Forbes, 2000). Optimal values for operation are computed at regular intervals and implemented as setpoints of the control system.

In the period from one optimization run to the next the disturbances will change and the operation is no longer optimal.

In addition uncertainties in the controlled variable measurements cause an operation that deviates from the true optimal operation. The disturbance error and control error are sources of a disturbance and control loss, (Skogestad et al., 1998). These losses depend highly on the control variables selected for implementation of the optimization result and the control variables are selected such that this loss is minimized. If some process constraint is active for all expected variations in the disturbances, this variable should be selected as a controlled variable. This is active constraint control, (Maarleveld and Rijnsdorp, 1970). The variable is then held at its optimal value for all disturbance variations.

If the controlled system has infeasible solutions (constraint violations), with the selected control structure, for some disturbance a back-off from constraints must be computed. The back-off is computed such that the controlled system has feasible solutions for all expected disturbances (Perkins, 1998).

To simplify the analysis, several assumptions have been made. The controlled variables selection is solely based on steady state considerations and no evaluation of possible dynamic control problems are made. A prefect model is assumed. Estimated parameters and process variables (reconciled values) are assumed to have no uncertainty. By these assumptions the computed optimal values, based on reconciled measurements and model parameters, describe the true process optimum.

## 6.2 The optimization problem

A typical process optimization problem has a linear economic objective function, nonlinear process model and some operational constraints. The optimization problem can be formulated as

$$\begin{aligned} \max_x J &= p^T x \\ \text{st.} \quad g(x, d_0, \beta) &= 0 \\ x_{\min} \leq x &\leq x_{\max} \end{aligned} \tag{6.1}$$

where the process variables are included in $x$. The objective, $J$, is typically product price times product flow minus feed price times feed flow and energy price times energy flow. The process model is included as an equality constraint, $g(x, d_0, \beta) = 0$, where $d_0$ are the nominal disturbance values $\beta$ are the model parameters. Inequality constraints are typically bounds on single process variables e.g. high temperature limits or a low flow limit. In this problem there are $n$ variables (in $x$), $m$ process equations ($g(x, \beta)$) and $m_d$ disturbances. The solution, $x^*(d_0)$, to 6.1 is referred to as the nominal optimum.

## 6.3 Implementation of optimal values

The solution to the optimization problem in 6.1, $x^*$, is implemented as setpoints to $n_f$ variables using a controller $C$. The controller may be included in the system as a set of linear constraints $Cx = r_0$ where each row in $C$ has one nonzero element, equal to one, corresponding to the selected controlled variable.

$$\begin{aligned} g(x, d, \beta) &= 0 \\ Cx &= r_0 \end{aligned} \tag{6.2}$$

The controller setpoints equal the nominal optimum, $r_0 = Cx^*$. The controlled system has the solution $x_c(d, r_0)$ and objective $J_c(d, r_0) = p^T x_c(d, r_0)$. A requirement on the controller is that the controlled variables are independent such that the controlled system has rank equal to the number of variables, i.e.

$$\text{rank} \begin{bmatrix} \frac{\partial g(x,d,\beta)}{\partial x} \mid_{x^*} \\ C \end{bmatrix} = n \tag{6.3}$$

## 6.4 The loss function

The disturbance loss function, (Skogestad et al., 1998), is defined as the difference of the optimal objective of some disturbance $d$, $J^*(d)$ and the objective achieved by using

a control structure $C$, with nominal optimal values as setpoints. The loss function can be written as

$$L(d) = J^*(d) - J_c(d, r_0) \tag{6.4}$$

where $J^*(d)$ is the objective of the optimal operation with a known disturbance $d$ (solution of problem 6.1) and $J_c(d, r_0)$ the objective of the controlled system using the controller $C$ with the nominal optimum as setpoints (solution to problem 6.2).

The disturbance loss function describes the loss of keeping the old setpoints (not re-optimizing) when the disturbance $d$ has changed to a value different from $d_0$.

In addition to the loss of a disturbance change there is a loss due to implementation errors or control errors. The variables selected as control variables varies around the optimal setpoint due to dynamic disturbances, measurement inaccuracy and noise. The control error loss function can be written as

$$L(\triangle r_e) = J^*(d_0) - J_c(d_0, r_0 + \triangle r_e) \tag{6.5}$$

where $\triangle r_e$ is the control error. The disturbance loss and control error loss is greater than zero for all values of $d$ and $\triangle r_e$. In the nominal point where $\triangle r_e = 0$ and $d = d_0$ the loss is zero. This definition of loss gives one loss function for each disturbance. In the case of two or more disturbances a single resulting loss function or a scalar measure of the loss would be preferable. A resulting loss function may be approximated as the sum of the individual loss functions where the individual disturbances are scaled by their variation range. A scalar measure can be calculated as the area below the loss function or the integral of $L(\delta_d)$ from $\delta_d = -1$ to $\delta_d = 1$. A similar scalar loss value can be calculated for the control error loss. The total loss for a control structure is calculated as the sum of the disturbance loss and control loss. With this simplification the loss is calculated along each of the disturbance axis. Other measures, as the sum of all corner points or the resulting loss of a Monte Carlo simulation could also be used.

## 6.5 Disturbance analysis

In the above analysis the aim is to find a controller which minimizes the loss in presence of disturbances. A key issue is to find and use a good representation of the disturbance variation. The normal variation of the disturbance variables should preferably be computed from process measurements. If measured data is unavailable, disturbance variations may be estimated based on experience from similar processes and design information. It is reasonable to expect that fast varying disturbances are mainly measurement noise and do not give a real contribution to the disturbance loss. Slow varying disturbances (slow compared to the RTO execution frequency) is detected by the data reconciliation and parameter estimation functions, and accounted for in the optimization results, and also gives a small contribution to the disturbance and control error loss. The intermediate rate of variation in the disturbances are the difficult ones as they gives a contribution to the loss in the period between RTO execution intervals.

When an RTO updates the optimal setpoints at regular intervals, an average of the disturbance standard deviation for each interval gives a measure of the expected disturbance change from one optimization run to the next. High frequency measurement noise must be removed prior to this computation. With this disturbance description the controller performance is evaluated with a disturbance change in one disturbance at a time. The total loss function is computed as the sum of the loss functions for each individual disturbance.

In a real process we often have the situation that the disturbances are correlated. The above analysis, evaluating the loss of one disturbance at a time, will fail to evaluate the loss with the most likely combinations of disturbances. By assuming a linear relation and using simple principal component analysis, (Jackson, 1991), the measured disturbances may be transformed into a reduced set of uncorrelated disturbances or principal components. The measured disturbance data in $\Psi = [d_1, d_2 ... d_p]$ is zero centered such that each variable has zero mean, $\Psi_{s_{(ij)}} = (d_{ij} - \bar{d}_j)$. The disturbance covariance matrix $X$ is computed as

$$X = \frac{1}{(K-1)} \Psi_s^T \Psi_s \tag{6.6}$$

where $K$ is the number of disturbance data samples in $\Psi_s$. The principal components, $Z$, or uncorrelated disturbance values are computed as $Z = \Psi_s P^T$, where $P$ are the eigenvectors of $X$. The columns of $Z$ are the $n_d$ new uncorrelated variables, $z_j$. Based on this linear transformation a new set of disturbances for evaluation of the selected controller may now be computed as $d = d_0 + p_j \triangle z_j$ where $\sigma_{zi} \leq \triangle z_i \leq \sigma_{zi}$. The variance of each principal component is computed for RTO execution intervals as described above. The fraction of variation in the disturbance data, described by each principal component $z_j$ is computed as $\lambda_j / \sum_j \lambda_j$ where $\lambda_j$ are the eigenvalues of $X$. The number of principal components used is selected such that the principal components describes the majority (i.e. 90% or 95%) of the variance in the measured data. This representation of the disturbance data provides a more realistic basis for selection of the minimum loss control structure.

## 6.6 Case study

In the crude unit the crude (CRU) is preheated in a heat exchanger network where heat is recovered from the hot products and circulating refluxes. As shown in figure 6.1 the cold crude is separated into seven parallel streams (A-G). The flow in each pass provides the degrees of freedom necessary for optimization. Changes in product yields and bottom circulating reflux (BSR) duty are the main disturbances to the heat exchanger network. The yield changes may be caused by feed composition changes or operational changes. The optimization objective is to save energy by recovering as much heat as possible. The heater is the main energy input in the process and heater outlet temperature is held constant. The minimum energy is then achieved by

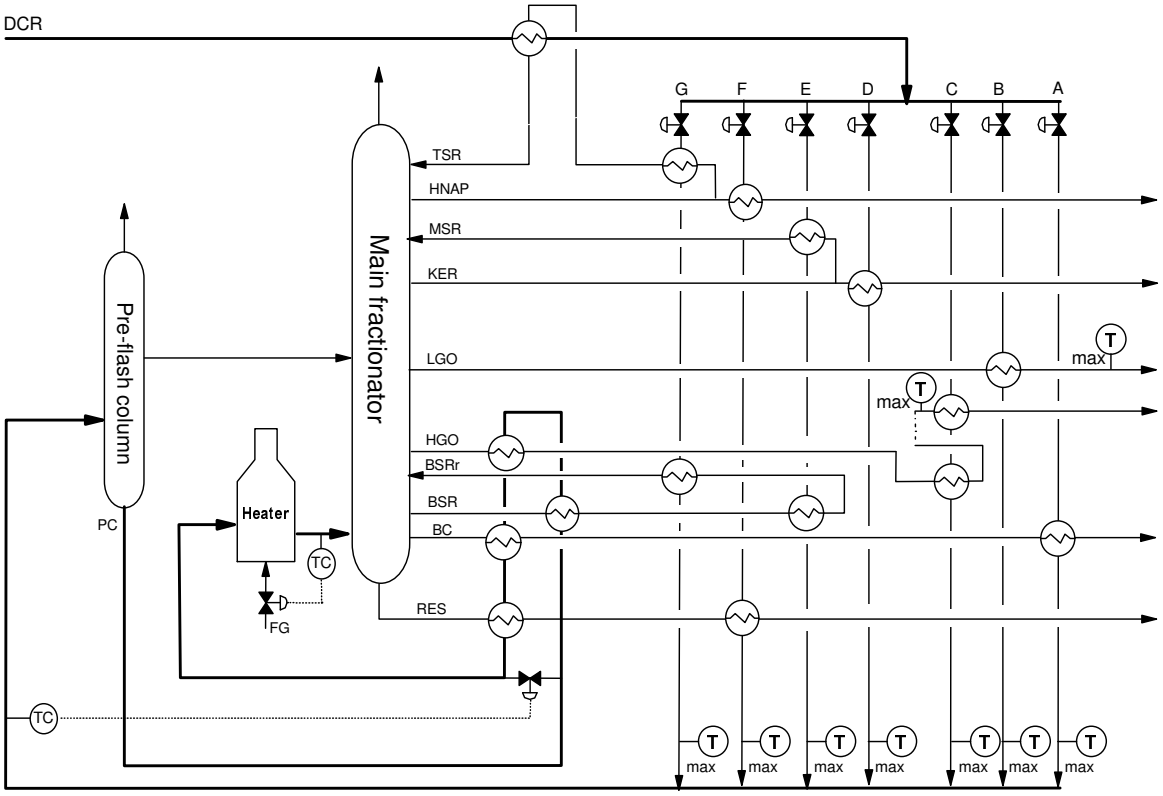


Figure 6.1: Simplified crude unit overview

maximizing the heater inlet temperature. A detailed description of the process, steady state model, data reconciliation and optimization is presented in Lid and Skogestad (2001).

### 6.6.1 Disturbances

There are 23 disturbance variables. These are the flows and temperatures of streams flowing into the heat exchanger network. The data used in this analysis are 35 days of 12 minutes averages sampled from normal process operation . The RTO execution interval is one hour. The disturbance measurements where reduced to four principal components using PCA as described in section 6.5. The average variance of the principal components within each optimization interval was computed and used as disturbance variation.

### 6.6.2 Control structure evaluation

There are a large number of possible controllers for implementation of the optimization result. The only requirement is that all 5 degrees of freedom in the process must be specified or that the controlled system rank requirement is satisfied. In this case study two control strategies are evaluated.

Strategy 1: the optimal result is implemented as setpoints to the flow controllers in each pass (open loop implementation).

Strategy 2: the optimal result is implemented as setpoints to pass outlet temperature controllers (closed loop implementation) where the temperature controllers manipulate the corresponding pass flow. The rank requirement, in equation 6.3, for the controller with the open or closed loop implementation strategy may be stated by two simple rules. First, the flow or temperature in pass D and G can not be specified simultaneously since then it would not be possible to control the total BSR duty. Second, only five flows or temperatures in the seven passes can be specified simultaneously since the sum of all seven pass flows is specified and constant. This makes effectively one of the flows as a dependent variable.

11 different control structures exists in the open loop implementation strategy which satisfies the rank requirement. In Table 6.1 all possible flow control combinations are numbered 1-11 and in Table 6.2 all possible temperature control combinations are numbered 12-22. For each control structure the disturbance loss, control loss and total loss are computed. The control variable selections in table 6.1 and 6.2, are sorted by total loss. The results show that the best open loop implementation strategy is to select the flow controllers of pass A,B,C,D and E as controlled variables. The setpoints of these controllers is set equal to the current nominal optimum. Pass G is used for total BSR duty control and pass F is used for total flow control. In table 6.2 the loss functions for different temperature control combinations are listed. The total loss for

the best controller is reduced by 57% when the outlet temperatures of pass A,B,C,D and E are used as controlled variables.

| No. | CV | $L_d$ | $L_{\triangle r_e}$ | $L$ |
|---|---|---|---|---|
| 1 | ABCDE | 0.013 | 0.009 | 0.021 |
| 4 | ACDEF | 0.015 | 0.018 | 0.034 |
| 7 | ABCEG | 0.040 | 0.010 | 0.050 |
| 2 | ABCDF | 0.021 | 0.031 | 0.052 |
| 6 | ABCEF | 0.021 | 0.032 | 0.053 |
| 3 | ABDEF | 0.023 | 0.031 | 0.054 |
| 10 | ACEFG | 0.053 | 0.020 | 0.073 |
| 5 | BCDEF | 0.038 | 0.047 | 0.084 |
| 8 | ABCFG | 0.068 | 0.034 | 0.102 |
| 9 | ABEFG | 0.080 | 0.034 | 0.114 |
| 11 | BCEFG | 0.123 | 0.050 | 0.173 |

Table 6.1: Flow control

| No. | CV | $L_d$ | $L_{\triangle r_e}$ | $L$ |
|---|---|---|---|---|
| 12 | ABCDE | 0.002 | 0.007 | 0.009 |
| 15 | ACDEF | 0.002 | 0.015 | 0.017 |
| 13 | ABCDF | 0.005 | 0.024 | 0.029 |
| 14 | ABDEF | 0.004 | 0.025 | 0.029 |
| 17 | ABCEF | 0.007 | 0.023 | 0.030 |
| 16 | BCDEF | 0.006 | 0.038 | 0.043 |
| 18 | ABCEG | 0.101 | 0.054 | 0.156 |
| 21 | ACEFG | 0.123 | 0.072 | 0.195 |
| 19 | ABCFG | 0.183 | 0.101 | 0.284 |
| 20 | ABEFG | 0.183 | 0.105 | 0.288 |
| 22 | BCEFG | 0.245 | 0.145 | 0.390 |

Table 6.2: Temperature control

Independent of disturbance representation the selection of pass A,B,C,D and E as controlled variables gives the minimum loss both for the open and closed loop implementation strategy. From table 6.1 to 6.2 it is clear that controllers including flow or temperature in pass G and F as controlled variables generally give a large loss.

The difference in loss for the flow control structures may be explained by the fraction of crude flow trough each pass. At the nominal optimum the fractions in pass A-G is [6 15 12 16 10 33 8]% respectively. Pass F has the largest flow and should be used to control the total flow since this will give the smallest relative error in presence of feed flow disturbances. A similar argument applies to the selection of pass E or G to control BSR total duty. The heat transferred from BSR is 4.2MW to pass G and 2.2MW to pass E. The pass receiving the largest duty should be selected to control the total duty in the BSR since this will give the smallest relative change in presence of disturbances.

The loss computed using principal components is in general smaller than the loss computed using the disturbances independently. This is explained with the fact that

the mass and energy balance in the process is always "zero". If the cold feed flow increases, the hot product flows will also increase. If there is a change in the product yield the flow of a hot product may decrease. The product temperature increases due to the same yield change, leaving the heat content almost unchanged. These dependencies in the disturbances cancel some of the effects on the total loss.

## 6.7 Conclusion

A method for selection of controlled variables for implementation of real-time optimization results based on the loss function is described (Skogestad et al., 1998). The analysis is solely based on steady state considerations and no evaluation of the resulting control problem is made. An open equation model formulation, typically for data reconciliation and optimization problems, is used in the analysis with no reformulation of model equations. The selection is based on how the controlled process will act in presence of disturbances compared to optimal operation. Some control structures are proposed and evaluated in presence of single disturbance variation and a description of disturbances using principal components. The minimum loss control structure is achieved by selecting the outlet temperature of pass A,B,C,D and E as controlled variables. The worst case loss, using temperature control, is 0.39°C which is more than 10% of the RTO system heater inlet temperature gain. This shows that proper selection of controlled variables is vital for achievement of maximum RTO benefits.

# Chapter 7

# Conclusions and further work

## 7.1 Conclusions

Data reconciliation and optimization have been applied to example processes and to real refinery processes. A first principle process model is used for data reconciliation and optimization. The process model has both measured and unmeasured variables. Typical model parameters, like heat transfer coefficients and efficiency, are included in the model as unmeasured variables. This selection of variables integrates data validation, model update and data reconciliation. The reconciled values are the basis of the optimization of the actual operation where the variable values of model parameters and variables like feed composition, feed temperature are fixed, leaving a few degrees of freedom for optimization. The optimal operation is implemented as set points in the control system for the controlled variables. The controlled variables are selected such that the presence of disturbances only causes a small deviation of the objective from is optimal value.

A generic process modeling framework for building steady state models has been developed. The procedure is based on unit models that interact through a shared variable vector. The unit models and specifications form an "open equation" set, well suited as nonlinear constrains in an optimization problem. In the suggested structure each unit model can be developed, tested and scaled individually before it is added to the overall process model. This simplifies the modeling work and saves a lot of troubleshooting. A new scaling procedure, which is applied at unit model level, results in a significant improvement in the overall numerical properties of the model.

The numerical examples of the flash process optimization shows that proper scaling reduces the number of iterations used for solving each case. More important though, it makes the results more reliable.

Data reconciliation is used to estimate the current state of the process based on available measurement and a first principle process model. The measurements are classified as redundant or non-redundant, and the unmeasured variables as observable, barely ob-

servable and unobservable. If gross errors are present (systematic errors) these can be detected and the corresponding measurements removed or a robust objective function can be selected.

The reconciliation problem analysis also levels the expectations of what can be achieved by the use of data reconciliation methods. If only random measurement errors are present the least squares objective function, based on a Gaussian error distribution, results in a maximum likelihood estimate of the process state.

When systematic or gross errors are present, the data reconciliation problem is more challenging. The simple evaluation in section 3.4 does not give a clear indication of which method or objective function to select. The preferred method is dependent of its numerical properties and the error characteristics.

The gross error detection method with measurement removal is a sequential method where one measurement is removed as long as a gross error is detected. In each iteration, a data reconciliation problem has to be solved.

The robust objective functions evaluated are the Gauss, Combined Gaussian, Cauchy and Fair function. The Cauchy function has good performance but has poor numerical properties. The influence function approaches zero for large values of e and the probability of converging at a local minima is high, compared to the other methods. The Gauss, Combined Gaussian and Fair functions are all numerically robust. The Combined Gaussian had the overall best performance in the example and was selected as the preferred method to be used in later chapters.

In Chapter 4 a refinery naphtha reformer is modeled using the described modeling framework. The proposed scaling of variables and equations improves the numerical properties of the model. The condition number of the model equations is reduced from $2.3 \times 10^{12}$ to $3.6 \times 10^{4}$. The model equations are solved using seven iterations using "best guess" initial values.

The model is fitted to 21 different data points using data reconciliation. The results show significant variations in catalyst efficiency parameters and deviation in reactor outlet temperatures. A good fit in one data set is not sufficient to claim that the model is a good description of the process.

The data reconciliation problem is analyzed and unobservable variables are identified. This example also shows that if a variable is defined as observable by the observability test it still may be practically unobservable. This is consistent with the computed uncertainly of the estimate, where the "barely observable variable" has a uncertainty 6800 times its value.

The computed uncertainty of the measured values shows that the uncertainty in the estimate of reactor inlet and outlet temperatures, compared with the measurement, is typically reduced by 2%.

Optimal operation is computed for two common operational cases defined by a low or high product price. The optimum operation has in case 1 seven active constraints and in case 2 four active constraints. In both cases active constraints are selected as con-

trolled variables. In case 2, three degrees of freedom are unconstrained. The remaining three degrees of freedom are specified by adding three reactor inlet temperature differences as "self optimizing control variables". A MPC (Model Predictive Control), with prioritizing of set points and constraints, has the required flexibility for implementation of the proposed control structure. This simple analysis also shows that the benefits of a real time optimizer (RTO), or computation of the set points for the unconstrained variables, are small.

Chapter 5 describes the data reconciliation and optimization crude unit heat exchanger network where the objective is to maximize heat recovery. A process model describing the mass and energy balance is used for data reconciliation and optimization. The model is fitted to the measured values by data reconciliation and optimal feed split fractions are computed and implemented in the control system once an hour. The reconciled values provide valuable information about the current condition of the measurement equipment and of the condition of the heat exchangers. Comparison of reconciled values and measured values has detected several flow measurements with pour performance and also a temperature measurement that was found to be installed in the wrong pipe. The evolution of heat transfer coefficients during operation is also used to detect fouling and schedule cleaning of the heat exchangers. The model is sufficiently detailed for optimization purposes and the predicted optimal heater inlet temperature is achieved in the process.

Chapter 6 describes a method for selection of controlled variables for implementation of real-time optimization results based on the loss function, (Skogestad et al., 1998). The analysis is based on steady state considerations and no evaluation of the resulting control problem is made. The selection of control variables is based on how the controlled process will act in presence of disturbances compared to optimal operation.

Some control structures are proposed and evaluated in presence of single disturbance variation. The individual disturbances are strongly correlated and a description of the dominating disturbance variation is created using principal components.

The minimum loss control structure is achieved by selecting the outlet temperature of pass A,B,C,D and E as controlled variables. The worst case loss, using temperature control, is 0.39°C which is more than 10% of the RTO system heater inlet temperature gain. This shows that proper selection of controlled variables is vital for achievement of maximum RTO benefits.

## 7.2 Further work

Future work The thesis has only considered steady-state models for data reconciliation and optimization.

The reason is that that this is sufficient for the majority of applications in the refining industry. However, extensions to include dynamics are important in some cases and should be included for future work.

The modeling framework described in Chapter 2 can be extended from the current steady state unit models to dynamic unit models. The scaling procedure and computation of first order derivatives are also applicable using a solver for differential algebraic equations (DAE).

By use of dynamic models, one may be able to adjust more quickly to changes and disturbances, as one does not need to wait for a new steady-state before performing data reconciliation (estimation) and optimization.

In this work the unit models are programmed as Matlab m files. This code could have been more efficient and better structured if it was converted to a true object oriented programming language like C++ or Java. If the Matlab environment is preferred as solver and analysis tool the model can be called trough a proper interface.

# Bibliography


L. T. Biegler and J. E. Cuthrell. Improved infeasible path optimization for sequential modular simulators-II: The optimization algorithm. *Computers & Chemical Engineering*, 9(3):257–267, 1985.

R. Bogusch and W. Marquardt. A formal representation of process model equations. *Computers & Chemical Engineering*, 19:S211–S216, 1995.

D. Bommannan, R. D. Srivastava, and D. N. Saraf. Modeling of catalytic naphtha reformers. *Canadian journal of chemical engineering*, 67:405–411, 1989.

H. I. Britt and R. H. Luecke. Estimation of parameters in nonlinear implicit models. *Technometrics*, 15(2):233–247, May 1973.

Xuayu Chen, Ralph W. Pike, Thomas A. Hertwig, and Jack R. Hopper. Optimal implementation of on-line optimization. *European Symposium on Computer Aided Process Engineering*, pages 435–442, 1998.

C. M. Crowe. Reconciliation of process flow rates by matrix projection, Part II: Nonlinear case. *AIChE Journal*, 32(4):881–888, April 1986.

C. M. Crowe, Y. A. Garcia Campos, and A. Hrymak. Reconciliation of process flow rates by matrix projection, Part I: Linear case. *AIChE Journal*, 29(6):881–888, November 1983.

Cameron M. Crowe. Observability and redundancy of process data for steady state reconciliation. *Chemical Engineering Science*, 44(12):2909–2917, 1989.

Cameron M. Crowe. Data reconciliation - progress and challanges. *Journal of Process Control*, 6(2/3):89–98, 1996.

J. Fraser Forbes and Thomas E. Marlin. Design cost: A systematic approach to technology selection for model-based real-time optimization systems. *Computers & Chemical Engineering*, 20(6/7):717–734, 1996.

J. Edward Jackson. *A user's guide to principal components*. Wiley series in probability and mathematical statistics. Applied probability and statistics. John Wiley & Sons, Inc., New York, 1991. ISBN 0-471-62267-2.

Lloid P. M. Johnston and Mark A. Kramer. Maximum likelihood data rectification: Steady state systems. *AIChE Journal*, 41(11):2415–2426, November 1995.

J. Y. Keller, M. Zasadzinski, and M. Darouach. Analytical estimator of measurement error variances in data reconciliation. *Computers & Chemical Engineering*, 16(3): 185–188, 1992.

Jeffrey Dean Kelly. Techniques for solving industrial nonlinear data reconciliation problems. *Computers & Chemical Engineering*, 28:2837–2843, 2004.

J. W. Lee, Y. C. Ko, Y. K. Jung, K. S. Lee, and E. S. Yoon. A modeling and simulation study on a naphtha reforming unit with catalyst circulation and regeneration system. *Computers & Chemical Engineering*, 21:S1105–S1110, 1997.

Tore Lid and Sigurd Skogestad. Implementation issues for real time optimization of a heatexchanger network. *European Symposium On Computer Aided Process Engineering-11*, 2001.

Tore Lid and Sigurd Skogestad. Effective steady state models for simulation, data reconciliation and optimization. *Computers & Chemical Engineering*, http://dx.doi.org/10.1016/j.compchemeng.2007.04.003, 2007.

Tore Lid, Sigurd Skogestad, and Stig Strand. On line optimization of a crude unit heat exchanger network. *Chemical Process Control-6, AIChE Symposium Series*, (326), 2002.

David G. Luenberger. *Linear and nonlinear programming.* Addison-Wesley, Reading, Massachusetts, second edition, 1984.

A Maarleveld and J. E. Rijnsdorp. Constraint control on distillation columns. *Automatica*, 6:51–58, 1970.

Richard S. H. Mah. *Chemical process structures and information flows.* Butterworths series in chemical engineering. Butterworths, Boston, 1990. ISBN 0-409-90175-x.

W. Marquardt. Trends in computer-aided modelling. *Computers & Chemical Engineering*, 20:591–609, 1996.

Matlab. *Optimization Toolbox Version 2.1.* The MathWorks Inc., 3 Apple Hill Drive, Natick, MA 01760-2098, UNITED STATES, 2000.

Mano Ram Maurya, Raghunthan Rengaswamy, and Venkat Venkatasubramanian. A systematic framework for the development and analysis of signed digraphs for chemical processes. 1. algorthms and analysis. *Industrial & Engineering Chemistry Research*, 42(20):4789–4810, 2003.

Anthony F. Mills. *HEAT AND MASS TRANSFER.* The Richard D. Irwin series in heat transfer. RICARD D. IRWIN, INC, first edition, 1995.

NIST. *NIST Chemistry WebBook*. National Institute of Standards and Technology, http://webbook.nist.gov/chemistry/, 2005.

Jorge Nocedal and Stephen J. Wright. *Numerical optimization*. Springer series in oprations research. Springer, New York, 1999.

Derya B. Özyurt and Ralph W. Pike. Theory and practice of simulaneous data reconciliation and gross error detection for chemical processes. *Computers & Chemical Engineering*, (28):381–402, 2004.

Constantinos C. Pantelides. The consistent initialisation of differential-algebraic systems. *SIAM Journal on Scientific and Statistical Computing*, 9(2):213–231, March 1988.

J. D. Perkins. Plant-wide optimization: Opportunities and challenges. *FOCAPO III, Snowbird, Utah*, pages 15–26, July 1998.

M. A. Rodriguez-Toral, W. Morton, and D. R. Mitchell. The use of new SQP methods for the optimization of utility systems. *Computers & Chemical Engineering*, 25: 287–300, 2001.

Massimo Roma. Dynamic scaling based preconditioning for truncated newton mathods in large scale unconstrained optimization. *Optimization Methods and Software*, 20 (6):693–713, December 2005.

J. A. Romagnoli and G. Stephanopoulos. Rectification of process measurement data in the presense of gross errors. *Chemical Engineering Science*, 36(11):1849–1863, 1981.

S. Skogestad, I. J. Halvorsen, and J. C. Morud. Self-optimizing control: The basic idea and taylor series analysis. *Presented at AIChE Annual Meeting, Miami Beach,16-20 Nov;paper 229c*, 1998.

R. B. Smith. Kinetic analysis of naphtha reforming with platinum catalyst. *Chemical Engineering Progress*, 55(6):76–80, 1959.

G. M. Stanley and R. S. H. Mah. Observability and redundancy in process data estimation. *Chemical Engineering Science*, 36:259–272, 1981.

Unmesh Taskar and James B. Riggs. Modeling and optimization of a semiregeneratiove catalytic naphtha reformer. *AIChE Journal*, 43(3):740–753, 1997.

I. B. Tjoa and L. T. Biegler. Simultaneous strategies for data reconciliation and gross error detection of nonlinear systems. *Computers & Chemical Engineering*, 15(10): 679–690, 1991.

A. W. Westerberg, H. P. Hutcison, R. L. Motard, and P. Winter. *Process flowsheeting*. Cambridge university press, London, 1979.

Douglas. C. White. Online optimization:what, where and estimating ROI. *Hydrocarbon Processing*, pages 43–51, June 1997.

Yale Zhang and J. Fraser Forbes. Extended design cost: a performance criterion for real-time optimization systems. *Computers & Chemical Engineering*, 24:1829–1841, 2000.

Detong Zhu. An affine scaling projective reduced hessian algorithm for minimum optimization with nonlinear equality and linear inequality constraints. *Applied mathematics and Computaion*, 166(1):131–163, 2005.

# Appendix A

# Unit models

A unit model describes a small part of the process like a heater, flash drum or compressor. The process model equations of a unit model are organized such that any connections between unit models are established by process streams. In this modeling framework, a process stream is defined as a set of shared variables describing the process stream properties. In this case the process stream variables are selected to be molar component fractions $\boldsymbol{x}$, molar flow $F$, stream temperature $T$ and stream pressure $P$.

## A.1 Heater

The heater is modeled as a direct heat input to the process stream. The inlet and outlet streams in the vapor phase and no phase changes occur. The heater has one inlet and one outlet stream as shown in figure A.1. The heater unit model has $n_z = 2(NC+3)+1$

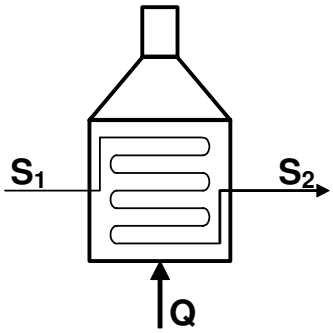


Figure A.1: Heater

variables where the $2(NC+3)$ variables describe the properties of the inlet and outlet streams and the additional variable is a internal variable, the heat input $Q$.

The process model is based on the mass balance, energy balance, mole fraction summation and pressure flow relation. The pressure drop is proportional to the squared outlet stream volume flow. The unit model has $n_f = NC+3$ equations and the degrees of freedom $n_z - n_f = NC + 4$. The equations of the heater unit model are written as

$$F_1\boldsymbol{x}_1 - F_2\boldsymbol{x}_2 = 0 \tag{A.1}$$

$$F_1 h_v(\boldsymbol{x}_1, T_1) - F_2 h_v(\boldsymbol{x}_2, T_2) + Q = 0 \tag{A.2}$$

$$\sum_{i=1}^{NC} \boldsymbol{x}_2(i) - 1 = 0 \tag{A.3}$$

$$P_2 - P_1 - k_p \left( F_2 \frac{RT_2}{P_2} \right)^2 = 0 \tag{A.4}$$

$$\tag{A.5}$$

where $k_p$ is a fixed pressure drop constant ([Pa/(m$^3$/s)$^2$]).

## A.2 Reactor (CSTR)

The CSTR unit model is used as an element in the reactor model. This unit model as shown in figure A.2 has one inlet and one outlet stream which both are in the vapor phase. The unit model has $2(NC + 3)$ variables describing the properties of the inlet

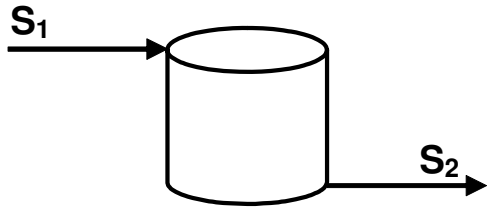


Figure A.2: Plug flow reactor element

and outlet streams and one internal variable, $A_c$. $A_c$ is a catalyst efficiency factor and has a value close to 1. The unit model total number of variables $n_z = 2(NC + 3) + 1$. The CSTR is modeled by a mass and energy balance, sum of molar fractions and a

pressure-flow equation.

$$F_1\boldsymbol{x}_1 - F_2\boldsymbol{x}_2 + A_c m_c N^{\mathrm{T}} r(T_2, P_2) = 0 \tag{A.6}$$

$$F_1 h_v(\boldsymbol{x}_1, T_1,) - F_2 h_v(\boldsymbol{x}_2, T_2) + A_c m_c H_r r(T_2, P_2) = 0 \tag{A.7}$$

$$\sum_{i=1}^{NC} \boldsymbol{x}_2(i) - 1 = 0 \tag{A.8}$$

$$P_2 - P_1 - k_p \left( F_2 \frac{RT_2}{P_2} \right)^2 = 0 \tag{A.9}$$

$$\tag{A.10}$$

where $m_c$ is the mass of catalyst, $N$ the stoichiometric matrix and $r(T, P)$ the reaction rates. $H_r$ is the heat of reaction. The reactor pressure drop is proportional with the squared of the reactor outlet volume flow. The CSTR unit model has $n_f = NC + 3$ equations and the degrees of freedom $n_z - n_f = NC + 4$.

## A.3 Separator with water cooling

The cooling water heat exchanger and separator is modeled as one unit model, as shown if figure A.3. Feed stream one are in the vapor phase and feed stream two are in the liquid phase. Outlet stream three are in the vapor phase and outlet stream four are in the liquid phase. The heat transfer is modeled as a pure countercurrent heat exchanger where the hot side has liquid and vapor inlet and outlet streams. This unit model has

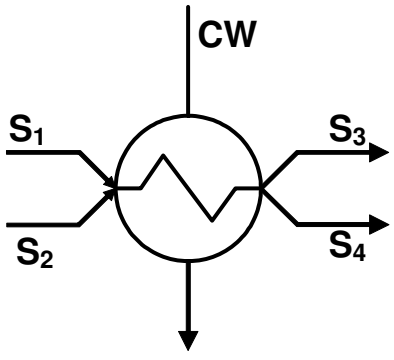


Figure A.3: Flash drum

$4(NC + 3)$ variables describing the properties of the inlet and outlet streams and five internal variables. Three internal variables describe the cooling water flow, inlet and outlet temperature and two internal variables are used for heat transfer coefficient $U$ and transferred heat, $Q$. The total number of model variables $n_z = 4(NC + 3) + 5$

The heat transfer is modeled using the $\epsilon$-Ntu method as described in Mills (1995). There is no pressure drop assumed in the system and the inlet and outlet streams have equal pressures.

The equations of this unit model are the hot side mass balance, hot side energy balance, sum of molar fractions of the hot side liquid and vapor outlet streams, hot side vapor liquid equilibrium, hot side vapor and liquid pressure-flow relation (zero pressure drop), equal temperature in vapor and liquid outlet streams, cold side energy balance (water) and finally a equation describing the heat transfer.

$$F_1\boldsymbol{x}_1 + F_2\boldsymbol{x}_2 - F_3\boldsymbol{x}_3 - F_4\boldsymbol{x}_4 = 0 \tag{A.11}$$

$$F_1 h_v(\boldsymbol{x}_1, T_1) + F_2 h_l(\boldsymbol{x}_2, T_2) - F_3 h_v(\boldsymbol{x}_3, T_3) - F_4 h_l(\boldsymbol{x}_4, T_3) + Q = 0 \tag{A.12}$$

$$\sum_{i=1}^{NC} \boldsymbol{x}_3(i) - 1 = 0 \tag{A.13}$$

$$\sum_{i=1}^{NC} \boldsymbol{x}_4(i) - 1 = 0 \tag{A.14}$$

$$\boldsymbol{x}_3 - K(T_4, P_4)\boldsymbol{x}_4 = 0 \tag{A.15}$$

$$P_1 - P_4 = 0 \tag{A.16}$$

$$P_2 - P_4 = 0 \tag{A.17}$$

$$T_3 - T_4 = 0 \tag{A.18}$$

$$F_{CW} Cp_{CW}(T_{CWo} - T_{CWi}) - Q = 0 \tag{A.19}$$

$$\varepsilon \cdot \mathrm{C_{min}}(T_1 - T_{CWi}) - Q = 0 \tag{A.20}$$

The subscript $CW$ refers to cooling water where $F_{CW}, T_{CWo}, T_{CWi}$ refers to cooling water flow, outlet and inlet temperature respectively. Fixed specific heat capacity $Cp_{CW}$ is assumed for cooling water.

For a pure countercurrent heat exchanger the efficiency ($\varepsilon$) is defined as

$$\varepsilon = \frac{1 - e^{(-\mathrm{Ntu}(1-\mathrm{R_C}))}}{1 - \mathrm{R_C}\, e^{(-\mathrm{Ntu}(1-\mathrm{R_C}))}} \tag{A.21}$$

where $\mathrm{R_C}$ is the capacity ratio and Ntu the number of transfer units. $\mathrm{R_C}$ and Ntu are defined as

$$\mathrm{R_C} = \frac{\mathrm{C_{min}}}{\mathrm{C_{max}}} \quad \mathrm{Ntu} = \frac{\mathrm{UA}}{\mathrm{C_{min}}} \tag{A.22}$$

where $U$ is the heat exchanger heat transfer coefficient and $A$ the heat exchanger area of heat transfer. The minimum and maximum capacity is defined as

$$\mathrm{C_{min}} = \min(\mathrm{C_h}, \mathrm{C_c}) \quad \mathrm{C_{max}} = \max(\mathrm{C_h}, \mathrm{C_c}) \tag{A.23}$$

where $\mathrm{C_h}$ $\mathrm{C_c}$ is the hot and cold side capacity respectively.

$$\mathrm{C_h} = F_h C_{ph} \qquad \mathrm{C_c} = F_c C_{pc} \tag{A.24}$$

where $F_h$ is the hot side flow and $C_{ph}$ is the hot side specific heat capacity. Similar for the cold side.

The $\epsilon$-Ntu method for calculation of heat transfer is based on hot and cold side fluids with constant specific heat. In this case the hot side fluid is a mixture of vapor and liquid and condensation of vapor occurs. In order to still be able to use this method an approximation of the hot side specific heat is used. The average $C_p = h/\Delta T$. In this case $\bar{h}$ is the average enthalpy of the inlet and outlet of the heat exchanger. The specific enthalpy at the inlet is the weighted average of the liquid and vapor specific enthalpy. The average enthalpy at the inlet and outlet is calculated as

$$\bar{h}_i = \frac{F_1 h_v(\boldsymbol{x}_1, T_1) + F_2 h_l(\boldsymbol{x}_2, T_2)}{F_1 + F_2} \qquad \bar{h}_o = \frac{F_3 h_v(\boldsymbol{x}_3, T_3) + F_4 h_l(\boldsymbol{x}_4, T_4)}{F_3 + F_4} \tag{A.25}$$

In the reformer model the inlet vapor and liquid stream are both saturated and are at the same temperature and pressure. The same is also valid for the heat exchanger hot side outlet stream. The average specific heat for the hot side stream is calculated as

$$Cph = \frac{\bar{h}_o - \bar{h}_i}{T_4 - T_2} \tag{A.26}$$

The separator with cooling unit model has $n_f = 2NC + 8$ equations and has $n_z - n_f = 2NC + 9$ degrees of freedom.

## A.4 Compressor

The compressor unit model, as shown in figure A.4, has one inlet and one outlet stream. The unit model has $2(NC+3)$ variables describing the properties of the process streams and three internal variables. The internal variables are shaft work $W$, compressor efficiency $\psi$ and isentropic outlet temperature (reversible compression) $T_s$. The number of variables adds up to $n_z = 2(NC + 3) + 3$. The compressor unit model equations

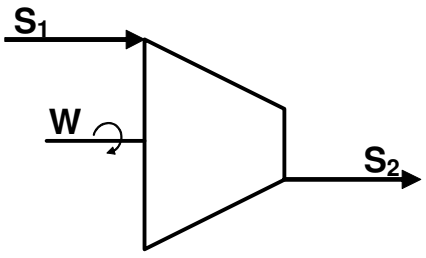


Figure A.4: Compressor

are the mass balance, energy balance for reversible and irreversible compression, sum

of outlet stream mole fractions and reversible compression zero entropy production.

$$F_1\boldsymbol{x}_1 - F_2\boldsymbol{x}_2 = 0 \tag{A.27}$$

$$F_1 h_v(\boldsymbol{x}_1, T_1) - F_2 h_v(\boldsymbol{x}_2, T_s) + \psi W = 0 \tag{A.28}$$

$$F_1 h_v(\boldsymbol{x}_1, T_1) - F_2 h_v(\boldsymbol{x}_2, T_2) + W = 0 \tag{A.29}$$

$$\sum_{i=1}^{NC} \boldsymbol{x}_2(i) - 1 = 0 \tag{A.30}$$

$$F_1 s_v(\boldsymbol{x}_1, T_1, P_1) - F_2 s_v(\boldsymbol{x}_2, T_s, P_2) = 0 \tag{A.31}$$

This compressor model has $n_f = NC + 4$ equations and $n_z - n_f = NC + 5$ degrees of freedom.

## A.5 Reactor effluent heat exchanger

The reactor effluent heat exchanger unit model, shown in figure A.5, has phase changes in both the hot and the cold side. The cold side inlet stream $S_1$ is in the vapor phase and $S_2$ is in the liquid phase. The outlet of the cold side $S_3$ is in vapor phase.

The hot side feed $S_4$ is superheated vapor, which is partially condensed into the hot side liquid and vapor outlet streams $S_5$ and $S_6$. This model has $6(NC + 3)$ variables

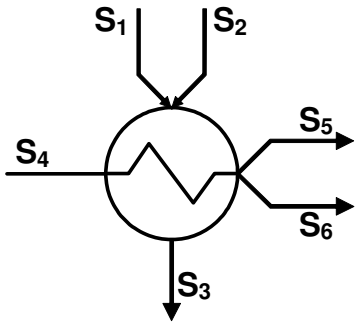


Figure A.5: Heat exchanger

describing the properties of the hot and cold side inlet and outlet streams. In addition there are two internal variables,heat exchanger duty $Q$ and the heat transfer coefficient U. The total number of variables $n_z = 6(NC + 3) + 2$.

The cold side model is the mass balance, energy balance, sum of outlet stream molar fractions and cold side pressure flow relation (zero pressure drop). The hot side side model is the mass balance, energy balance, sum of outlet streams molar fractions, vapor-liquid equilibrium and hot side pressure flow relation (zero pressure drop).

Finally, the heat transfer is modeled using the $\epsilon$-Ntu method.

$$F_1\boldsymbol{x}_1 + F_2\boldsymbol{x}_2 - F_3\boldsymbol{x}_3 = 0 \tag{A.32}$$

$$F_1 h_v(\boldsymbol{x}_1, T_1) + F_2 h_l(\boldsymbol{x}_2, T_2) - F_3 h_v(\boldsymbol{x}_3, T_3) + Q = 0 \tag{A.33}$$

$$\sum_{i=1}^{NC} \boldsymbol{x}_3(i) - 1 = 0 \tag{A.34}$$

$$P_1 - P_3 = 0 \tag{A.35}$$

$$P_2 - P_3 = 0 \tag{A.36}$$

$$F_4\boldsymbol{x}_3 - F_5\boldsymbol{x}_5 - F_6\boldsymbol{x}_6 = 0 \tag{A.37}$$

$$F_4 h_v(\boldsymbol{x}_4, T_4) - F_5 h_v(\boldsymbol{x}_5, T_5) - F_6 h_l(\boldsymbol{x}_6, T_6) - Q = 0 \tag{A.38}$$

$$\sum_{i=1}^{NC} \boldsymbol{x}_5(i) - 1 = 0 \tag{A.39}$$

$$\sum_{i=1}^{NC} \boldsymbol{x}_6(i) - 1 = 0 \tag{A.40}$$

$$\boldsymbol{x}_5 - K(T_6, P_6)\boldsymbol{x}_6 = 0 \tag{A.41}$$

$$P_4 - P_5 = 0 \tag{A.42}$$

$$T_5 - T_6 = 0 \tag{A.43}$$

$$\varepsilon \cdot \mathrm{C}_{\min}(T_4 - T_1) - Q = 0 \tag{A.44}$$

The calculation of the heat transfer term in equation A.44 is similar to the description in section A.3 equation A.21.

This heat exchanger unit model has $n_f = 3NC + 10$ equations and $n_z - n_f = 3NC + 10$ degrees of freedom.

## A.6 Vapor-liquid stream mixer

This unit model, shown in figure A.6, is used to describe the mixing of the liquid feed and recycle gas. There are four process streams in the model, one vapor and one liquid inlet stream, and one vapor and one liquid outlet stream. The inlet stream $S_1$ and

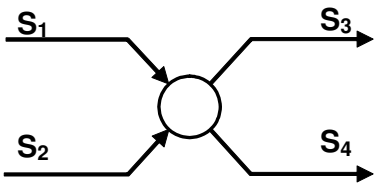


Figure A.6: Mixing of vapor and liquid streams

outlet stream $S_3$ are in the vapor phase and inlet steam $S_2$ and outlet stream $S_4$ in

the liquid phase. There are $n_z = 4(NC + 3)$ variables describing the properties of the input and output streams.

The stream mixing model are the mass balance, energy balance, sum of outlet streams molar fractions, vapor-liquid equilibrium and pressure-flow relations (zero pressure drop).

$$F_1\boldsymbol{x}_1 + F_2\boldsymbol{x}_2 - F_3\boldsymbol{x}_3 - F_4\boldsymbol{x}_4 = 0 \tag{A.45}$$
$$F_1 h_v(\boldsymbol{x}_1, T_1) + F_2 h_l(\boldsymbol{x}_2, T_2) - F_3 h_v(\boldsymbol{x}_3, T_3) - F_4 h_l(\boldsymbol{x}_4, T_4) = 0 \tag{A.46}$$
$$\sum_{i=1}^{NC} \boldsymbol{x}_3(i) - 1 = 0 \tag{A.47}$$
$$\sum_{i=1}^{NC} \boldsymbol{x}_4(i) - 1 = 0 \tag{A.48}$$
$$\boldsymbol{x}_3 - K(T_3, P_3)\boldsymbol{x}_4 = 0 \tag{A.49}$$
$$P_1 - P_3 = 0 \tag{A.50}$$
$$P_2 - P_3 = 0 \tag{A.51}$$
$$T_3 - T_4 = 0 \tag{A.52}$$

The unit model has $n_f = 2NC + 6$ equations and if the degrees of freedom in this model equals $n_z - n_f = 2NC + 6$.

## A.7 Stream split

The stream split unit model, shown in figure A.7 describes the split of one vapor stream into two vapor streams. The model has $n_z = 3(NC + 3)$ variables, describing

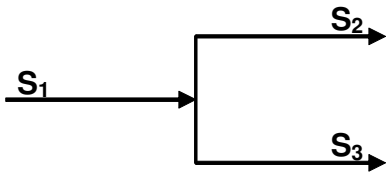


Figure A.7: Splitting of streams

the properties if the input and output streams.

The stream split model are the mass balance, energy balance, sum of molar fractions, outlet stream equal composition, outlet stream equal temperature, and pressure-flow

relations (zero pressure drop).

$$F_1\boldsymbol{x}_1 - F_2\boldsymbol{x}_2 - F_3\boldsymbol{x}_3 = 0 \tag{A.53}$$

$$F_1 h_v(\boldsymbol{x}_1, T_1) - F_2 h_v(\boldsymbol{x}_2, T_2) - F_3 h_v(\boldsymbol{x}_3, T_3) = 0 \tag{A.54}$$

$$\sum_{i=1}^{NC} \boldsymbol{x}_3(i) - 1 = 0 \tag{A.55}$$

$$\boldsymbol{x}_2 - \boldsymbol{x}_3 = 0 \tag{A.56}$$

$$T_2 - T_3 = 0 \tag{A.57}$$

$$P_1 - P_2 = 0 \tag{A.58}$$

$$P_1 - P_3 = 0 \tag{A.59}$$

The stream split unit model has $n_f = 2NC + 5$ equations and $n_z - n_f = NC + 4$ degrees of freedom.